B cells, T follicular helpers, and germinal centers as facilitators of chronic Graft-versus-Host disease

A DISSERTATION SUBMITTED TO THE FACULTY OF THE UNIVERSITY OF MINNESOTA BY

Ryan Patrick Flynn

IN PARTIAL FULFILLMENT OF THE REQUIREMENTS FOR THE DEGREE OF DOCTOR OF PHILOSOPHY

Dr. Bruce R. Blazar, M.D.

August 2014

Acknowledgements

I would like to thank the other MICaB students and staff.

I would like to thank the members of my thesis committee Drs. Chris Pennell, Jeff Miller, and Bryce Binstadt for supporting me throughout my graduate career.

I would like to thank members of the Blazar lab who have helped throughout my graduate career:

Pat Taylor who was always willing to listen and offer support. I greatly appreciated the scientific experience you were willing to share.

LeAnn Micek who made sure everything got done. I was always able to come to you with a question and leave with an answer. Stacy Maher who was always available to schedule meetings.

For the scientific support provided by all of the current and past lab members: Brent Koehn, Rachelle Veenstra, Cameron McDonald-Hyman, Dawn Reichenbach, Jing Du, Katelyn Goodman, Raju Thangavelu Kazutosi Ayoma, Asim Saha, Michelle Smith, Sarah Parker, Beau Webber, Randy Donelson, Chris Lees and Mark Osborn.

I would like to thank my family for motivating me to graduate and having me keep them informed on when that would actually happen. I would like to especially thank Megan Multhaup who never lost faith in me.

Finally, I would like to thank my advisor Dr. Bruce Blazar who has been the most important influence on my scientific and professional life. I am honored to have trained with you and am excited to continue working with you.

Abstract

Allogeneic hematopoietic stem cell transplantation is a potential cure for many malignant diseases. However, the possibility of chronic Graft-Versus-Host Disease (GVHD) is a major obstruction to the therapeutic results. Development of novel therapies has been hindered by an incomplete knowledge of the mechanism of disease. This is in part due to a lack of relevant mouse models. Using a new murine model of chronic GVHD we shed light on the mechanism of disease as well as proposed novel therapeutics that could be beneficial for the treatment of chronic GVHD. First, we demonstrate that B cells derived from the donor bone marrow are necessary for the progression of disease and that these B cells had to produce class-switched antibodies. The production of class-switched antibody is dependent on the germinal center reaction. The need for the germinal center is further highlighted by the requirement for the presence of T follicular helper cells. These specialized cells promote the germinal center reaction by providing survival signaling to B cells through the IL-21 cytokine and ICOS and CD40 costimulatory molecules. We further provide evidence that T follicular helper cells and the germinal center reaction are necessary by demonstrating that therapeutic depletion of B cells during active chronic GVHD is unable to prevent the progression of disease. Finally, we demonstrate the importance of B cell signaling following antigen stimulation. Inhibition of the B-cell signaling molecule Syk directly down-stream of B-cell receptor signaling is sufficient to prevent the progression of chronic GVHD. Collectively this work identifies important B-cell survival signals that are necessary for the development of chronic GVHD.

Table of Contents

List of Figures

Chapter I

Chapter II

Chapter III

Chapter IV

Chapter V

List of Abbreviations

APC	Antigen Presenting Cell
BAFF	B-cell Activating Factor
BCR	B-cell Receptor
BMT	Bone Marrow Transplant
BOS	Bronchiolitis Obliterans Syndrome
Btk	Bruton's Tyrosine Kinase
CD40L	CD40 Ligand
Cy	Cyclophosphamide
GC	Germinal Center
GVHD	Graft-versus-Host disease
HSC	Hematopoietic Stem Cell
HSCT	Allogeneic Hematopoietic Stem Cell Transplant
H-Y	Male Histocompatibility
ICOS	Inducible T-cell Costimulator
Ig	Immunoglobulin
IL	Interleukin
ITK	Interleukin-2 Inducible Kinase
KO	Knockout
LTβR	Lymphotoxin Beta Receptor
mAb	Monoclonal Antibody
MHC	Major Histocompatibility Complex
MiHA	Minor Histocompatibility Antigen

PDGF	Platelet Derived Growth Factor
PD-1	Programmed Death Protein 1
PDL1	PD-1 Ligand
Syk	Spleen Tyrosine Kinase
TBI	Total Body Irradiation
Tfh	T Follicular Helper
Th	T Helper
Treg	T Regulatory
Tg	Transgenic
TGF	Transforming Growth Factor
TNF	Tumor Necrosis Factor
WT	Wild Type

Chapter I: Introduction

Allogeneic Hematopoietic Stem Cell Transplantation

Development of blood cells takes place in the bone marrow, where hematopoietic stem cells (HSCs) differentiate into the cells that constitute the blood such as red blood cells, leukocytes, and platelets. The leukocyte population comprises the cells of the innate and adaptive immune system. Without these cells, hosts would be susceptible to infections and would not survive. These cells are also important for preventing the onset of malignancies.

Due to the rapid creation and turnover of the blood and bone marrow compartments there is a high risk of genetic mutations that can lead to the development of cancer. Leukemia and lymphoma are malignancies of the blood and bone marrow. There are over 30,000 new cases of leukemia annually and roughly 70% of people will die from the malignancy. For many of these diseases the only cure is a HSC transplantation (HSCT), where patients are ablated of their malignant bone marrow by chemotherapy and given healthy bone marrow from a donor. The donor bone marrow can come from the same host, a sibling, or a non-related host. There are many benefits and complications from each donor source. With an autologous, same, or sibling donor there is a decreased risk of graft-rejection compared to an allogeneic, non-related, donor. However, the risk of tumor relapse is decreased with an allogeneic donor compared to the autologous or sibling donor[1].

Allogeneic hosts offer an increased clearance of the leukemia or lymphoma following HSCT. However the risk of rejecting the recipient by the donor's immune-competent cells can occur. Graft-versus-Host disease (GVHD)

is a major complication following HSCT. GVHD can occur in 19-66% of sibling and 90% of unrelated allogeneic donors and leads to a mortality rate of about 15% of total HSCT recipients[2]. Due to the high tumor clearance of allogeneic HSCT and the relatively low existence of sibling donors – about one in four recipients – the need for better understanding of GVHD as well as better therapeutics is necessary.

Graft-versus-Host Disease

Graft-versus-host disease was fist observed as a secondary disease following irradiation and transplantation of hematopoietic cells[3]. Later Billingham R.E. defined the three criteria necessary for diagnosis of GVHD[4]. First, the graft must contain immunologically competent cells. It was demonstrated that addition of mature hematopoietic cells from the spleen or lymph nodes increased the severity of disease.[5] Further research has demonstrated that thymus-derived lymphocytes (T cells) are the key cell required for development of GVHD[6]. Depletion of T cells from the donor graft is able to prevent the development of GVHD, but the depletion also removes many beneficial effects as well, such as tumor clearance. Second, the recipient must be immune compromised so that they are unable to reject the graft. This occurs with the high levels of chemotherapy necessary for eliminating the malignancy. Finally, the recipient and donor must have antigen disparity. Major and minor histocompatibility antigens (MHC and MiHA respectively) generate immune responses to the host[7].

It is estimated that 1 in 100 T cells are able to recognize these histocompatibility antigens[8], in striking contrast to the 1 in 100,000 for other antigens[9].

GVHD can be divided into two distinct diseases: acute GVHD and chronic GVHD. Pathogenesis of acute GVHD beings with the initiation phase: cytoablative conditioning releases proinflammatory cytokines and damages epithelial tissues, most notably in the gastrointestinal tract. The release of the pro-inflammatory cytokines TNF-a and IL-1 increases with increased doses of irradiation[10]. These cytokines act to increase the activation state of host antigen presenting cells[11]. Damage to the epithelial lining also allows for the release of bacterial endotoxin, further amplifying the activation of host immune cells[12]. Furthermore, damage to thymic epithelial cells allows for decreased thymic output and an increase in potentially self-reactive T cells[13], which can lead to increased disease during chronic GVHD. During the activation phase, donor mature T cells present in the graft are activated in the pro-inflammatory environment created by conditioning. It remains controversial how donor T cells recognize antigen presented by host (MHC). T cells can recognize host antigen by either direct presentation or indirect presentation or some combination of both[14]. For direct recognition donor T cells recognize either the peptide bound to allogeneic MHC or the allogeneic MHC molecule themselves. In contrast, indirect recognition involves the T cell binding to degraded recipient MHC presented by graft MHC. Finally, activated T cells migrate to target tissues to cause significant host tissue destruction[15]. Acute GVHD is defined by necrosis of target tissues. Activation of CD8 cytotoxic T lymphocytes has been shown to be necessary for

the progression of disease. Each phase works to amplify the disease causing multi-organ system damage.

Whereas research in acute GVHD has greatly increased the survival rate for transplanted patients, the prevalence of chronic GVHD has increased. This is partially due a lack of definition for the disease and the dearth of relevant research tools to study disease[16]. Recently an NIH consensus consortium redefined the diagnosis and criteria for disease[17], establishing key pathological syndromes necessary for diagnosis as chronic GVHD. Previously, any complication following 100 days post transplantation was considered chronic GVHD. However, there is precedent of late-term acute GVHD that can manifest past the 100-day criteria. Therefore incorrect diagnosis and understanding of disease was unable to be defined by timing of disease. Finally, the presence of accurate research models has remained poor. Murine models of acute GVHD can mimic the human disease; however, models for chronic GVHD have not replicated the spectrum of the human disease. Many chronic GVHD models either do not have the complete cytoablative conditioning regiment or do not use cells from relevant donors to cause disease. Furthermore, manifestation of disease has been limited to only a couple target organs, such as skin, kidneys, and liver instead of a systemic multi-organ disease. Development and characterization of a more accurate model is necessary for the understanding and ultimately the development of new therapies for chronic GVHD.

Chronic GVHD

While chronic GVHD can have different disease manifestations in the lung, liver, and skin the pathology has the overlapping key characteristics of increased fibrosis (Figure 1). In several instances there has been evidence to suggest that B cells play a major role in disease. B cells are antibody-producing cells that develop in the bone marrow. After recognition of the cognate antigen they interact with specialized T cells to produce high-affinity antibodies in the germinal center (GC). Acute GVHD tends to be a B cell eliminating disease, however, B cells appear to be activated during chronic GVHD. Early studies demonstrated an increase in antibody production to known MiHA. It was demonstrated that male recipients receiving female grafts developed antibodies toward the male MiHA in the context of chronic GVHD[18]. This demonstrated that during chronic GVHD antibody to a known MiHA was produced. In addition, the level of B-cell activating factor (BAFF) is increased in patients with chronic GVHD[19, 20]. The increase of BAFF to B cell ratio is thought to increase the response rate and survival of pathogenic B cells.

Even though the role of B cells during chronic GVHD is not completely understood there is growing evidence that deposition of antibodies in target tissues causes disease. Antibody deposition can lead to activation of complement and antibody-dependent cellular cytotoxicity. This process involves the activation of macrophages or natural killer cells in target tissues by recognizing antibody bound to the cognate antigen. The activation of macrophages can cause release of pro-fibrotic cytokines that leads to tissue remodeling. The increase in antibody deposition in target tissues is correlated

with the increase in fibrosis; however, the processes that lead to increased fibrosis are not well understood. In some patients there are increases in pro-fibrotic cytokines such as TGFβ[21]. There is growing evidence that TGFβ is produced by donor macrophages activated by deposited antibody (JCI in press). However there are other mechanisms that have been seen in clinic. The activation of receptors, such as Platelet Derived Growth Factor Receptor (PDGFR), by activating antibodies has also been described[22, 23]. In this situation, antibodies might not be causing the tissue destruction as previously believed; instead receptor-activating antibodies might cause the increase in fibroproliferation.

Initiation of disease is dependent on T cells. Presence of mature T cells in the graft is necessary for disease in models of chronic GVHD[24]. B cells interact with T cells in the follicle of secondary lymphoid organs to form GC reactions. Here T cells provide survival signals to B cells during DNA mutation to the antibody locus in peripheral tissues following antigen stimulation in a process known as somatic hyper-mutation. After antigen stimulation, B cells upregulate activation induced cytosine deaminase (AID), causing point mutations to the Ig locus, these mutations are repaired by non-homologous end joing repair mechanism creating mutations in the region. DNA that affects the antigen-recognizing portion of the antibody it is selected by T cells by receiving cell pro-survival stimulation or is neglected and undergoes apoptosis[25]. Specialized T follicular helper cells (Tfh) provide cytokine support and selection for B cells undergoing somatic hyper-mutation. The cytokine IL21 has been demonstrated

to increase the B cell survival and maturation to memory and plasma cells even though the GC reaction is not dependent on the expression of IL21[26]. Signaling through the IL21 receptor increases the expression of proteins necessary for somatic hyper-mutation and survival factors in B cells. Tfh also provide contact dependent signals to B cells through ICOS and CD40 signaling. B cells that are able to produce higher affinity antibodies create more stable contacts receive increased support from the Tfh.

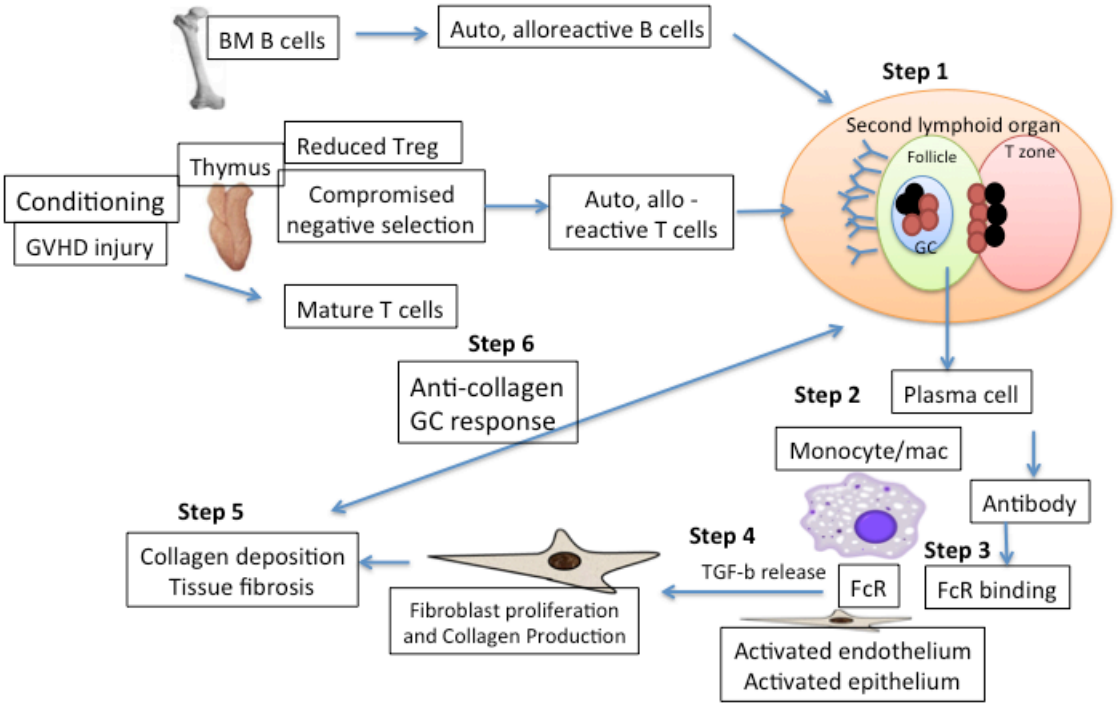

Figure 1: Proposed mechanism of chronic GVHD. Pre-transplant conditioning and alloreactive donor T cells leads to a compromised selection in the thymus and bone marrow allowing for allo/auto reactive T cells and B cells, respectively, to be generated. B cells and T follicular helper cells enter the secondary lymphoid organs and form germinal centers reactions to allo/auto reactive antigens. B cells differentiate into the antibody-producing cell, Plasma cells, which produce highly specific antibodies that bind target tissues and activate macrophages, releasing pro-fibrotic cytokines. This leads to a positive-feedback loop increasing fibrosis and tissue damage and allowing more allo/auto reactive B cells to undergo the germinal center reaction.

Chapter II: Donor B-cell alloantibody deposition and germinal center formation are required for the development of murine chronic GVHD and bronchiolitis obliterans

Originally published by the American Society of Hematology in the journal Blood
Srinivasan M, Flynn R, Price A, Ranger A, Browning JL, Taylor PA *et al*. *Blood* 2012; **119**(6)**:** 1570-80.

Chronic GVHD poses a significant risk for HSCT patients. Preclinical development of new therapeutic modalities has been hindered by models with pathologic findings that may not simulate the development of human chronic GVHD. Previously, we have demonstrated that chronic GVHD induced by allogeneic HSCT after a conditioning regimen of cyclophosphamide and total-body radiation results in pulmonary dysfunction and airway obliteration, which leads to bronchiolitis obliterans (BO), which is pathognomonic for chronic GVHD of the lung. We now report chronic GVHD manifestations in a wide spectrum of target organs, including those with mucosal surfaces. Fibrosis was demonstrated in the lung and liver and was associated with $CD4^+$ T cells and $B220^+$ B-cell infiltration and alloantibody deposition. Donor bone marrow obtained from mice incapable of secreting IgG alloantibody resulted in less BO and chronic GVHD. Robust germinal center reactions were present at the time of chronic GVHD disease initiation. Blockade of germinal center formation with a lymphotoxin-receptor–immunoglobulin fusion protein suppressed chronic GVHD and BO. We conclude that chronic GVHD is caused in part by alloantibody secretion, which is associated with fibrosis and chronic GVHD manifestations including BO, and that treatment with a lymphotoxin-β receptor–immunoglobulin fusion protein could be beneficial for chronic GVHD prevention and therapy.

Introduction

Chronic GVHD is a significant complication of allogeneic HSCT[27]. Progress in developing interventional strategies to counter chronic GVHD has been hampered by variable onset and pathologic manifestations of chronic GVHD, now better defined by the National Institutes of Health consensus conference,[17] and a dearth of robust preclinical venues that closely mimic conditions in which chronic GVHD is generated and manifested[16].

Although the exact causes of chronic GVHD are unknown, higher antibody levels have been associated with autoimmunity and implicated in chronic GVHD[28, 29]. Studies of newly diagnosed patients with extensive chronic GVHD showed that they had elevated soluble B-cell activating factor (BAFF) levels and anti-ds-DNA antibodies[30, 31]. Increased soluble BAFF in chronic GVHD was associated with higher circulating levels of pre–germinal center (GC) B cells and post-GC plasmablasts[19]. B cells from chronic GVHD patients are hyper-responsive to TLR-9 signaling and have up-regulated CD86 levels[32], which suggests an important participatory role for B cells in establishing chronic GVHD and emphasizes the need for further investigation into the immunologic role of B cells in chronic GVHD pathogenesis.

Existing murine chronic GVHD models simulate one or more of the pathologic manifestations, such as increased serum antibodies (typically anti-DNA antibodies), scleroderma, and fibrosis of skin and liver, and the less common immune complex deposition in kidneys and glomerulonephritis[33-35]. The type of multi-organ involvement and alloantibodies seen in chronic GVHD

patients often has not been well represented in these preclinical models. Moreover, some models do not involve conditioning regimens, whereas others rely on radiation alone. Previously, our laboratory has studied pulmonary dysfunction and chronic GVHD target-organ pathology in animals conditioned with high-dose cyclophosphamide (Cy) and lethal total-body irradiation (TBI) rescued with allogeneic BM and splenocytes[36]. The functional, physiologic, and pathologic assays demonstrated that Cy and TBI–conditioned recipients of low numbers of allogeneic T cells developed bronchiolitis obliterans (BO)[37, 38]. BO, characterized by airway blockade, peribronchiolar fibroproliferation, and obliteration of bronchioles, is a late-stage complication of GVHD, prevalent in 2%-3% of HSCT patients and up to 6% of patients who develop GVHD[39]. Patients diagnosed with BO have a 5-year survival rate of only 10% versus 40% in patients without BO[37]. According to the National Institutes of Health consensus criteria[17], BO is the only single pathognomonic manifestation of chronic GVHD of the lung; therefore, this is a bona fide chronic GVHD murine model.

In the present study, we identified the presence of $CD4^+$ Th cells and $B220^+$ B cells in the airways of mice that had BO, tissue-specific antibodies from sera, and alloantibody deposition in the lung and liver of chronic GVHD recipients. Through studies using wild-type (WT), knockout, and transgenic donor cells, we conclusively demonstrate that donor alloantibody secretion is essential for BO generation, providing a preclinical model in which to test interventional and prophylactic approaches for chronic GVHD.

The mainstay of treatment of chronic GVHD and BO is anti-inflammatory therapy. Corticosteroids are contained in many of the current regimens but are still associated with a high rate of progressive airway obliteration and subsequent mortality[40]. Treatment of steroid-refractory chronic GVHD patients with rituximab, a B cell–depleting anti-CD20 mAb, has shown a beneficial role in resolution of autoimmune disorders such as systemic lupus erythematosus and rheumatoid arthritis[41], as well as chronic GVHD[18, 42-44]. Aggregate analysis of 6 trials of steroid-refractory chronic GVHD showed overall response rates of 29%-36% for oral, hepatic, gastrointestinal, and lung chronic GVHD and 60% for cutaneous chronic GVHD[45].

Additional prevention and treatment strategies clearly are needed. We focused on GC formation, critical for efficient class switching and antibody secretion by mature B cells and plasma cells. Lymphotoxin-β (LTβ)–LTβ receptor (LTβR) interactions are essential for GC formation and maintenance, ensuring proper anchoring of GC B cells within the network of follicular dendritic cells (DCs) and correct GC formation. Inhibiting the GC reaction and subsequent antibody secretion has proved to be efficacious in some systemic lupus and other autoimmune models in which B cells and antibody secretion have been implicated in pathology[41]. LTβR-Ig is a novel fusion protein that binds circulating lymphotoxin and inhibits LT-LTβR signaling[46]. We show that LTβR-Ig treatment of transplanted animals susceptible to the establishment of chronic GVHD and BO resulted in improved lung function along with lower tissue-specific antibody levels

in the sera and fibrosis of the lung and liver. LTβR-Ig represents a potential new therapy for chronic GVHD prevention and treatment.

Results

Multiorgan pathology with fibrosis in Cy/TBI recipients experiencing chronic GVHD

B10.BR mice were conditioned with Cy/TBI and received either BM alone (BMT control group) or BM with low-dose splenocytes to induce a chronic alloresponse not associated with early post-BMT mortality. Weight curves (Figure 1 A) and 2-month survival rates were ≥ 90% and were comparable between groups (Figure 1 B). On day 60, PFTs in the chronic GVHD group (Figure 1 C) demonstrated lung dysfunction consistent with BO[36]. The PFTs showed an increase in airway resistance, which correlated with lung constriction, increased elastance, and decreased compliance, which signifies increased stiffness or rigidity of the lungs. These data simulate BO manifestations in chronic GVHD patients[39]. A decrease in pulmonary function and increased pathology was noticed as early as 28 days after transplantation (Figure 1 D; supplemental Figure 2). Therefore, this system is a bona fide model of chronic GVHD based on extrapolation of the National Institutes of Health's consensus criteria for chronic GVHD diagnosis in patients[17]. The chronic GVHD group displayed multiorgan pathophysiology consistent with chronic GVHD (Figure 2 A-B). Lung histology showed peribronchiolar infiltration and cuffling denoting the onset of obliteration of the bronchioles (Figure 2 A). Many animals displayed distal pathology in the

lungs, including protein exudation, macrophage infiltration, and the start of tissue remodeling (supplemental Figure 1). Lung pathology scores were significantly higher in the chronic GVHD group than in BMT controls (Figure 2 B). In the liver, perivascular infiltration was observed surrounding the bile duct and extending into the parenchyma (Figure 2 A), which resulted in a significant increase in the pathology score in the chronic GVHD versus the BMT control animals (Figure 2 B). Mice with higher pathology scores also had necrotic foci of cells in the parenchyma proper. Because patients with chronic GVHD may also have oral mucosal involvement, histopathology of the tongue and salivary glands was examined. Areas of infiltration, inflammation, and abscess formation were observed on the tongue near the taste receptors (Figure 2 A). The pathology score was significantly higher, albeit modest in magnitude, in the chronic GVHD group than in the BMT-only controls (Figure 2 B). Salivary glands displayed perivascular infiltration; however, this infiltration was also seen in the BMT controls, which suggests changes resulting from the conditioning (Figure 2A).

The thymus, known to be involved in human chronic GVHD[13], displayed necrotic foci and destruction of stromal matrix, which resulted in a significantly higher chronic GVHD pathology score. The spleen had abnormal architecture similar to the thymus, albeit only modest differences were seen in the pathology score. The colon displayed moderate pathology in the chronic GVHD cohorts, although it was not as extensive or invasive as in acute GVHD models. The ileum displayed the mild pathology seen in both the chronic GVHD and the BMT group, which suggests the role of pretransplantation conditioning.

Chronic GVHD has been characterized as a fibroproliferative disease, and therefore, collagen levels were quantified by trichrome staining. The lung and liver (Figure 2 C-D) both displayed a significant increase in collagen deposition around bronchioles and blood vessels. The organization of the collagen surrounding the bronchioles and blood vessels is highlighted and demonstrates that the increase in collagen was localized to specific structures and not uniformly distributed throughout the lungs and liver (Figure 2C). Fibrosis patterns in tongue and salivary glands were somewhat more variable between individual mice within a group, and trichrome staining was not increased significantly compared with the BMT controls (data not shown).

Overall, Cy/TBI conditioning followed by the transfer of a low-splenocyte infusion reproduced the pathology of chronic GVHD. It was distinguished from acute GVHD by the absence of significant weight loss early and overall mild losses later after transplantation, BO, involvement of the oral mucosa, and fibrosis in chronic GVHD target organs. Although pathology and fibrosis in the lung have been observed previously[36], documented reports of pathology in the other organs have not been evaluated.

$CD4^+$ T-cell and B-cell infiltration and alloantibody deposition in chronic GVHD target organs

We sought to determine the potential etiopathogenic mechanisms associated with chronic GVHD. We focused on the lung and liver as the two most severely affected chronic GVHD organs denoted by obstructive PFTs and the presence of fibrosis. $CD4^+$ T-cell infiltration was observed in peribronchiolar

areas in the chronic GVHD group but not in BMT-only controls (Figure 3A). The liver displayed substantial infiltration in the perivascular areas (Figure 3A) and, for some recipients, into the parenchyma (not shown). Because of the degree of lung inflation influencing the distribution of cells, percentages of lymphocytes were quantified in the lung versus the total number. The number of $CD4^+$ T cells in the lung (Figure 3B) and the liver (Figure 3C) was significantly higher in the chronic GVHD group than in the BMT-only control group, consistent with other models in which $CD4^+$ T cells could be found in chronic GVHD organs[33]. There was only minimal infiltration of $CD8^+$ T cells in both groups (data not shown). $B220^+$ B-cell infiltration in the lung and liver (Figure 3D) was seen in a pattern similar to that of $CD4^+$ T cells. A significant increase in total $B220^+$ B cells in the lung and liver was seen in the chronic GVHD group compared with the BMT controls (Figures 3E and 3 F, respectively). Salivary glands and the tongue had only minimal $B220^+$ B-cell infiltration (data not shown). Taken together, the pathology in the lung and liver was associated with $CD4^+$ T-cell and B-cell infiltration. We hypothesized that B cell–secreted antibodies might play a role in chronic GVHD pathology and determined whether antibody deposition could be observed in chronic GVHD organs on day 60 after transplantation. The lung and liver had deposits of mouse Ig within surrounding areas of infiltration and pathologic effects (Figure 4A). There were peribronchiolar deposits and perivascular deposits in both organs. Quantification of Ig deposition in the lung and liver (Figure 4B) revealed higher levels in the chronic GVHD group than in

the BMT controls. The predominant Ig type was IgG2c in the lung and liver (supplemental Figure 3 and data not shown).

To determine whether circulating anti-host tissue-reactive antibodies were present, sera from transplanted animals were incubated with tissues from a naive B10.BR mouse and then probed with fluorochrome-labeled anti-mouse Ig (Figure 4 C). Fluorescence was evident in the perivascular areas in lung and liver and in the peribronchiolar area in lung. These results indicate that circulating host tissue-reactive antibodies may contribute to chronic GVHD pathology.

chronic GVHD pathogenesis requires the production and secretion of anti-host reactive antibodies

To further test our hypothesis that B cells and secreted alloantibodies play a causative role in establishment of chronic GVHD, we used donor μMT mice that do not have membrane-bound IgM and are deficient in mature B cells (Figure 5). To limit the contribution of donor B cells and avoid any issues related to defective regulatory T-cell dysfunction reported in μMT mice, Cy/TBI-conditioned recipients received WT or μMT BM with or without supplemental WT T cells (0.33×10^6). Recipients of WT BM plus supplemental WT T cells versus low-dose splenocytes had comparable survival and weight and had significant increases in resistance and elastance, with a lowering of compliance that was characteristic of BO. When recipients of B cell–deficient BM and WT T cells were compared with mice with chronic GVHD that received WT BM with WT T cells, PFTs demonstrated lower resistance, elastance, and higher compliance (Figure

5A). Control recipients of WT compared with μMT BM had comparable parameters. Recipients of B cell–deficient BM with WT T cells had resistance and elastance comparable to that of recipients of B cell–deficient BM without supplemental T cells. Thus, donor allogeneic T cells and BM-derived mature B cells are required for BO generation. In contrast to recipients of WT BM plus T cells versus BM alone, there were no significant differences in the histopathology scores of lung and liver between mice given μMT BM plus T cells and those given WT BM (supplemental Figure 4). Of note, although lymphocyte infiltration and inflammation were observed in recipients of μMT BM and T cells, there was no destruction of the bronchioles or bile ducts, and the degree of fibrosis mirrored the extent of pathologic injury (Figure 5B). The somewhat higher amounts of fibrosis in recipients of μMT BM with or without WT T cells may be due to the known Treg defect in μMT mice[47], which then could have failed to control the inflammatory response in the lung and liver in chronic GVHD mice, offsetting in part the effect of B-cell deficiency. Moreover, Ig was not deposited in the lung or liver of mice that received μMT BM and T cells (Figure 5C), findings that correlated with results of PFTs.

We cannot exclude the possibility that antibody deposition is a bystander in the disease process and that the critical pathogenic mechanism is the APC function rather than Ig capacity of activated B cells. To distinguish between these two fundamental mechanisms, we used (m+s)IgMxJhD BALB/c donors. These mice are capable of generating membrane-bound IgM and secreting IgM, but they produce and secrete ≥ 100-fold less antigen-specific IgG than similarly

immunized WT controls[48]. They also do not appear to have a regulatory T-cell defect like the μMT mice (supplemental Figure 5). Recipients were given WT BM or transgenic BM alone or with WT splenocytes. Day 60 PFTs in conditioned B10.BR recipients of (m+s)IgMxJhD BM and WT splenocytes had significantly lower lung resistance and elastance and higher compliance than recipients of WT BM with splenocytes (Figure 6 A). These data indicate that the lack of IgG alloantibody secretion by donor BM-derived B cells precluded the pulmonary dysfunction associated with BO. This was confirmed by staining tissues for total Ig in the lung and liver (Figure 6 D). Mice given (m+s)IgMxJhD BM only and mice given (m+s)IgMxJhD BM with splenocytes both had decreased deposition of Ig surrounding bronchioles and bile ducts compared with mice transplanted with WT BM and splenocytes. Collagen deposition was significantly reduced in mice that received (m+s)IgMxJhD BM with splenocytes compared with the WT BM plus splenocytes (Figure 6 B). However, infiltrating $CD4^+$ cells were still observed in the lung and liver of both mice given WT BM and splenocytes and those given (m+s)IgMxJhD BM and splenocytes (Figure 6 C). These data suggest that inflammation is not regulated by Ig deposition per se, and therefore, other mechanisms (chemokines) are not affected by Ig deposition. The pathogenicity of Ig deposition in adversely affecting PFTs may not be the result of changes in inflammation but rather in situ injury from complement binding to deposited alloantibody or the Ig-facilitated activation of inflammatory or resident cells in situ.

Blockade of GC formation is sufficient to prevent BO and hence chronic GVHD generation

Because BM-derived B-cell production and secretion of anti-host reactive antibody appear to be critical for chronic GVHD generation, we sought to prevent antibody production by interrupting GC formation. GCs are sites where mature B cells rapidly proliferate, differentiate, and undergo somatic hypermutation that results in the production of class-switched antibody. LTβ, produced by T and B cells, and LTβR signaling are required for proper establishment of the follicular DC network and the organizational network of functional GCs in lymphoid tissues. Given the role of LTβR signaling and our finding that the dominant Ig isotype deposited in chronic GVHD target organs was IgG2c, we sought to determine whether disruption of LT-LTβR signaling by infusion of a known blocking reagent, mouse LTβR-Ig fusion protein, would reduce chronic GVHD pathology. Recipients were treated with LTβR-Ig or control fusion protein from days 28-52 after transplantation (Figure 7). Treatment began on day 28 because of decreases in PFTs (Figure 1 D) and increased GC size and frequency (supplemental Figure 8), which indicated early initiation of chronic GVHD. To determine the effect of LTβR-Ig on GC formation in chronic GVHD versus BM recipients, spleens were analyzed by immunofluorescence (Figure 7 A); peanut agglutinin and IgM staining detects GC B cells, whereas VCAM-1 stains follicular DCs. Untreated and control mAb-treated mice with chronic GVHD pathology displayed prominent GC structures with a well-organized follicular DC network, which signifies a robust GC reaction. Mice treated with LTβR-Ig showed

disrupted GC structures with an ill-formed follicular DC network. A decrease in size and frequency of GC was seen in LTβR-Ig–treated mice (Figure 7 B-C).

Consistent with the finding that disruption of GC formation would diminish BO and chronic GVHD generation, day 60 PFTs in the chronic GVHD cohorts indicated that LTβR-Ig–treated but not control protein-treated recipients displayed lower resistance and elastance and higher compliance (Figure 7 D). Both liver and pulmonary fibrosis was reduced by LTβR-Ig (Figure 7 E). Thus, LTβR-Ig treatment given after transplantation ameliorated the development of BO and chronic GVHD. The pathologic scores showed that mean lung scores of mice given BM plus splenocytes plus MOPC21 were ~5-fold higher than those that received BM plus splenocytes plus LTβR-Ig (supplemental Figure 7), although these differences did not reach statistical significance. For the liver, recipients given BM with splenocytes treated with MOPC21 had a reduction in mean scores compared with those given BM plus splenocytes and no Ig control, thereby making it difficult to assess the extent to which LTβR-Ig was superior to MOPC21. However, we can state that recipients of BM plus splenocytes had higher scores than those of mice BM with splenocytes and treated with LTβR-Ig, indicating that the LTβR-Ig did indeed reduce the severity of pathological injury. These data are supportive of our findings that LTβR-Ig reduces chronic GVHD as measured by PFTs, fibrosis, Ig deposition, and GC formation, all of which showed a marked reduction in BO and chronic GVHD manifestations.

To test our hypothesis that LTβR-Ig treatment works by inhibiting antibody secretion by class-switched B cells, we assayed for the presence of host tissue–

reactive antibodies in the sera of transplanted animals using a serum-binding assay. Compared with control mAb–treated recipients, sera from mice that were treated with LTβR-Ig had reduced fluorescence in the peribronchiolar area of the lung and perivascular area of the liver (Figure 7 F), which indicates that LTβR-Ig but not control protein leads to a decrease in the production of anti-host reactive antibody, consistent with the improvement in PFTs.

These results suggest that B cells, via their antibody secretory capability, contribute to pulmonary dysfunction and liver pathology in animals that have chronic GVHD after transplantation, and interventional strategies that inhibit pathways involved in B-cell function and antibody secretion may be useful in the prevention or treatment of chronic GVHD.

Discussion

We report that Cy/TBI-conditioned allogeneic recipients given low splenocyte or T-cell doses developed multiorgan system pathology with fibrosis and BO pathognomonic of chronic GVHD of the lung. chronic GVHD development was associated with IgG2c deposition in the lung and liver and IgG2b in the liver, which was abrogated if the donor BM was deficient in mature B cells or incapable of producing anti-host reactive IgG. Robust GC formation was seen in mice with chronic GVHD. By disrupting GC formation with LTβR-Ig, BO was reduced. Together, these data indicate that GC formation and IgG secretion by donor BM-derived mature B cells are necessary for chronic GVHD pathology.

The use of Cy, which exacerbates TBI-induced glutathione redox reactions in the lung[49], along with sublethal doses of donor T cells (to avoid acute GVHD) favored the generation of chronic GVHD. The histologic changes in this model were similar to the findings in human chronic GVHD[28]. The lungs showed peribronchiolar and perivascular cuffing and infiltration of the airway epithelium. The pathology appeared predominantly bronchiolar, with some alveolar involvement. Completely occluded bronchioles are observed in 20% of the animals in this model[36]. The pattern of inflammation along with increased collagen deposition surrounding nonobliterated bronchioles was similar to the pathology that defines occluded bronchioles in humans[50]. The liver had inflammation and lymphocytic infiltration, along with collagen deposition in the vascular epithelium and around the bile ducts and apoptotic foci in the parenchyma. Salivary gland pathology is an important clinical manifestation of chronic GVHD; patients suffer from xerostomia, histopathologic analysis shows mononuclear infiltration and fibrosis[51, 52], and salivary gland injury is a known finding in a minor mismatch mouse model of chronic GVHD[53]. The parotid and submandibular salivary glands displayed lymphocytic infiltrates in both the BM and chronic GVHD groups, likely because of transplantation conditioning. In the tongue, there was a quantifiable difference in the histology; however, the extent of inflammation and infiltration was mild to moderate and isolated to small regions of the epithelium. Similar profiles of fibrosis were seen in the tongue and salivary glands for both control and chronic GVHD groups, which suggests that the oral mucosa did not manifest chronic GVHD or that the kinetics were delayed

compared with the liver and lung. The absence of any inflammatory or fibrotic changes in the skin differs from some other models in which the predominant feature is scleroderma (reviewed in Sarantopoulos et al[19]). This systemic histologic profile reinforces the observation that in mice, as in humans, the pathologic manifestations of chronic GVHD are heterogeneous.

The role of $CD4^+$ T cells in both acute GVHD and chronic GVHD has been well chronicled. We also observed the presence of $CD4^+$ T cells in the zones of inflammation in both lung and liver of affected animals. A significantly higher number of $B220^+$ B cells were found clustered with the $CD4^+$ T cells, which sets up a situation in which $CD4^+$ T-cell help for B-cell alloantibody production might occur in situ in chronic GVHD target organs. Although donor $CD8^+$ T-cell involvement has been reported to play a causative role in airway obliteration after BMT[50], we did not observe a higher incidence of $CD8^+$ T cells in the inflamed and affected regions of the lungs or livers (data not shown). We detected antibody deposition in the target areas of lung and liver, which confirms the involvement of B cells. Examining sera from these animals, we detected the presence of lung and liver tissue–specific antibodies. Further characterization is required to identify whether these antibodies are donor-versus-host alloreactive or autoreactive because of a breakdown in the tolerance processes after BMT. Thus, it appears that the tissue modifications and fibrosis stem from a coordinated $CD4^+$ T-cell and B-cell response.

Alleviation of physiologic and histologic symptoms in animals that received B cell–deficient BM compared with WT BM confirms the requirement of B cells

for lung dysfunction and inflammation and fibrosis in the lung and liver. These animals displayed a less restrictive pulmonary physiology and a lower incidence of occluded and fibrotic airways, which signifies healthier lungs. The liver displayed less intensive inflammation and fibrosis, consistent with a study that reported attenuated liver fibrosis after toxin injury in B cell–deficient mice[54]. The use of (m+s)IgMxJhD mice that can only secrete IgM and not IgG2[48] as donors excluded the capacity of donor B cells to facilitate chronic GVHD manifestations because of enhanced pathogenic antibody production as a product of class switching and affinity maturation. B cells and follicular DCs have intact APC function, although the B-cell receptor repertoire is restricted because of the use of a fixed IgM-Vh region[55]. On day 60 after transplantation, the lung physiology showed a significantly healthy phenotype compared with the chronic GVHD group. The lack of secreted antibody other than IgM alleviated the functional consequences of chronic GVHD in the lung. These data indicate that either IgG secretion is necessary for pathogenicity or a full B-cell receptor repertoire is required to promote disease. The repertoire in turn could control the quality and specificity of the alloreactive antibodies secreted, as well as any required APC function of specific B cells for pathogenic $CD4^+$ T cells. Further work will be required to dissect these two related possibilities.

Given a role for IgG antibodies, we propose that alloantibody binding to chronic GVHD organs could enable tissue destruction and modifications via donor cell–mediated antibody-dependent cellular cytotoxicity or antibody-dependent phagocytosis. Alternatively, the pathology could be defined by the

specific function of these secreted antibodies. For example, elevated titers of anti-PDGFR antibody have been detected in sera of patients with extensive chronic GVHD[22]. This antibody has been implicated in a signal transduction pathway that ultimately leads to the induction of type 1 collagen production and fibrosis[29]. Pathogenic antibody production, therefore, is likely to be an important inducer of chronic GVHD, and targeting this specific function of the B cells is an attractive strategy to prevent or treat early manifestations of chronic GVHD. Treatment of chronic GVHD with the anti-CD20, B cell–depleting antibody rituximab ameliorates some manifestations of chronic GVHD, but it rarely results in complete remission of chronic GVHD[29]. In studies using mice and monkeys, it has been shown that rituximab treatment is more successful in removal of B cells from the blood than from spleen and lymph nodes[56, 57]. GC B cells display lower susceptibility to rituximab-mediated clearance, probably because they reside in a nonoptimal environment for antibody-based depletion[41]. Our observation that GC B cells are critical to the development of chronic GVHD suggests that agents that are more effective at disrupting the GC might be more useful clinically. We are unaware of the use of rituximab in a systemic fashion to determine the effects on BO in chronic GVHD patients. Such studies would require patients with the same duration of onset and severity of BO. To the best of our knowledge, the relative number and frequency of infiltrated B cells have not been evaluated in the secondary lymphoid organs of patients with chronic GVHD, although high GC formation could occur because of increased BAFF levels[58]. GCs are specialized regions found in secondary lymphoid organs in which activated B cells undergo

diversification and affinity maturation that result in differentiation into both memory B cells and long-lived plasma cells that produce high-affinity, antigen-specific, class-switched antibodies. GCs are required for a sustained humoral immune reaction to alloreactive antigens but also could result in the production of autoreactive antibodies and a dysregulated autoimmune response, which might be relevant in patients who have chronic GVHD symptoms[59]. Follicular B cells express LT-αβ, whereas follicular DCs express LTβR. One of the important consequences of the LT-LTβR interaction between these cells is the proper positioning of GC B cells and establishment of GC architecture. LT-LTβR signaling also enhances the follicular DC–B cell interactions by up-regulating expression of adhesion factors such as VCAM-1 on the follicular DCs. Inhibition of this interaction by use of the LTβR-Ig fusion protein prevents GC formation[60]. Treatment with LTβR-Ig had a direct effect on the symptoms of chronic GVHD, at least in part by blocking GC formation. These effects included an alleviation of pulmonary dysfunction. There was also a decrease in tissue-specific Ig levels in the sera. This confirms that inhibition of antibody secretion from post-GC B cells and plasmablasts elicits a positive response in animals that have pulmonary GVHD. The presence of IgG2c deposits in lung and liver further supports the notion that successful GC reactions that result in class switching are an important parameter in establishing lung and liver pathology. The fusion protein could work as a potential therapeutic agent for GVHD by causing a breakdown in GC architecture, resultant antibody production, and conversion of B cells into memory cells and plasmablasts.

LTβR-Ig blocks both LTαβ and LIGHT, which is expressed on activated T cells and on B cells[60]. LIGHT has been demonstrated to have a role in the fibrosis, smooth muscle hyperplasia, and airway hyperresponsiveness associated with two murine models of chronic asthma. Pharmacologic inhibition of LIGHT resulted in better lung function, and this was linked to the reduced production of TGF-β and IL-13, cytokines involved in airway remodeling after injury[61]. The efficacy of LTβR-Ig as a chronic GVHD interventional strategy may be the result of multiple mechanisms of action, including disruption of GCs and antibody production.

In summary, we have observed a requirement for B cells in development of chronic GVHD symptoms in lung and liver in a myeloablative conditioning model of allogeneic HCST. B cells, presumably via pathogenic antibody secretion by products of the GC reaction, including long-lived antibody-forming cells, play a causal role in modulating the physiology of the lung and pulmonary dysfunction. Our studies have therefore identified important immunologic processes that are involved in chronic GVHD and indicate that LTβR-Ig could be a potential clinical interventional strategy for prevention and therapy of chronic GVHD.

Materials and Methods

Mice

C57Bl/6 ($H2^b$) mice were purchased from the National Cancer Institute. B10.BR ($H2^k$), BALB/c ($H2^d$), and B6.129S2-Igh-6tm1Cgn/J mice on a C57Bl/6

background (referred to as μMT mice) were purchased from The Jackson Laboratory. BALB/c (m+s)IgMxJhD transgenic mice were bred at the University of Minnesota animal facility. Mice were housed in a specific pathogen-free facility and used with the approval of the University of Minnesota's institutional animal care committee.

BM transplantation

B10.BR recipients were conditioned with Cy on days −3 and −2 (120 mg · kg^{-1} · d^{-1} intraperitoneally). On day −1, recipients received TBI by x-ray (7.5 Gy). Donor BM was T-cell depleted with anti-Thy1.2 mAb followed by rabbit complement. T cells were purified from lymph nodes by incubation with phycoerythrin-labeled anti-CD19 (eBioscience), followed by anti-PE beads and depletion with a magnetic column (Miltenyi Biotec). On day 0, recipients received 10 × 10^6 BM cells with or without allogeneic splenocytes (0.75-1 × 10^6) or purified T cells (0.33 × 10^6), as indicated. Weights of individual mice were recorded twice weekly. Where indicated, recipients in chronic GVHD groups were given murine LTβR-Ig or control murine MOPC21 provided by Biogen Idec at 200 μg per dose intraperitoneally every 3 days from days 28-52.

Pulmonary function tests

Anesthetized mice were weighed, and lung function was assessed by whole-body plethysmography with the Flexivent system (SCIREQ) and analyzed with Flexivent Version 5.1 software.

Frozen tissue preparation

All organs harvested were embedded in optimal cutting temperature compound, snap-frozen in liquid nitrogen, and stored at −80°. Lungs were inflated by infusion of 1 mL of optimal cutting temperature compound:PBS (3:1) intratracheally before harvest.

Histology and trichrome staining

Six-micrometer cryosections were fixed for 5 minutes in acetone and stained with H&E to determine pathology and with a Masson trichrome staining kit (Sigma-Aldrich) for detection of collagen deposition. Histopathology scores were assigned as described previously. Collagen deposition was quantified on trichrome-stained sections as a ratio of area of blue staining to area of total staining by use of the Adobe Photoshop CS3 analysis tool.

Immunohistochemistry

Acetone-fixed 6-μm cryosections were immunoperoxidase stained with biotinylated mAbs for CD4, CD8, and B220 (BD Pharmingen). Stained sections were examined under 200× magnification, and images were captured with an Olympus BX51 microscope. Antibody-binding–positive cells were quantified by counting a 100-mm^2 area for liver or obtaining a ratio of positive to total cells in a 100-mm^2 area for lung.

Immunofluorescence

For Ig deposition, 6-μm cryosections were fixed with acetone, blocked with horse serum, and stained with either FITC-labeled anti–mouse Ig (BD Pharmingen) or goat anti–mouse IgM, goat anti–mouse IgG1, goat anti–mouse IgG2b, goat anti–mouse IgG2c, or goat anti–mouse IgG3, followed by FITC-labeled donkey anti–goat Ig (Jackson ImmunoResearch). For detection of tissue-specific serum antibodies, fixed cryosections of organs from a naive B10.BR mouse were incubated with sera from the BM-transplanted (BMT) recipients. Sections were incubated with FITC-labeled anti–mouse Ig. Confocal images were acquired on an Olympus FluoView500 confocal laser scanning microscope at 200× magnification, analyzed with FluoView 3.2 software (Olympus), and processed with Adobe Photoshop CS3 Version 9.0.2. Antibody deposition was quantified by scoring sections by use of a scale from 1-3.

GC detection

Fixed 6-μm spleen cryosections were stained with rat anti–mouse VCAM1 followed by Cy3-labeled goat anti–rat, FITC-labeled rat anti–mouse IgM, and biotinylated peanut agglutinin (Vector Laboratories), followed by streptavidin Cy5. Confocal images were obtained as described in “Immunofluorescence.”

Statistical analysis

Survival data were analyzed by life-table methods, and actuarial survival rates are shown. Group comparisons were made by log-rank test statistics. Group

comparisons of cell counts and flow cytometry data were analyzed by Student *t* test.

Figure Legends

Figure 1: Allogeneic transfer of BM and low concentrations of splenic cells in hosts treated with Cy/TBI-caused chronic GVHD and BO. B10.BR mice treated with 120 mg · kg−1 · d−1 Cy (day −3, −2) and lethally irradiated (day −1) were transplanted with BM alone or BM plus 0.75-1 × 106 splenocytes from C57Bl/6 mice. n = 10 mice/group. Weights of the animals (A) and survival (B) were tracked up to 60 days after transplantation. PFTs were performed on anesthetized animals at day 60 (C) and day 28 (D) after transplantation. Animals were artificially ventilated, and resistance, elastance, and compliance were measured as parameters of distress in lung function in animals receiving low-dose splenocytes or T cells. Representative data from 3 individual experiments. **P < .01.

Figure 2: Multiorgan disease in mice with chronic GVHD; immune infiltration and collagen deposition.(A) Tissues (lung, liver, tongue, salivary glands [SG], thymus, spleen, ileum, and colon) were harvested at day 60 after transplantation and stained with H&E to determine pathology. Bright-field images were captured at 100× magnification with an Olympus BX51 microscope. (B) Inflammation, immune infiltration, and parenchymal changes were scored with a cumulative scoring system. (C) Collagen deposition was determined with a Masson trichrome staining kit; blue indicates collagen deposition. (D) Collagen deposition was quantified as a ratio of blue area to total area of tissue. Quantification was performed with the analysis tool in Photoshop CS3. Data from

2 individual experiments were pooled to obtain pathology scores; n = 12. *P < .05; **P < .01; ***P < .005.

Figure 3: $CD4^+$ T-cell and $B220^+$ B-cell infiltration is seen in lungs and livers of transplanted animals. Liver and lung tissues were harvested at day 60 after transplantation from animals receiving BM only and BM plus splenocytes (BM + spleen) and analyzed by immunohistochemistry and methyl blue counterstaining. Representative images from 3 individual experiments are shown for CD4 (A) and B220 (D). Images were captured with a bright-field microscope at 200× magnification. For lung, infiltration was quantified by obtaining a ratio of $CD4^+$ (B) or $B220^+$ (E) cells to total cells in a 100-mm^2 field of view under the microscope. Shown is an average of the count from 4 representative fields. For liver, CD4 (C) and B220 (F) cell infiltration was quantified by counting the number of antibody binding–positive cells and obtaining an average of counts from 4 representative fields. n = 6. *P < .05; **P < .01; ***P < .005.

Figure 4: Antibody deposition detected in target areas of lung and liver in diseased animals. Six-micrometer sections of frozen lung and liver tissues harvested at day 60 after transplantation were analyzed by immunofluorescence. Tissues were incubated with FITC-conjugated anti-mouse Ig. (A) Representative images for lung and liver from 3 individual experiments. n = 8. (B) Ig deposition was quantified on a 0-3 scale to determine the amount of antibody in the tissues. (C) Serum from animals given BM only and animals given BM plus splenocytes

was collected at day 60 after transplantation and incubated with healthy B10.BR lung and liver tissue followed by FITC-conjugated anti-mouse Ig to detect the presence of tissue-specific antibodies in the serum of diseased animals. White arrows depict areas of Ig deposition. Fluorescence was detected with an Olympus FluoView 500 confocal laser scanning microscope at a magnification of 200×.

Figure 5: Animals receiving B cell–deficient BM show a decrease in pathology. B10.BR recipients were transplanted with WT BM or BM from μMT knockout mice with or without WT T cells. (A) At 60 days after transplantation, mice were anesthetized and artificially ventilated to measure pulmonary function parameters. (B) Collagen deposition was quantified from trichrome-stained samples as a ratio of blue area to total area of tissue. Quantification was performed with the analysis tool in Photoshop CS3. (C) Lung and liver tissues were harvested, and 6-μm frozen sections were stained with FITC-conjugated anti–mouse Ig for antibody deposition within the tissues. White arrows denote areas of Ig deposition. Images shown are representative images of 3 individual experiments; n = 4. *P < .05; ***P < .005; P = .4066 for lung BM (μMT) only vs BM (μMT) + T cells; P = .2860 for liver BM (μMT) only vs BM (μMT) + T cells.

Figure 6: Secreted antibody is required for pulmonary dysfunction in animals with chronic GVHD. (A) B10.BR mice were transplanted with BM ± splenocytes from WT or (m+s)IgMxJhD BALB/c mice and anesthetized at day 60

after transplantation for PFTs. Resistance, compliance, and elastance were measured; n = 8. (B) Collagen deposition was quantified from trichrome-stained samples as a ratio of blue area to total area of tissue. Quantification was performed with the analysis tool in Photoshop CS3. (C) Infiltration of $CD4^+$ cells in the lung and liver of transplanted mice. (D) Lung and liver tissues were harvested, and 6-μm frozen sections were stained with FITC-conjugated anti-mouse Ig for antibody deposition within the tissues. White arrows denote areas of Ig deposition. Representative image from 2 independent experiments; n = 8. *P < .05; **P < .01; ***P < .005.

Figure 7: Disruption of GC formation by LTβR-Ig treatment reduces lung dysfunction and chronic GVHD organ tissue fibrosis. B10.BR recipients were transplanted as per Figure 1. A cohort of animals receiving BM + splenocytes were treated with 200 μg of murine LTβR-Ig or the control Ab, murine MOPC21, every 3 days beginning on day 28 after transplantation until day 52. (A) Spleen tissue harvested from these animals at day 60 was analyzed by immunofluorescence for GC structures. GCs were detected by colocalization of IgM (green), VCAM-1 (blue), and peanut agglutinin (red); merged images show overlap (white) to discriminate GC. White arrows highlight GC. Images were captures with an Olympus FluoView 500 confocal laser scanning microscope at 100× magnification; n = 5. (B) The size of the GC was quantified by measuring the area of peanut agglutinin staining in Photoshop C3. (C) Frequency of GCs was quantified by counting the number of GCs in 1 mm^2 of spleen section. (D) PFTs were performed on anesthetized animals on day 60 after transplantation to

measure lung function. (E) Animals treated with LTβR-Ig and MOPC21 were examined for fibrosis in the lung and liver. (F) Presence of deposited lung and liver tissue–specific antibodies in animals treated with LTβR-Ig and MOPC21 was determined by immunofluorescence by staining with FITC-conjugated anti–mouse Ig. White arrows depict Ig deposition. Images were captured at 200× magnification and are representative of 2 individual experiments; n = 5. *P < .05; **P < .01.

Supplemental Figure 1: Increased peripheral pulmonary pathology associated chronic GVHD. Representative image of three independent experiments, hematoxylin and eosin stained lung tissue from chronic GVHD group taken day 60 post transplant. * denotes protein exudation, closed arrow denotes macrophage infiltration. Image was captured at 200x magnification. Representative image from 3 experiments.

Supplemental Figure 2: sections of frozen lung and liver tissues harvested at day 28 after transplantation and stained with Hematoxylin and Eosin to determine pathology. Inflammation, immune infiltration and parenchymal changes were scored, using a cumulative scoring system used previously[26], n=4 per group. * *P<0.05, *** P<0.005.*

Supplemental Figure 3: Deposition of IgG2c in the lung of mice with chronic GVHD compared to BM only controls. 6um sections of frozen lung tissues harvested at day 60 after transplantation were analyzed by immunofluorescence. Tissues were incubated with either goat anti-mouse IgM,

IgG1, IgG2b, IgG2c or IgG3 and followed by donkey anti-goat Ig-FITC. White arrow denotes area of Ig deposition. Representative images for lung from two individual experiments are displayed.

Supplemental Figure 4 : Decreased μMT pathological scores. 6um sections of frozen lung and liver tissues harvested at day 60 after transplantation and stained with Hematoxylin and Eosin to determine pathology. Inflammation, immune infiltration and parenchymal changes were scored, using a cumulative scoring system used previously[26]. Representative scores n=5 per group. * *P<0.05*; p=0.3228 for lung BM (μMT) versus BM (μMT)+T cells; p=0.2893 for liver BM (μMT) versus BM (μMT)+T cells.

Supplemental Figure 5: Tregs from (m^+s)IgMxJhD Balb/c mice are able to suppress $CD4^+$ T cells at the same level as WT Balb/c Tregs. T cells from Thy1.1 Balb/c mice were labeled with CFSE and mixed with different proportions of $CD4^+$ $CD25^+$ T cells from either WT Balb/c (WT) or (m^+s)IgMxJhD (m^+s) with 0.25 mg/mL of anti-CD3 in complete DMEM. After 4 days, division of $CD4^+$ $Thy1.1^+$ cells was analyzed by dilution of CFSE on the BD LSRFortessa.

Supplemental Figure 6: Pathological scores of mice transplanted with (m^+s)IgMxJhD BM have elevated pathology scores compared to BM only. 6um sections of frozen lung and liver tissues harvested at day 60 after transplantation and stained with Hematoxylin and Eosin to determine pathology.

Inflammation, immune infiltration and parenchymal changes were scored, using a cumulative scoring system used previously[26]. Representative scores n=4 per group. * *P<0.05*; p=0.4881 for lung (m^+s)IgMxJhD BM only versus (m^+s)IgMxJhD BM+spleen; p=0.6704 for liver (m^+s)IgMxJhD BM only versus (m^+s)IgMxJhD BM+spleen.

Supplemental Figure 7: Pathological scores of mice treated with LTbR-Ig demonstrate infiltration in treated mice. 6um sections of frozen lung and liver tissues harvested at day 60 after transplantation and stained with Hematoxylin and Eosin to determine pathology. Inflammation, immune infiltration and parenchymal changes were scored, using a cumulative scoring system used previously[26]. Representative scores n=4 per group. * *P<0.05*; p=0.2029 for lung BM+spleen MOPC21 versus BM+spleen LTbR-Ig; p=0.5543 for liver BM+spleen MOPC21 versus BM+spleen LTbR-Ig.

Supplemental Figure 8: Increased Germinal Center size and frequency on Day 28 post transplantation. 6um sections of frozen lung and liver tissues harvested on day 28 after transplantation and stained with Biotin-PNA and FITC-IgM followed by SA-PE. The size of the GC was quantified by measuring the area of PNA staining in Photoshop C3. Frequency of the GC was quantified by counting the number of GCs in 1 mm^2 of spleen section, representative experiment n=4. * *P<0.05, *** P<0.005*

Figure 1

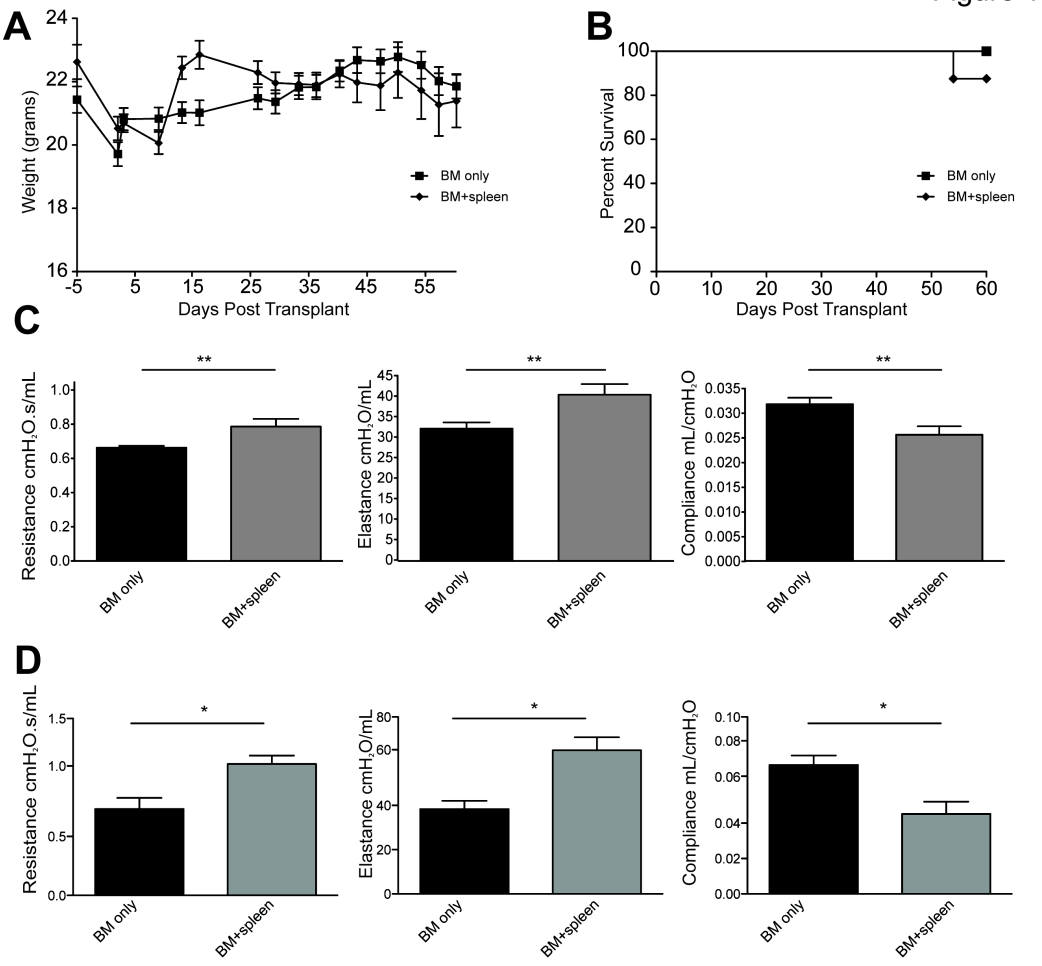
A
Weight (grams)
Days Post Transplant
BM only
BM+spleen
B
Percent Survival
Days Post Transplant
BM only
BM+spleen
C
Resistance cmH2O.s/mL
Elastance cmH2O/mL
Compliance mL/cmH2O
BM only
BM+spleen
D
Resistance cmH2O.s/mL
Elastance cmH2O/mL
Compliance mL/cmH2O
BM only
BM+spleen

Figure 2

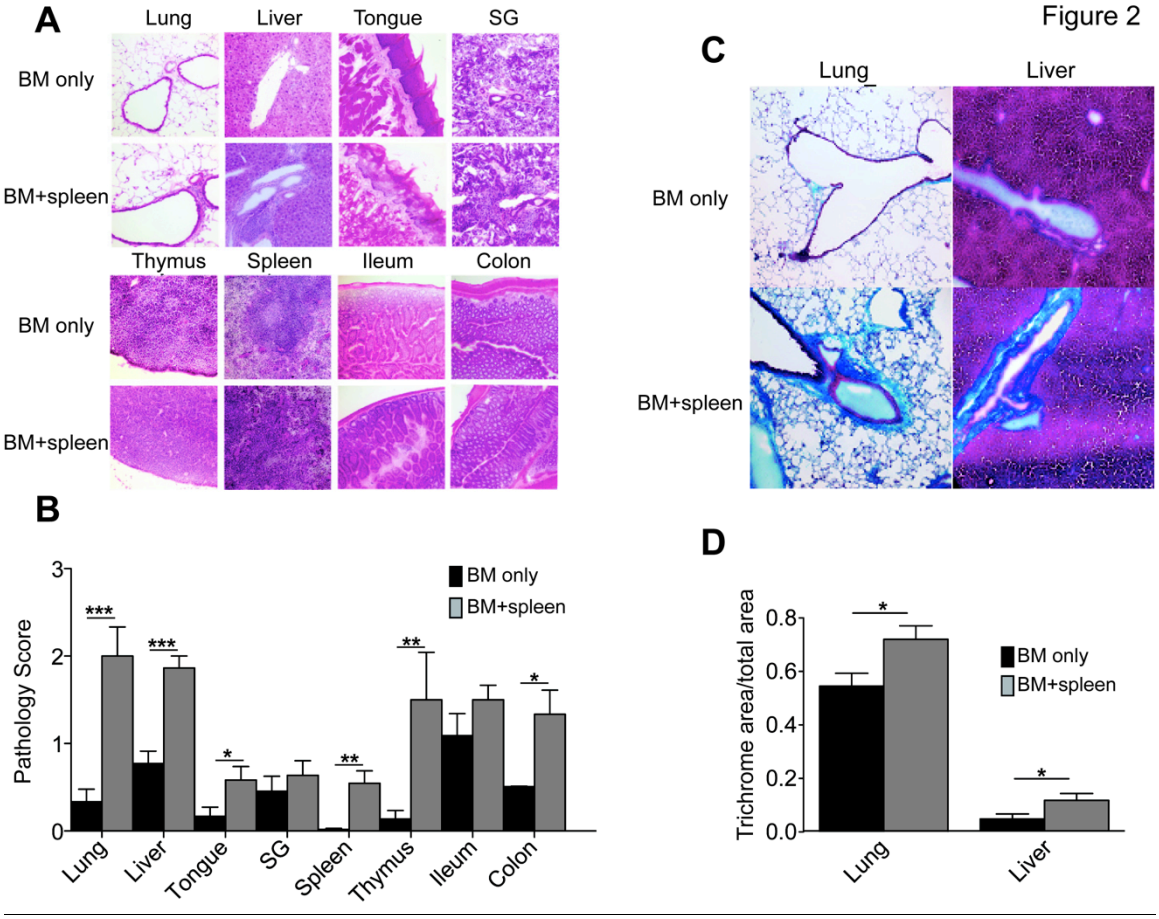
A
Lung
Liver
Tongue
SG
BM only
BM+spleen
Thymus
Spleen
Ileum
Colon
BM only
BM+spleen
C
Lung
Liver
BM only
BM+spleen
B
Pathology Score
BM only
BM+spleen
***
***
*
**
**
*
Lung
Liver
Tongue
SG
Spleen
Thymus
Ileum
Colon
D
Trichrome area/total area
BM only
BM+spleen
*
*
Lung
Liver

Figure 3

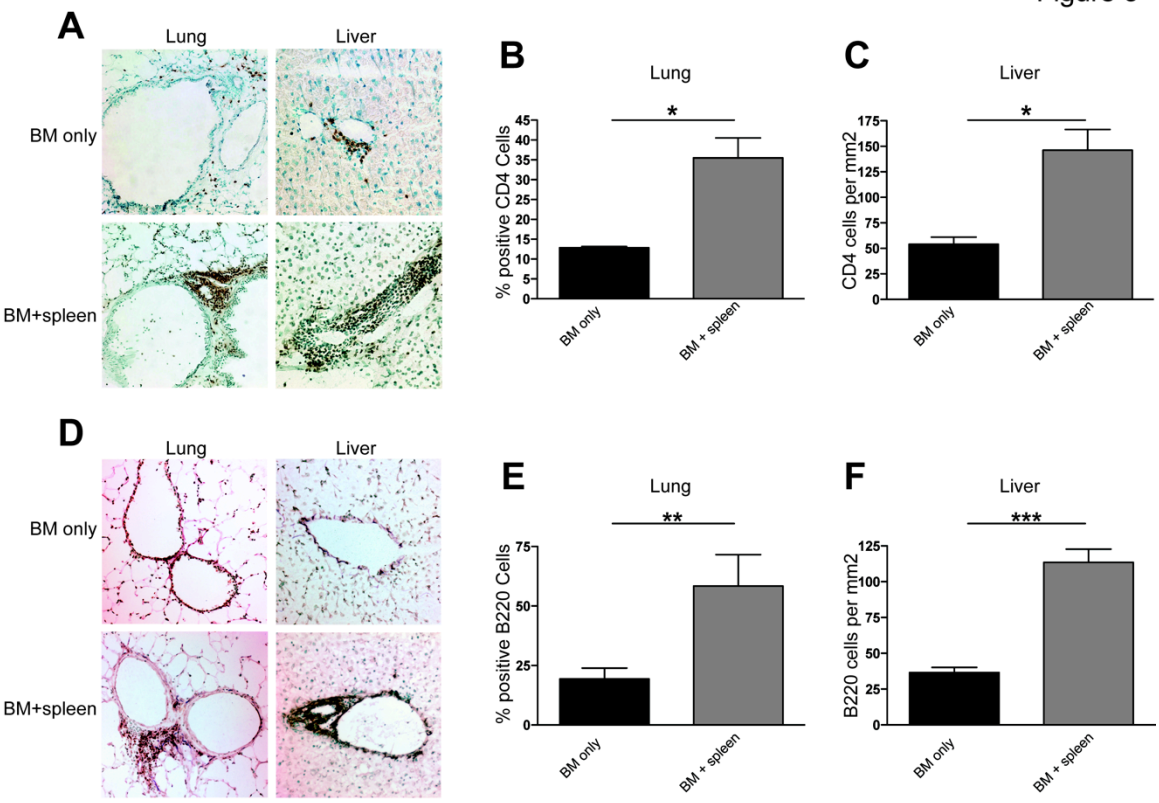
A
Lung
Liver
BM only
BM+spleen
B
Lung
*
% positive CD4 Cells
45
40
35
30
25
20
15
10
5
0
BM only
BM + spleen
C
Liver
*
CD4 cells per mm2
175
150
125
100
75
50
25
0
BM only
BM + spleen
D
Lung
Liver
BM only
BM+spleen
E
Lung
**
% positive B220 Cells
75
50
25
0
BM only
BM + spleen
F
Liver
***
B220 cells per mm2
125
100
75
50
25
0
BM only
BM + spleen

Figure 4

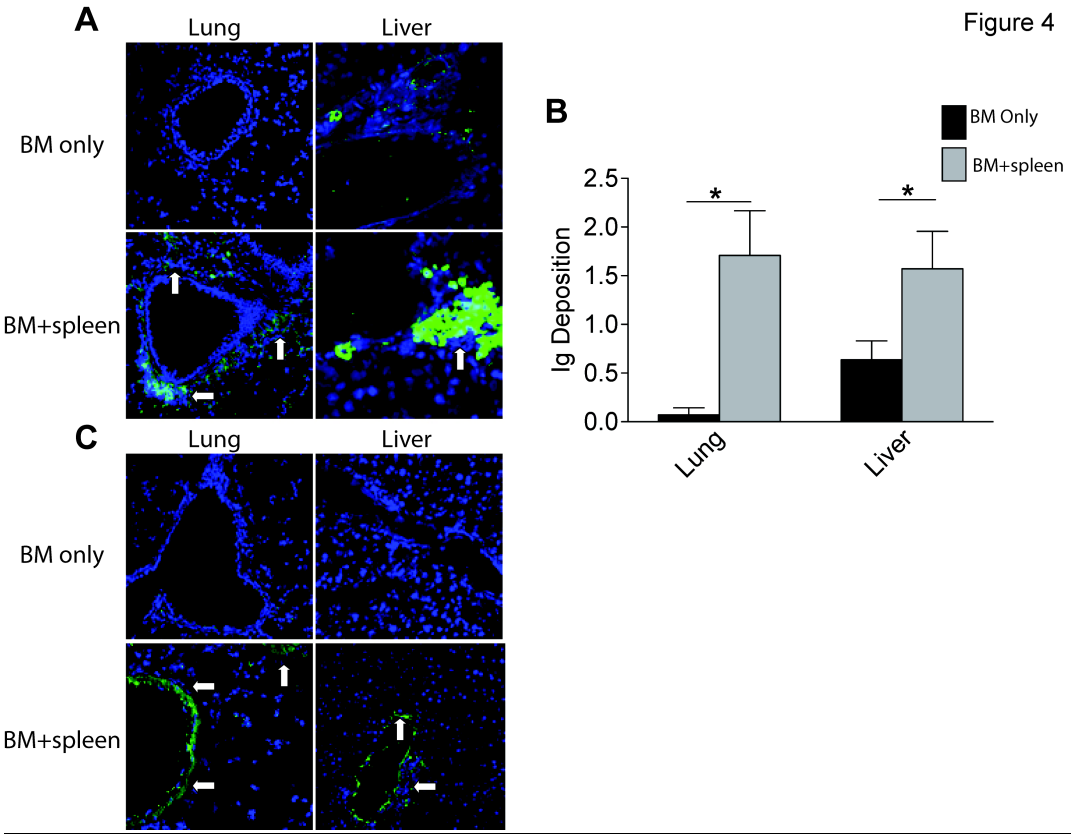
A
Lung
Liver
BM only
BM+spleen
C
Lung
Liver
BM only
BM+spleen
B
BM Only
BM+spleen
Ig Deposition
2.5
2.0
1.5
1.0
0.5
0.0
*
*
Lung
Liver

Figure 5

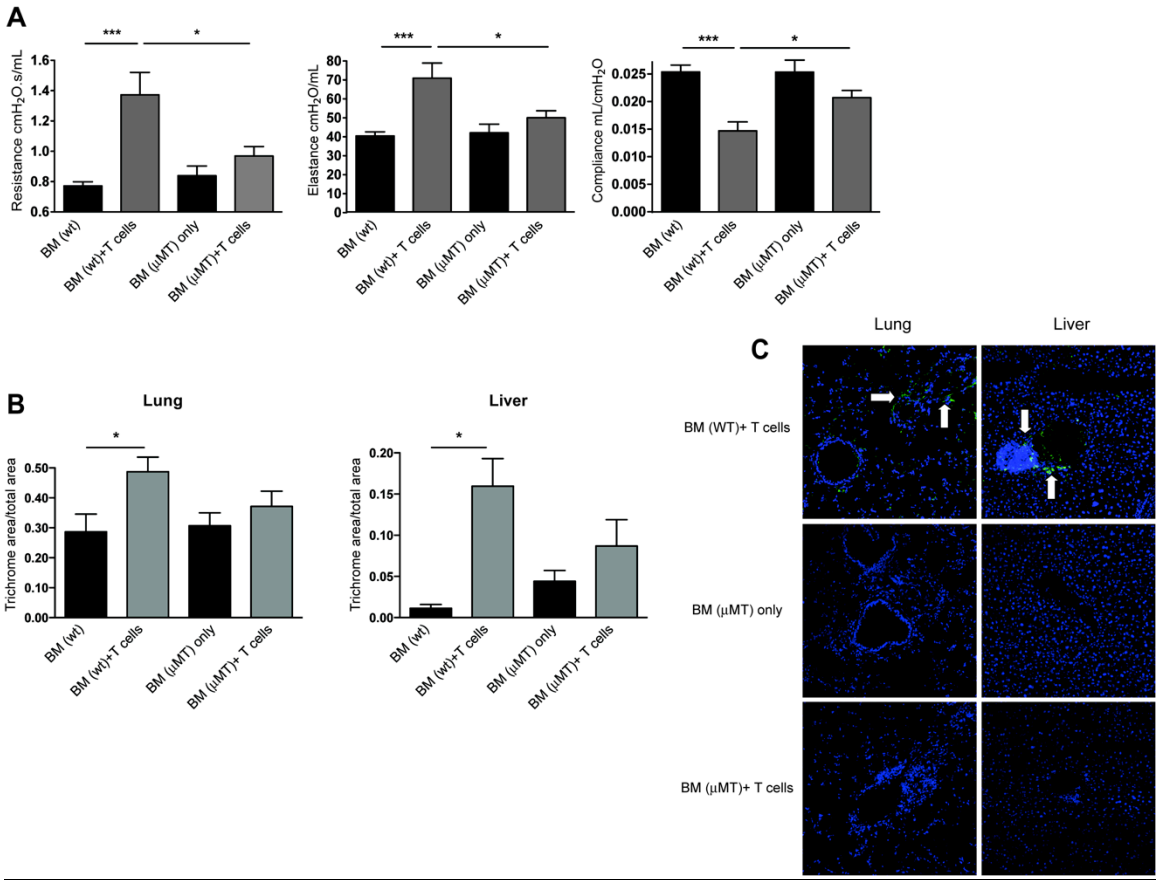
A
Resistance cmH2O s/mL
Elastance cmH2O/mL
Compliance mL/cmH2O
BM (wt)
BM (wt)+T cells
BM (µMT) only
BM (µMT)+T cells
B
Lung
Liver
Trichrome area/total area
C
Lung
Liver
BM (WT)+ T cells
BM (µMT) only
BM (µMT)+ T cells

Figure 6

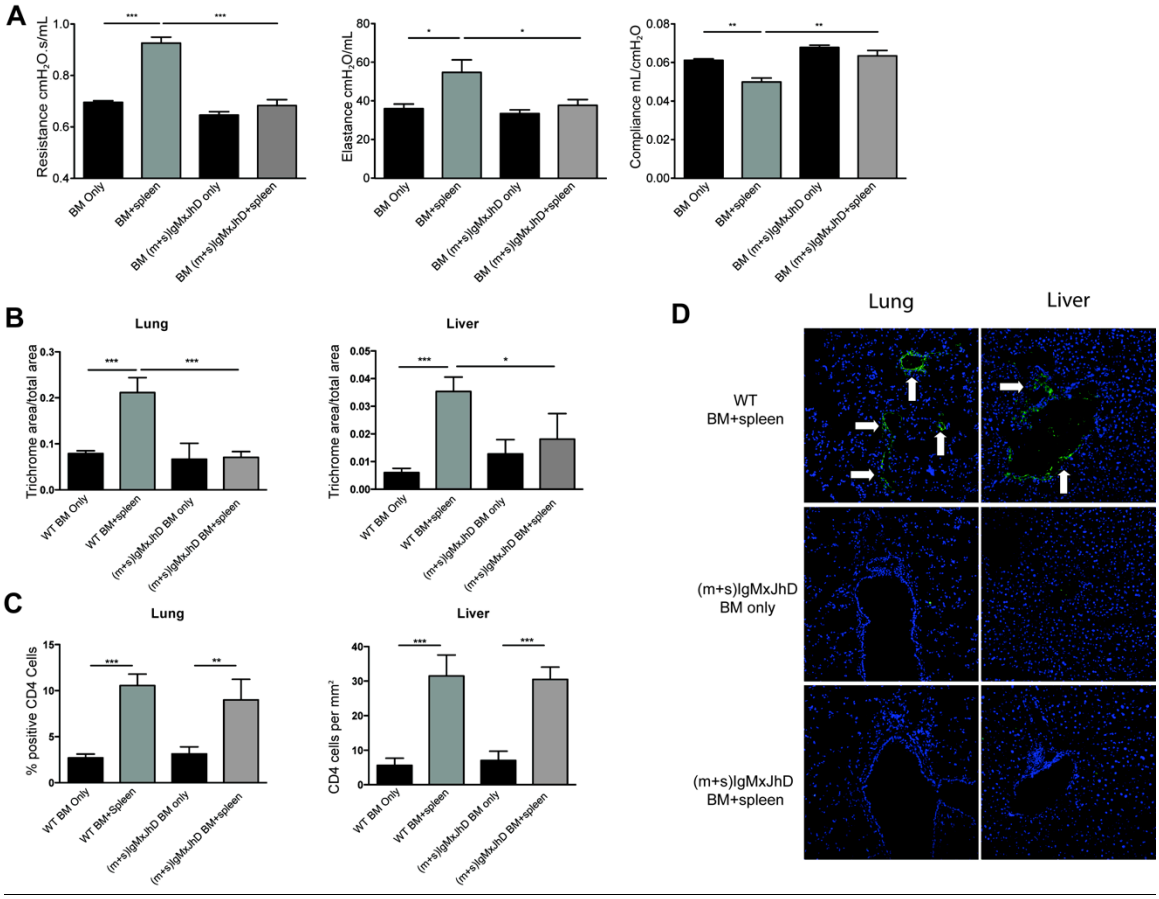
A
Resistance cmH2O s/mL
Elastance cmH2O/mL
Compliance mL/cmH2O
BM Only
BM+spleen
BM (m+s)IgMxJhD only
BM (m+s)IgMxJhD+spleen
B
Lung
Liver
Trichrome area/total area
WT BM Only
WT BM+spleen
(m+s)IgMxJhD BM only
(m+s)IgMxJhD BM+spleen
C
Lung
Liver
% positive CD4 Cells
CD4 cells per mm2
WT BM+Spleen
D
Lung
Liver
WT
BM+spleen
(m+s)IgMxJhD
BM only
(m+s)IgMxJhD
BM+spleen

Figure 7

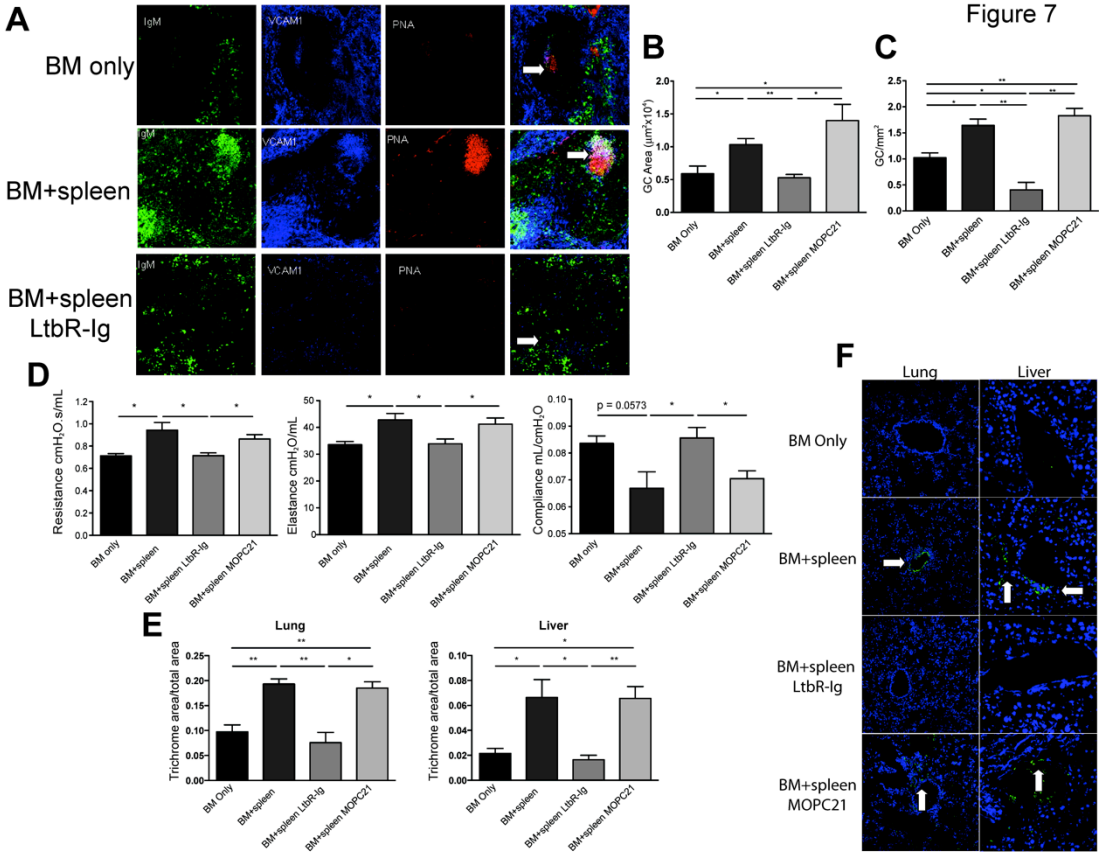
A
BM only
BM+spleen
BM+spleen LtbR-Ig
IgM
VCAM1
PNA
B
GC Area (μm²x10⁴)
C
GC/mm²
BM Only
BM+spleen
BM+spleen LtbR-Ig
BM+spleen MOPC21
D
Resistance cmH₂O.s/mL
Elastance cmH₂O/mL
Compliance mL/cmH₂O
p = 0.0573
E
Lung
Liver
Trichrome area/total area
F
Lung
Liver
BM Only
BM+spleen
BM+spleen LtbR-Ig
BM+spleen MOPC21

Supplemental Figure 1

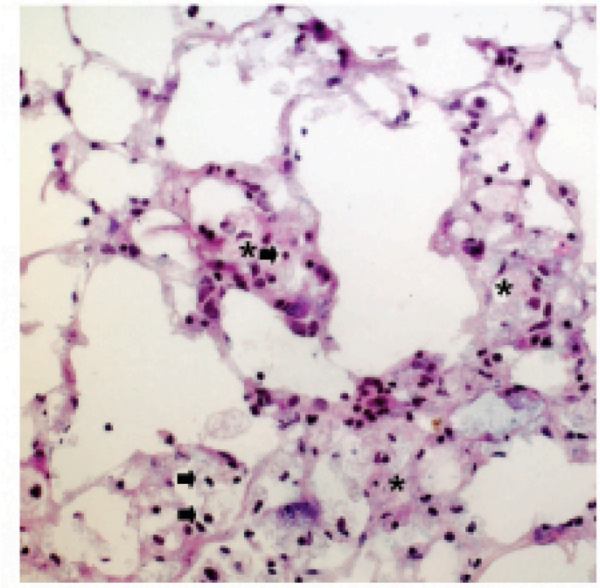

Supplemental Figure 2

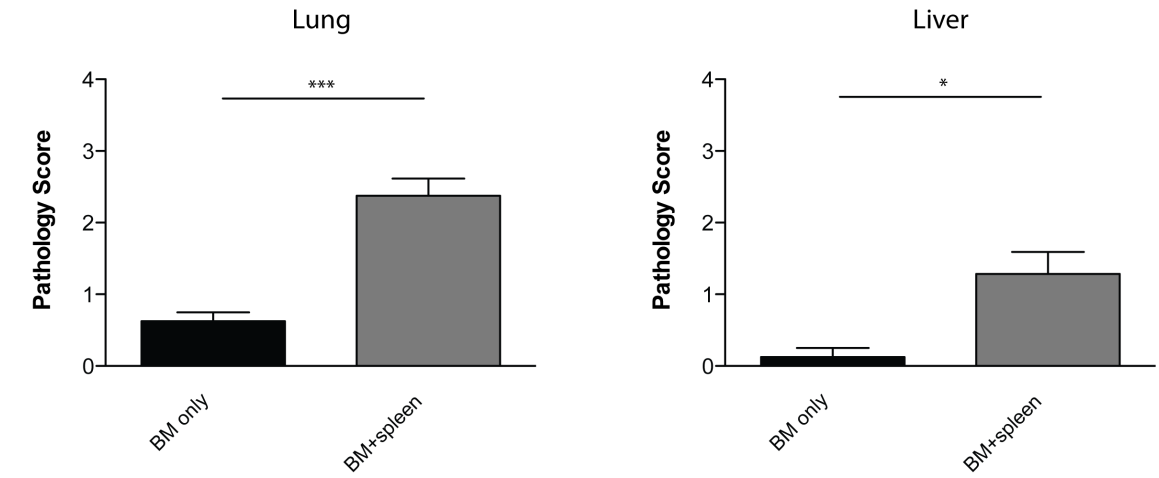

Supplemental Figure 3

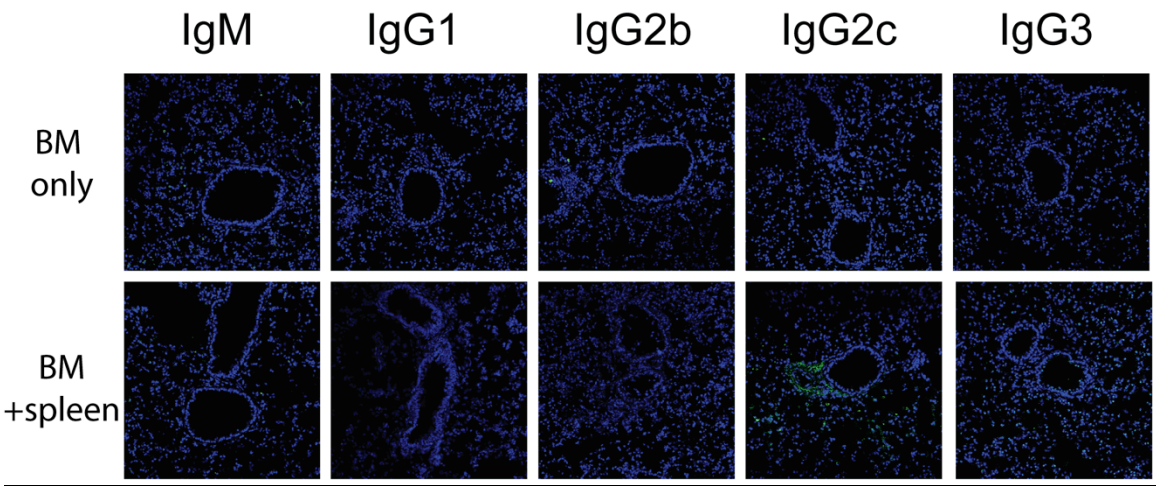

Supplemental Figure 4

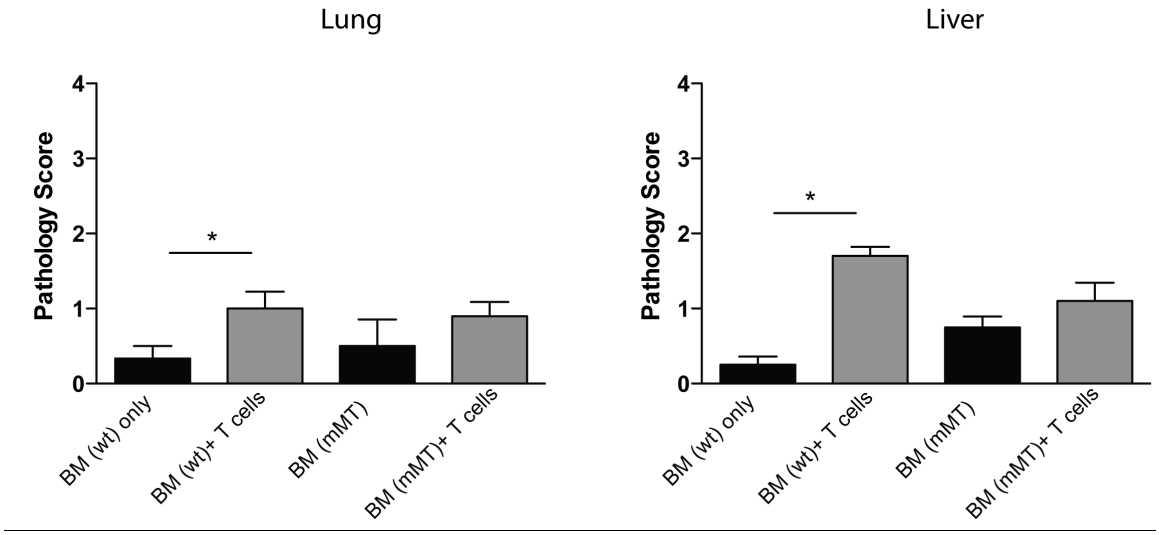

Supplemental Figure 5

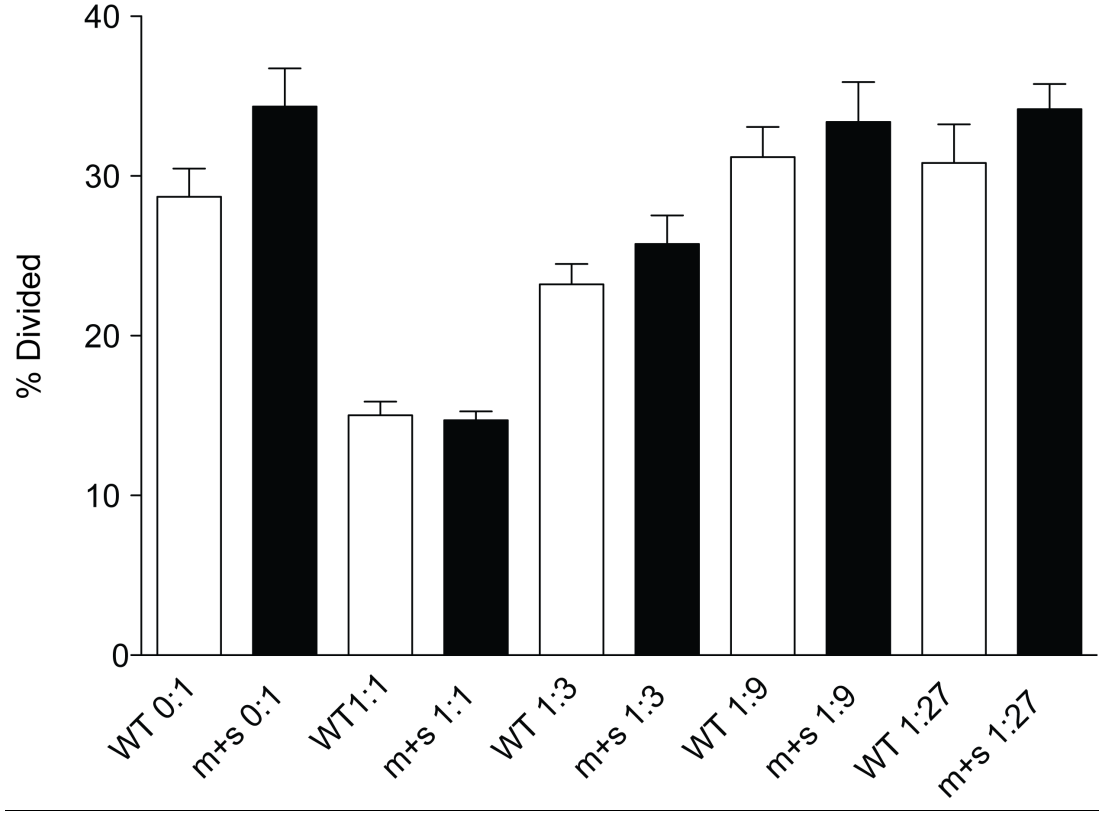

Supplemental Figure 6

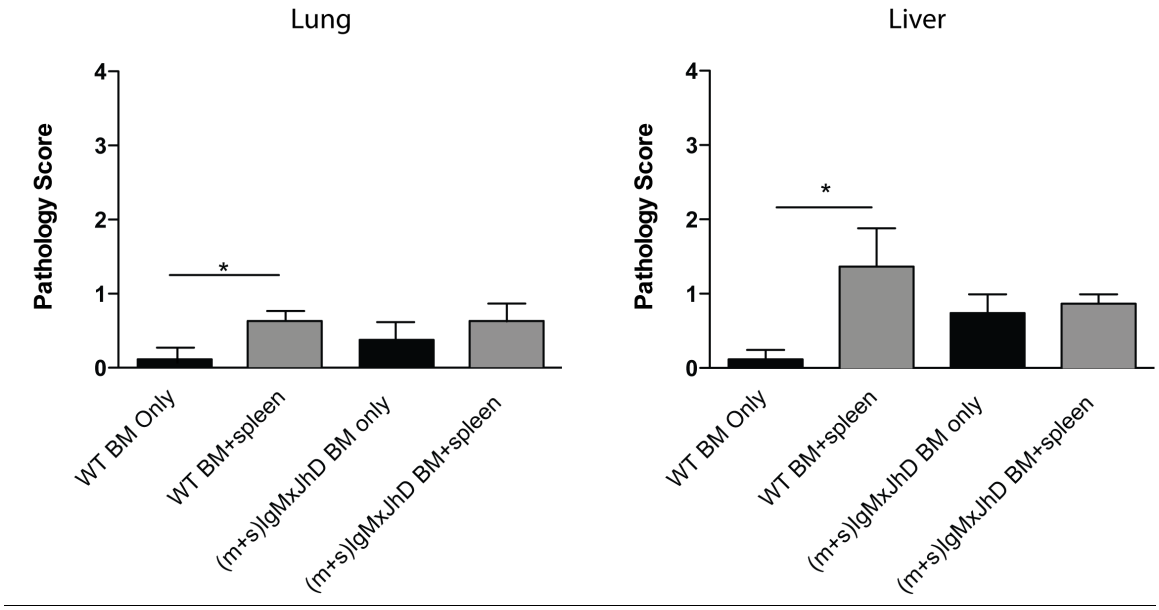

Supplemental Figure 7

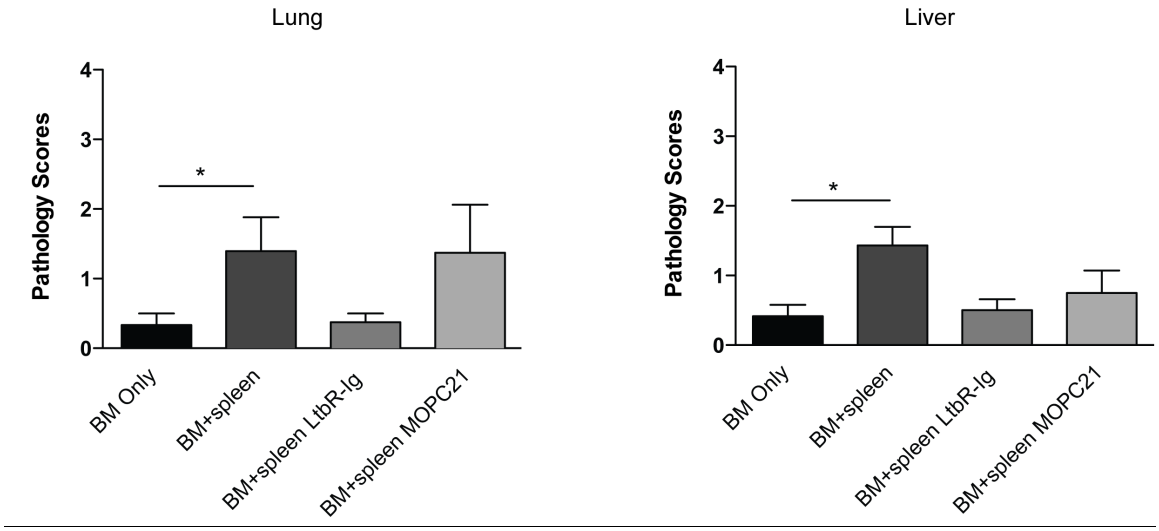

Supplemental Figure 8

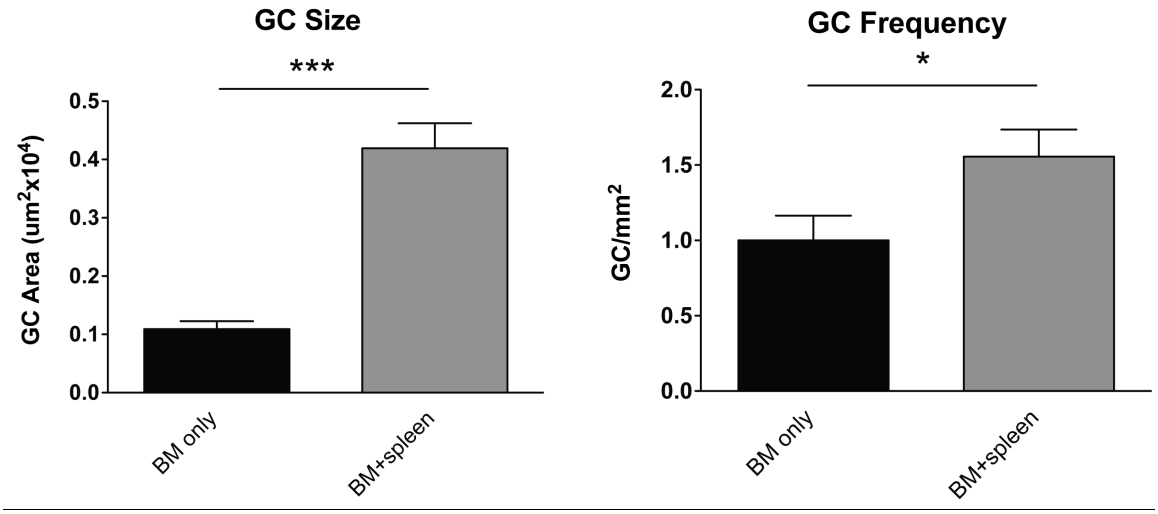

Chapter III: Increased T follicular helper cells and germinal center B cells are required for chronic GVHD and bronchiolitis obliterans

Originally published by the American Society of Hematology in the journal Blood
Flynn R, Du J, Veenstra RG, Reichenbach DK, Panoskaltsis-Mortari A, Taylor PA *et al. Blood* 2014; **123**(25)**:** 3988-98.

Chronic graft-versus-host disease is a leading cause of morbidity and mortality after allogeneic hematopoietic stem cell transplantation. Having shown that germinal center (GC) formation and immunoglobulin deposition are required for multiorgan system chronic GVHD and associated bronchiolitis obliterans syndrome (BOS) in a murine model, we hypothesized that T follicular helper (Tfh) cells are necessary for chronic GVHD by supporting GC formation and maintenance. We show that increased frequency of Tfh cells correlated with increased GC B cells, chronic GVHD, and BOS. Although administering a highly depletionary anti-CD20 monoclonal antibody (mAb) to mice with established chronic GVHD resulted in peripheral B-cell depletion, B cells remained in the lung, and BOS was not reversed. BOS could be treated by eliminating production of interleukin-21 (IL-21) by donor T cells or IL-21 receptor (IL-21R) signaling of donor B cells. Development of BOS was dependent upon T cells expressing the chemokine receptor CXCR5 to facilitate T-cell trafficking to secondary lymphoid organ follicles. Blocking mAbs for IL-21/IL-21R, inducible T-cell costimulator (ICOS)/ICOS ligand, and CD40L/CD40 hindered GC formation and chronic GVHD. These data provide novel insights into chronic GVHD pathogenesis, indicate a role for Tfh cells in these processes, and suggest a new line of therapy using mAbs targeting Tfh cells to reverse chronic GVHD.

Introduction

Chronic graft-versus-host disease is a major obstacle following allogeneic hematopoietic stem cell transplantation[62, 63]. Clinically representative models have increased our understanding of acute GVHD, but the dearth of relevant chronic GVHD murine models has limited our ability to interrogate its underlying pathophysiology[64, 65]. However, recent work with a novel murine model of multiorgan chronic GVHD that highlights lung pathology with the development of bronchiolitis obliterans syndrome (BOS) has provided new insight into research on chronic GVHD[24, 36].

Even though the exact mechanism of chronic GVHD is unknown, B cells and pathogenic antibody production are clearly implicated in both human and mouse models. Patients diagnosed with chronic GVHD had elevated soluble B-cell activating factor and increased proportions of pre-germinal center (GC) B cells and post-GC plasmablasts[19]. Furthermore, male patients who received grafts from female donors had an increase in antibody response to H-Y minor histocompatibility antigens, which correlated with chronic GVHD[18]. In addition, we have shown that B cells are required to induce chronic GVHD and associated BOS in this clinically relevant murine model[24]. Not only was the presence of B cells necessary but the development of tissue fibrosis was dependent on secretion of class-switched antibody. These data suggest that B-cell activation and maturation is necessary for chronic GVHD progression.

The ability of B cells to create high-affinity antibodies is dependent on the GC reaction and extrafollicular B cells. Once B cells recognize cognate antigen,

they can undergo somatic hypermutation and class switching with the aid of CD4 T cells in the B-T cell junction within secondary lymphoid organs. T cells are required to provide survival signals to B cells that are rapidly making random mutations to the complementary determining regions in the immunoglobulin (Ig) genes. This results in the negative selection of poor-affinity antibodies, while selecting for those B cells with mutations that increase antibody affinity. B cells that produce high-affinity class-switched antibodies are able to activate immune responses and, in the case of chronic GVHD, cause severe damage to the target tissues by activating complement or antibody-dependent cell-mediated cytotoxicity.

We sought to investigate the role of T follicular helper (Tfh) cells in the genesis of chronic GVHD in order to develop new interventions. Previously, we defined the role of antibody production by bone marrow (BM)-derived B-cell progeny in the initiation and maintenance of chronic GVHD in this clinically relevant murine model[24]. The ability of B cells to produce class-switched antibodies and the need for lymphotoxin β receptor signaling in the GC was highlighted, clearly defining the importance of GC maturation during chronic GVHD. Tfh cells are a subset of $CD4^+$ T cells that are located in the B-cell follicle and express the transcription factor Bcl6 along with high levels of the chemokine receptor CXCR5 and programmed cell death protein-1 (PD-1)[66]. These cells support the generation of GCs by providing signaling through interleukin-21 (IL-21), inducible T-cell costimulator (ICOS), and CD40[26, 67-69]. Having previously shown that B-cell production of class-switched antibody is necessary for chronic

GVHD, we hypothesized that maintenance of the GC by Tfh cells is necessary for the progression of chronic GVHD and associated BOS. Genetic deletions and interventional therapies were used to study the importance of Tfh cell signaling of GC B cells during murine chronic GVHD.

Results

Increased Tfh cell frequency during chronic GVHD

Previously, we demonstrated that mice with chronic GVHD have larger and more frequent GCs in the spleen compared with BM only (non-chronic GVHD) mice.[24] Therefore, we examined the presence of splenic Tfh cells in chronic GVHD mice because Tfh cell support is necessary for GC formation[36, 70, 71]. Spleens harvested from mice with chronic GVHD demonstrated an increased presence of $CD4^+$ cells in peanut agglutinin–positive GC areas compared with non-GVHD mice, co-localizing to regions of high PD-1 expression (Figure 1A). Localization of $CD4^+$ cells to the GC by the chemical gradient chemokine ligand CXCL13 binding with its receptor CXCR5 is a hallmark of Tfh cells[72]. During chronic GVHD, CD4 localization was associated with increased GC size and GC B cells, denoted by GL7 staining (Figure 1B; see also Figure 1E). Flow cytometry of purified splenocytes from BM only non-chronic GVHD and chronic GVHD mice showed a significant decrease in the proportion of B1a, B1b, $CD23^+$, IgM^+, and IgD^+ follicular B cells (Figure 1C). Even though there are fewer follicular B cells, there is an increase in the frequency of B cells entering the GC. In addition, there was a twofold increase in the frequency of splenic Tfh cells, defined as PD-

1^{hi}CXCR5^{+} CD4 T cells in chronic GVHD mice compared with non-chronic GVHD mice (Figure 1D), which correlated with a twofold increase in the percentage of GL7^{+}, Fas^{+}, and CD38^{-} GC B cells (Figure 1E).

Anti-CD20 therapy does not prevent the development of chronic GVHD

Rituximab therapy has been used as an attractive treatment for some patients with chronic GVHD to eliminate pathogenic B cells. We sought to determine the therapeutic effect of anti-CD20 in our mouse model of chronic GVHD, which is dependent on B-cell activation and GC reaction. B10.BR mice were transplanted with wild-type (WT) B6 BM cells and WT B6 T cells and allowed to develop chronic GVHD over 28 days, at which point mice were given anti-CD20 to deplete B cells. When analyzed on day 60, >98% of the splenic B cells were depleted (Figure 2B). However, mice still developed chronic GVHD. PFTs demonstrated decreased functional capacity of the lungs as evidenced by increased resistance and elastance and decreased compliance similar to irrelevant mAb–treated chronic GVHD mice (Figure 2A). Furthermore, anti-CD20–treated chronic GVHD mice had increased collagen deposition surrounding the bronchioles, consistent with BOS compared with BM only mice (Figure 2C). Tissues were analyzed for the deposition of IgG2c antibody. Compared with BM only controls and despite peripheral B-cell depletion by anti-CD20 mAb, chronic GVHD mice given anti-CD20 mAb had increased IgG2c, but not the isotype of anti-CD20 mAb (IgG1) (Figure 2D and supplemental Figure 1). We examined potential reasons why anti-CD20 therapy was not able to decrease development of BOS and chronic GVHD. First, plasma cells (CD138^{+} CD19^{lo}),

which do not express CD20, were significantly increased in the BM and spleen of mice treated with anti-CD20 mAb (Figure 2E and data not shown). This suggests that depletion therapy increases selection of CD20-deficient further differentiated antibody-producing cells. Next, anti-CD20 therapy was unable to deplete $CD19^+$ B cells within the target organs, including the lung (Figure 2F). Finally, even though there was a significant depletion of total B cells, there was a threefold increase in the relative frequency of GC B cells in the B-cell compartment of mice treated with anti-CD20 therapy compared with irrelevant mAb–treated chronic GVHD control mice ($P < .05$; data not shown). The increase in frequency highlights the relative resistance of GC B cells to B-cell–depleting therapy[73]. Thus, B-cell depletion therapy for treatment of active chronic GVHD had little effect on the progression of the disease likely because of the inability to deplete all GC B cells.

T cell Trafficking to the B-cell follicle by the chemokine receptor CXCR5 is necessary in chronic GVHD

Trafficking of Tfh cells to the B-cell zone is dependent on the expression of the chemokine receptor CXCR5, which binds CXCL13 secreted by follicular dendritic cells. Without CXCR5, Tfh cells are unable to localize to the B-cell follicle and cannot interact with GC B cells. To determine the requirement for such Tfh cell migration during chronic GVHD, we transplanted mice with T cells deficient in CXCR5. Compared with positive control mice with chronic GVHD, which received WT BM and WT T cells, recipients of WT BM cells with CXCR5

KO T cells had PFTs that were significantly improved and comparable to BM-only controls (Figure 3A). In recipients given CXCR5 KO T cells, there was a significant decrease in the amount of Ig found in the lungs of these mice (Figure 3B-C), and collagen surrounding the bronchioles was significantly decreased as demonstrated by trichrome staining (Figure 3D-E). Together, these data demonstrate that CXCR5 expression on donor T cells is needed for chronic GVHD associated with BOS.

IL-21 is a required cytokine for the development of chronic GVHD

Tfh cells are able to drive GC reactions by multiple mechanisms, including cell-to-cell contact and secretion of key cytokines. IL-21 is a major cytokine produced by Tfh cells. Although IL-21 is not essential for GC formation, it is important for the production of memory B cells with high-affinity antibody production[74]. Therefore, we investigated the role of IL-21 in chronic GVHD and its possible requirement for the production of class-switched IgG that is deposited in chronic GVHD organs. Mice were transplanted with WT BM and either no T cells or WT or IL-21 KO splenocytes. Recipients of IL-21 KO splenic T cells did not develop symptoms of BOS as demonstrated by PFTs (Figure 4A). A decrease in the GC sizes (Figure 4B) was also seen. Deposition of Ig in the tissues was restored to healthy control levels (Figure 4C), leading to a twofold decrease in collagen (Figure 4D) in recipients of IL-21 KO splenic T cells compared with chronic GVHD controls. There was a two-fold decrease in frequency of splenic Tfh cells; moreover, the frequency of GC B cells was significantly decreased

compared with the recipients of WT splenic T cells (Figure 4E-F). Profibrotic effects of IL-21 may contribute to chronic GVHD and BOS[75]. To determine the extent to which the profibrotic vs B-cell activating functions of IL-21 accounted for improved PFTs, we transplanted mice with BM from WT or IL-21R KO donors with or without WT splenic T cells. Compared with recipients of WT BM and WT splenic T cells, mice transplanted with the IL-21R KO BM and WT splenic T cells had significantly improved PFTs (Figure 5A) and reduced GC area (Figure 5B) associated with reduced frequencies of PD-1^{hi}CXCR5^{+} Tfh cells (Figure 5C) and GL7^{+}CD38^{lo} GC B cells (Figure 5D) that was not different from BM only no chronic GVHD controls. Concordant with these findings, Ig (Figure 5E-F) and collagen (Figure 5G-H) were detected at levels less than that found in BM only controls. Together these data demonstrate a requirement for both donor T-cell IL-21 production and donor BM IL-21R expression in generating Tfh cells, GCs, and chronic GVHD with BOS.

Blocking signaling from ICOS and CD40 has a therapeutic benefit in chronic GVHD

ICOS and CD40 signals are required for GC formation[69]. ICOS is highly expressed on Tfh cells and is necessary for secretion of IL-21 following engagement with ICOS ligand–expressing B cells. CD40 is expressed on B cells in the GC, and signaling through CD40 by CD40 ligand–expressing T cells is necessary for the survival of B cells in the GC. Disruption of ICOS/ICOS ligand and CD40/CD40 ligand has been shown to decrease antibody formation in murine lupus models and to be important in the progression of acute GVHD[76, 77].

To determine whether ICOS and CD40 are necessary signals in chronic GVHD, mice with WT BM and splenic T cells were administered anti-ICOS– and anti-CD40 ligand–blocking mAbs beginning 28 days after transplantation, when chronic GVHD has been established[24]. Mice given either anti-ICOS or anti-CD40 ligand blocking mAbs had PFTs comparable to those of BM only controls (Figure 6A). Mice treated with anti-ICOS or anti-CD40L had a 95% reduction in GC formation (Figure 6B). The decrease in overall size of GCs correlated with a threefold reduction in Tfh cells and GC B cells present in the spleen (Figure 6C-D). Furthermore, IgG2c deposition surrounding the bronchioles in the lung was decreased (Figure 6E-F). Finally, the mice treated with anti-ICOS or anti-CD40L mAb did not have increased collagen surrounding the bronchioles (Figure 6G-H). Consistent with anti-ICOS–blocking mAb data, PFTs in recipients of ICOS KO vs WT T cells indicated normalization compared with BM only controls (supplemental Figure 2). These data indicate that the ICOS and CD40 signaling in the GC is necessary for the development of chronic GVHD.

Therapeutic effect of IL-21 mAb in mice with chronic GVHD and BOS

Blocking cytokine signaling was shown to be effective in many autoimmune diseases, including systemic lupus erythematous and rheumatoid arthritis[78, 79]. To determine whether the effects of neutralizing IL-21 would be a potential therapeutic for the progression of chronic GVHD and establishment of BOS, mice were transplanted with WT BM and WT splenic T cells and were treated with irrelevant or anti-IL-21 neutralizing mAb starting on day 28 after BM transplant. Mice treated with anti-IL-21 mAb demonstrated normalized pulmonary

function comparable to that in BM only recipients (Figure 7A). Anti-IL-21 mAb was effective at decreasing the frequency of GC B cells and Tfh cells in the spleen (Figure 7B-C). By blocking IL-21 in the chronic GVHD mice, we were able to limit the GC reaction and Ig deposition in the lung (Figure 7D). Finally, there was no increase in collagen deposition in mice treated with anti-IL-21 mAb (Figure 7E). These data demonstrate a novel potential therapy for the treatment of chronic GVHD and associated BOS.

Discussion

In this study, we defined a novel role of Tfh cells in the activation of GC B cells in the production and deposition of pathologic Ig and collagen, ultimately causing BOS and multiorgan system chronic GVHD. Although chronic GVHD B cells are activated and primed for survival via B-cell activating factor and BCR-associated signaling pathways[80], the direct mechanism underpinning B-cell activation has yet to be clearly defined. By using a preclinical chronic GVHD model, our data strongly suggest that donor T-cell–derived Tfh cells are necessary for the activation of donor BM–derived B cells that differentiate into GC B cells, resulting in Ig deposition in BOS lesional tissue. Consistent with this notion, preliminary data indicate that recipients of either BM or T cells from bcl6 KO donors are unable to cause chronic GVHD (data not shown), pointing to the requirement for Tfh cells and GC B cells in chronic GVHD generation and/or maintenance under these conditions. The increase in GC size (Figure 1A-B) is independent of the number and frequency of follicular B cells present during

chronic GVHD (Figure 1C) and, in fact, $CD19^{+}B220^{+}CD5^{hi}$ B1a cells (that produce broadly reactive natural IgM) and $CD19^{+}B220^{+}CD5^{lo}$ B1b B cells (that produce adaptive IgG antibody, especially to T-cell–independent type 2 antigens) are significantly decreased in chronic GVHD mice. Together, these data indicate that there is not a general increase in the B-cell population, but there is a selective increase in the frequency of GC B cells and GC number per area. Although splenic B-cell and GC populations were largely depleted by anti-CD20 mAb therapy for established chronic GVHD, there was no impact on chronic GVHD BOS (Figure 2). Possible explanations include inadequate B-cell depletion in chronic GVHD target organs (Figure 2F) and/or failure to deplete preformed plasma cells residing in the BM (Figure 2E). The increased activation state of GC B cells during chronic GVHD has the potential to make monoclonal cellular depletion therapies less effective, as seen in other autoimmune disorders[17, 81]. The production of class-switched antibodies requires the ability of T cells to localize to the GC and provide survival signals to B cells during chronic GVHD. Interruption of trafficking of T cells to the B-cell follicle by CXCR5 was sufficient for preventing GC response and preventing chronic GVHD (Figure 3). Expression of CXCR5 is a hallmark of Tfh cells, and without this essential chemokine receptor, GCs failed to increase posttransplant during conditions that otherwise were conducive to chronic GVHD generation. Di Carlo et al[82] demonstrated that cardiac allo-rejection was highly associated with production of CXCL13 and increased GC formation.

Robust GC reactions during chronic GVHD were dependent on the production of IL-21 from donor T cells (Figures 4 and 5). Tfh cells are dependent on the antigen-presenting function of B cells in the GC for maintenance[83]. In chronic GVHD, a decrease in IL-21 could potentially play multiple roles independent of Tfh cell involvement, including increase in induced T regulatory cells[84], possibly including T follicular regulatory cells. For example, IL-21 is important in the production of higher-affinity antibodies by stabilizing the expression of Bcl6[68]. This is consistent with our findings that IL-21 signaling in B cells is necessary to produce Ig that is deposited in the lung and associated with BOS (Figure 5). Our data using IL-21 KO T cells, IL-21R KO BM cells, and neutralizing anti-IL-21 mAb collectively indicate that the IL-21/IL-21R pathway is a promising target for therapeutics. Together, these data suggest that naïve donor T cells differentiate into Tfh cells that support GC formation after alloactivation, resulting in the upregulation of CXCR5, ICOS, CD40L, and IL-21 production, which then work in concert to migrate to secondary lymphoid organs and drive GC B-cell differentiation and GC formation.

ICOS and CD40 signaling are required for the establishment of GCs and have been demonstrated to eliminate GC reactions upon blockade[82, 85]. The presence of Tfh cells and the stability of GC are contingent upon ICOS and CD40 expression[85] and are necessary for the progression of chronic GVHD in our model (Figure 6 and supplemental Figure 2). ICOS could also be necessary for T-cell activation independent of GCs, as demonstrated when ICOS KO T cells are used in acute GVHD[76]. By using either blocking anti-ICOS or anti-CD40

ligand mAbs, we have demonstrated that disease progression is prevented or even reversed, revealing that the maintenance of GCs is essential in chronic GVHD. Although data presented here suggest that ICOS, CD40, and IL-21 blockade are effective in treating chronic GVHD associated with the dampening of the Tfh cell response, alternative mechanisms may exist. For example, it has previously been demonstrated that anti-IL-21 can increase peripheral-derived T regulatory cells[84]. The increase in T regulatory cells may dampen the GC response. Moreover, alloactivated T effector cells might directly contribute to tissue injury and work alone or in concert with Tfh cells to cause chronic GVHD. By blocking IL-21, ICOS, or CD40L signaling, T-cell proliferation, survival, or effector function may be compromised, resulting in reduced tissue injury and chronic GVHD, independent of the requirement for Tfh cells in the chronic GVHD process.

The use of this BOS murine model of chronic GVHD should be readily translatable to human chronic GVHD. The National Institutes of Health consensus group defined the diagnosis of BOS as a pathognomonic symptom of lung chronic GVHD[86]. By using clinically relevant functional, histopathologic, and immunologic markers of chronic GVHD as readouts, we can confirm the chronic GVHD disease state. Moreover, Srinivasan et al[24] demonstrated that the BOS model represents a multiorgan syndrome that is consistent with human chronic GVHD pathology. Finally, prior to interventions, we established chronic GVHD instead of taking a prophylactic approach. This is consistent with diagnosis and starting patients on treatment following allogeneic hematopoietic stem cell

transplantation. However, it is important to point out that there are several potential adverse events associated with the proposed therapeutics. For example, blocking IL-21, ICOS, or CD40L with mAbs might increase either T-cell responsive infections or the rate of leukemia relapse as a result of dampening of peripheral immune surveillance mechanisms. Finally, our discovery that Tfh cells are upregulated in murine chronic GVHD warrants investigation of this cell population in the peripheral blood[87] of chronic GVHD patients. If correlations are noted with chronic GVHD onset or severity, Tfh cells could be targeted, as we have done in this study, which may prove useful for treating or perhaps preventing chronic GVHD in the clinic.

Materials and Methods

Mice

C57Bl/6 (B6; $H2^b$) mice were purchased from the National Cancer Institute. B10.BR ($H2^k$), $CXCR5^{-/-}$, and $ICOS^{-/-}$ B6 knockout (KO) mice were purchased from Jackson Laboratories. B6 IL-$21^{-/-}$ and IL-21 receptor (IL-21R)$^{-/-}$ KO mice were bred at the University of Minnesota animal facility. Mice were housed in a specific pathogen-free facility and used with the approval of the University of Minnesota institutional animal care facility.

Bone marrow transplant and therapeutic intervention

B10.BR recipients were conditioned with Cy on days −3 and −2 (120 mg/kg per day intraperitoneally). On day 1, recipients received total-body irradiation by x-ray (8.3 Gy). B6 donor BM was T-cell depleted with anti-Thy1.2 monoclonal antibody (mAb) followed by rabbit complement. T cells were purified from spleens by incubation with phycoerythrin-labeled anti-CD19 (eBioscience), followed by anti-phycoerythrin beads and depletion with a magnetic column (Miltenyi-Biotec). On day 0, recipients received 10×10^6 T-cell–depleted BM cells with or without allogeneic spleen cells (0.75×10^6 to 1×10^6) or purified splenic T cells (0.1×10^6), as indicated. Weights of individual mice were recorded each week. Where indicated, recipients in chronic GVHD groups were given anti-CD20 (250 μg per animal every 2 weeks; clone 18B12, IgG2a; kindly provided by Biogen Idec), anti-IL-21 (250 μg per animal twice a week; clone Ch268.5.1, mIgG1, kindly provided by Novo Nordisk), anti-ICOS (200 μg per animal three times a week; clone 7E.17G9.G1, rIgG2b), or anti-CD40L (200 μg per animal twice a week; clone MR1, hamster IgG), or irrelevant isotype antibody as previously reported.

Pulmonary function tests

Pulmonary function tests (PFTs) were performed as described.[6] Briefly, anesthetized mice were weighed, and lung function was assessed by whole-body plethysmography using the Flexivent system (Scireq) and was analyzed by using the Flexivent software version 5.1.

Frozen tissue preparation

All organs harvested were embedded in Optimal Cutting Temperature compound, snap-frozen in liquid nitrogen, and stored at −80° centigrade. Lungs were inflated by infusing 1 mL of optimum cutting temperature compound:phosphate-buffered saline (3:1) intratracheally prior to harvest.

Trichrome staining

Cryosections (6 μm) were fixed for 5 minutes in acetone and stained with Masson's trichrome staining kit (Sigma) for detection of collagen deposition. Collagen deposition was quantified on trichrome-stained sections as a ratio of area of blue staining to area of total staining by using the Adobe Photoshop CS3 analysis tool (Adobe Systems)

Immunofluorescence

For Ig deposition, 6-μm cryosections were fixed with acetone and then blocked with horse serum and streptavidin-biotin blocking kit (Vector) and stained with fluorescein isothiocyanate (FITC)-labeled anti-mouse-Ig (BD Pharmingen) or goat-anti-mouse-IgG2c followed by FITC-donkey-anti-goat Ig (Jackson ImmunoResearch). Antibody deposition was quantified by area of Ig staining per 100-μm section. Fixed 6-μm spleen cryosections were stained with rhodamine-peanut agglutinin (Vector Laboratories), anti-PD-1 FITC, anti-GL7 FITC, anti-CD4 biotin or anti-CD19 biotin followed by Cy5-conjugated streptavidin to detect the presence of B cells and T cells in the GC. Confocal images were acquired on an

Olympus FluoView500 Confocal Laser Scanning Microscope at ×200, analyzed by using FluoView3.2 software (Olympus), and processed with Adobe Photoshop CS3, version 9.0.2.

Flow Cytometry

For flow cytometric analysis of Tfh cells and GC B cells, single-cell suspensions from spleens or the peritoneal cavity were obtained and labeled with anti-CD4, anti-CXCR5, anti-PD-1, anti-CD19, anti-GL7, anti-CD38, anti-IgM, anti-IgD, anti-CD23, or anti-CD5 (eBioscience). Cells were analyzed on a BD LSRFortessa cell analyzer.

Statistics

Group comparisons of cell counts and flow cytometry data were analyzed by Student *t* test.

Figure Legends

Figure 1: Increased Tfh in chronic GVHD. B10.BR mice were transplanted with BM only or BM and splenic T cells from B6 donor mice and spleens were harvested on D60. A) Representative spleens harvested from BM only and BM+spleen (S) mice on day 60 showing CD4 (Blue), PD-1 (Green) and PNA (Red) or B) CD19 (Blue), GL7 (Green) and PNA (Red). Arrows highlight germinal center areas. C) Composition of B cells in the spleen and the peritoneal cavity. D) Frequency of Tfh cells and E) GC B cells. * $P < 0.05$, *** $P < 0.001$.

Figure 2: B cell depletion by anti-CD20 therapy is not sufficient to prevent chronic GVHD and associated BOS. Chronic GVHD was established in B10.BR mice transplanted with WT B6 BM and WT B6 spleen cells and mice were treated with anti-CD20 or irrelevant mouse IgG1 antibody starting D28-56. A) Pulmonary function tests for mice treated with irrelevant or anti-CD20 antibody. B) Number of B cell purified from the spleens of mice on D56. C) Trichrome deposition and D) Ig deposition in the lung of mice harvested on D56. E) Representative images of frozen lung tissues stained with anti-CD19 FITC and DAPI. Representative data from 2 experiments n=8 mice per group. ** $P < 0.01$; *** $P < 0.001$.

Figure 3: Chemokine receptor CXCR5 on donor mature T cells is necessary for chronic GVHD. B10.BR mice were transplanted with WT B6 BM and WT B6 T cells or B6 CXCR5 KO T cells. A) Mice were evaluated for pulmonary function.

B) Lung sections were stained with FITC conjugated anti-mouse Ig and the area of Ig deposition was measured C) representative images. D) Lungs of mice were stained for Trichrome and the ratio of collagen stain to total stain was measured surrounding the bronchioles E) representative images. Representative data from 3 experiments with n=8 mice per group. * $P < 0.05$; ** $P < 0.01$; *** $P < 0.001$.

Figure 4: IL21 production from donor T cells is required for chronic GVHD pathology. B10.BR mice were transplanted with WT B6 BM and splenocytes from either WT B6 or B6 IL21 KO mice. A) Mice were evaluated for pulmonary function. B) Lungs of mice were stained for Trichrome and the ratio of collagen stain to total stain was measured surrounding the bronchioles. C) Lung sections were stained with FITC conjugated anti-mouse Ig and the area of Ig deposition was measured. D) Whole spleens sections were stained with Rhodamine conjugated PNA and the size of the PNA positive sections was measured. Representative data from 3 experiments with n=8 mice per group. * $P < 0.05$; ** $P < 0.01$; *** $P < 0.001$.

Figure 5: B cells need IL21R for full maturation and progression of chronic GVHD. B10.BR recipients were transplanted with either WT BM or IL21R KO BM and WT T cells. A) Mice were evaluated for pulmonary function. B) Lungs of mice were stained for Trichrome and the ratio of collagen stain to total stain was measured surrounding the bronchioles. C) Lung sections were stained with FITC conjugated anti-mouse Ig and the area of Ig deposition was measured. D) Whole

spleens sections were stained with Rhodamine conjugated PNA and the size of the PNA positive sections was measured. Representative data from 3 experiments with n=8 mice per group. * P < 0.05; ** P < 0.01; *** P < 0.001.

Figure 6: ICOS or CD40L costimulatory pathway blockade is sufficient for reducing GCs and preventing BOS. chronic GVHD was established in B10.BR mice transplanted with WT B6 BM and WT B6 T cells and mice were treated with either anti-ICOS, anti-CD40L or irrelevant rat antibody from D28-56. A) Pulmonary function test. GC size was analyzed in situ by measuring the PNA positive sections in transplanted spleens from D56. Splenocytes were harvested from transplanted mice on D56 and made into single-cell suspension and analyzed for C) Tfh or D) GC B cells. E) Amount of Ig deposited in the lungs of transplanted mice on D56 with F) representative images. G) Quantified Trichrome present in the lungs of mice on D56 with H) representative images. Representative data from 2 experiments with n=8. * P < 0.05; ** P < 0.01; *** P < 0.001.

Figure 7: Anti-IL21 mAb reverses BOS. chronic GVHD was established in B10.BR mice transplanted with WT B6 BM and WT B6 T cells and mice were treated with either irrelevant mouse IgG1 or anti-IL21. A) PFTs from mice treated with either neutralizing anti-IL21 mAb or irrelevant mAb. Splenocytes were isolated and analyzed for B) GC B cells or C) Tfh cells. D) Ig and E) ratio of trichrome positive to total area surrounding bronchioles in Trichrome stain.

Representative data from 3 experiments with n=8. * $P < 0.05$; ** $P < 0.01$; *** $P < 0.001$.

Supplemental Figure 1: Pathogenic antibody deposition in lungs of anti-CD20 treated mice. Lungs from day 60 B10.BR mice transplanted with WT B6 Bone Marrow and splenic T cells were stained for specific IgG subtype: either irrelevant/anti-CD20 antibody (IgG1) or pathogenic antibody (IgG2c).

Supplemental Figure 2: ICOS deficiency in donor derived T cells is necessary for development of pathogenic pulmonary function. Day 60 pulmonary function tests for mice transplanted with BM and splenic T cells from WT or ICOS deficient B6.

Figure 1

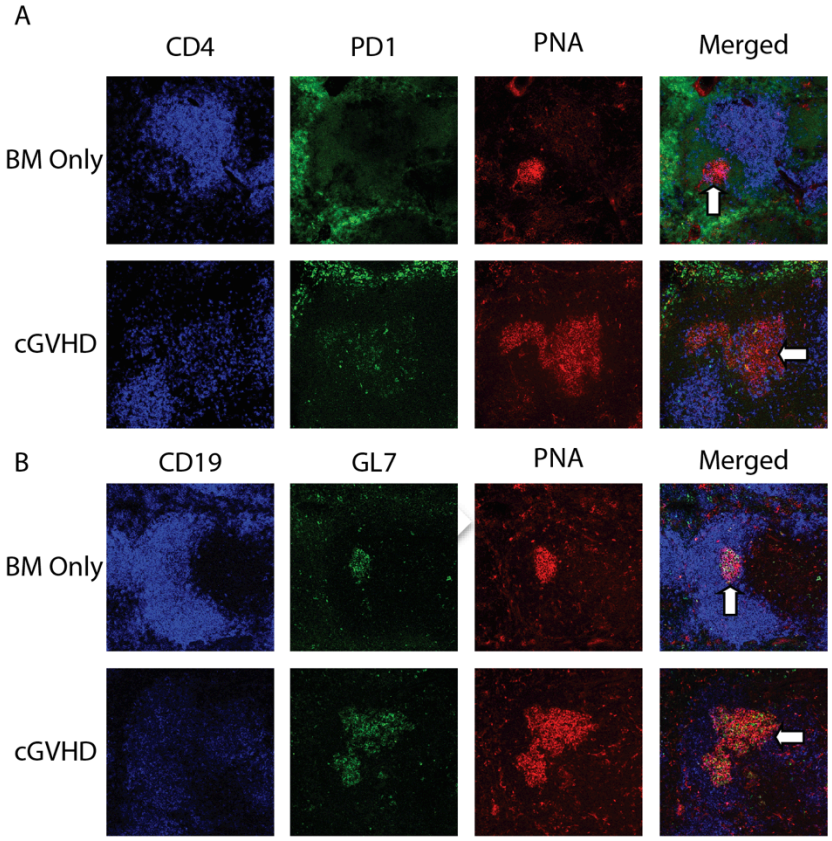
A
CD4
PD1
PNA
Merged
BM Only
cGVHD
B
CD19
GL7
PNA
Merged
BM Only
cGVHD

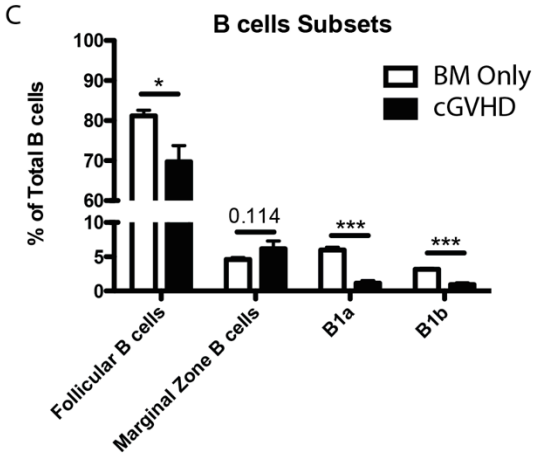
C
B cells Subsets
BM Only
cGVHD
% of Total B cells
100
90
80
70
60
10
5
0
*
0.114
***
***
Follicular B cells
Marginal Zone B cells
B1a
B1b

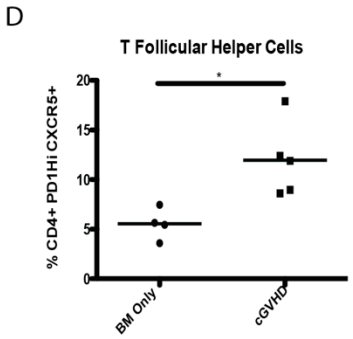
D
T Follicular Helper Cells
% CD4+ PD1Hi CXCR5+
20
15
10
5
0
*
BM Only
cGVHD

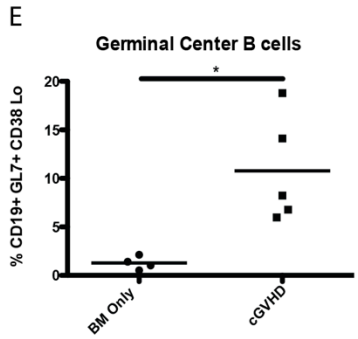
E
Germinal Center B cells
% CD19+ GL7+ CD38 Lo
20
15
10
5
0
*
BM Only
cGVHD

Figure 2

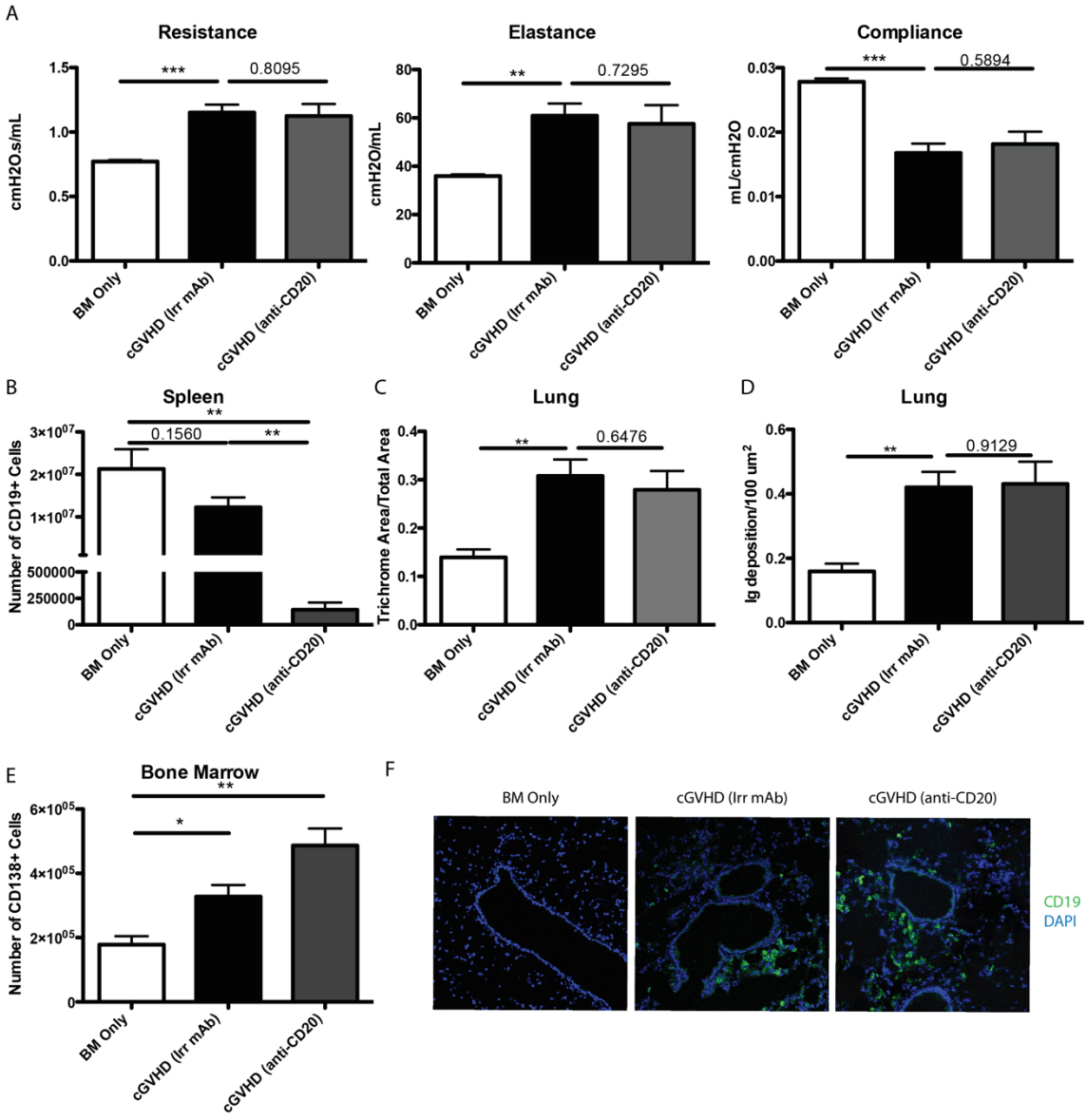
A
Resistance
cmH2Os/mL
***
0.8095
Elastance
cmH2O/mL
**
0.7295
Compliance
mL/cmH2O
***
0.5894
BM Only
cGVHD (Irr mAb)
cGVHD (anti-CD20)
B
Spleen
Number of CD19+ Cells
**
0.1560
**
C
Lung
Trichrome Area/Total Area
**
0.6476
D
Lung
Ig deposition/100 um²
**
0.9129
E
Bone Marrow
Number of CD138+ Cells
**
*
F
BM Only
cGVHD (Irr mAb)
cGVHD (anti-CD20)
CD19
DAPI

Figure 3

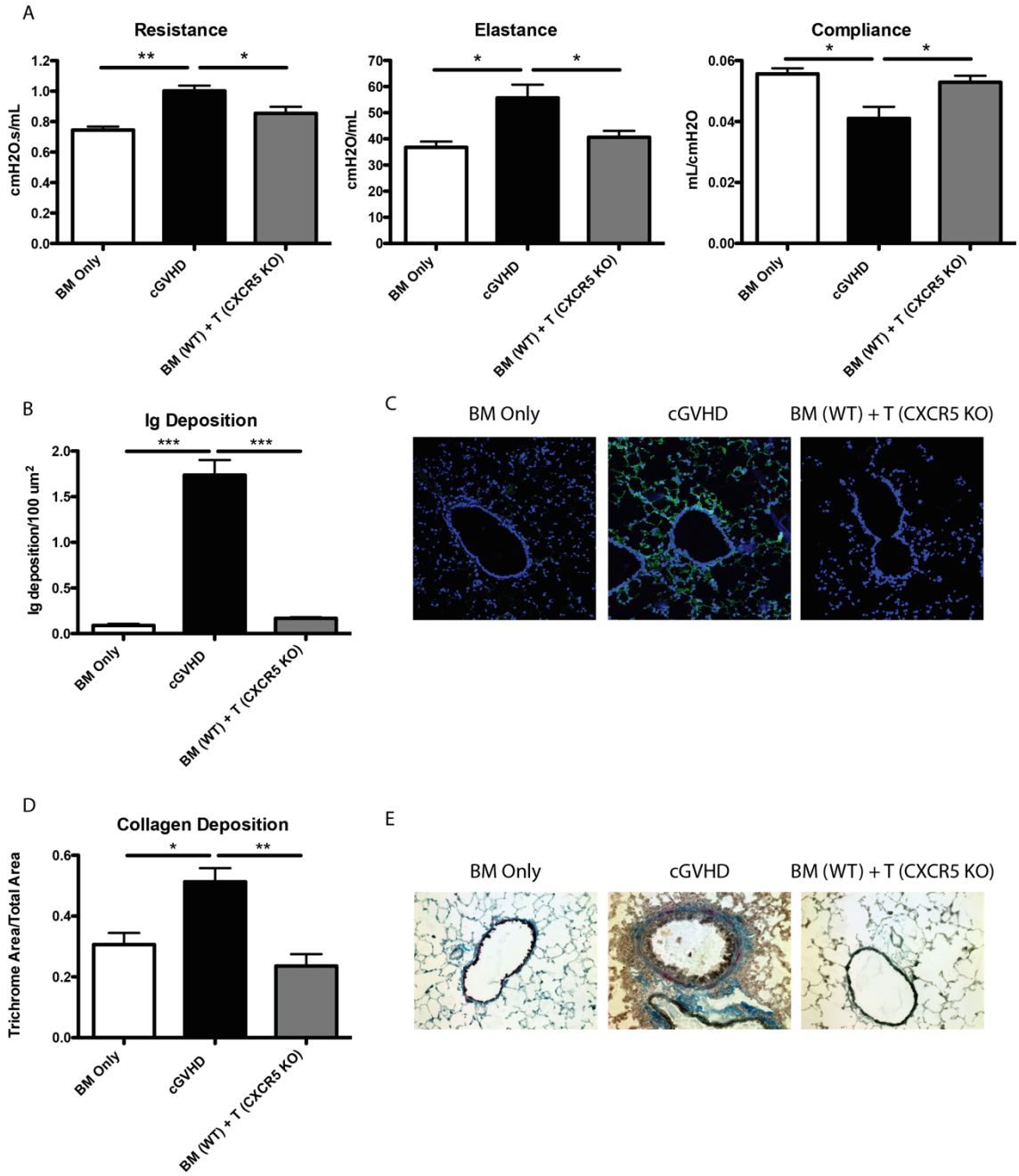
A
Resistance
cmH2Os/mL
1.2
1.0
0.8
0.6
0.4
0.2
0.0
**
*
BM Only
cGVHD
BM (WT) + T (CXCR5 KO)
Elastance
cmH2O/mL
70
60
50
40
30
20
10
0
*
*
BM Only
cGVHD
BM (WT) + T (CXCR5 KO)
Compliance
mL/cmH2O
0.06
0.04
0.02
0.00
*
*
BM Only
cGVHD
BM (WT) + T (CXCR5 KO)
B
Ig Deposition
Ig deposition/100 um2
2.0
1.5
1.0
0.5
0.0
***
***
BM Only
cGVHD
BM (WT) + T (CXCR5 KO)
C
BM Only
cGVHD
BM (WT) + T (CXCR5 KO)
D
Collagen Deposition
Trichrome Area/Total Area
0.6
0.4
0.2
0.0
*
**
BM Only
cGVHD
BM (WT) + T (CXCR5 KO)
E
BM Only
cGVHD
BM (WT) + T (CXCR5 KO)

Figure 4

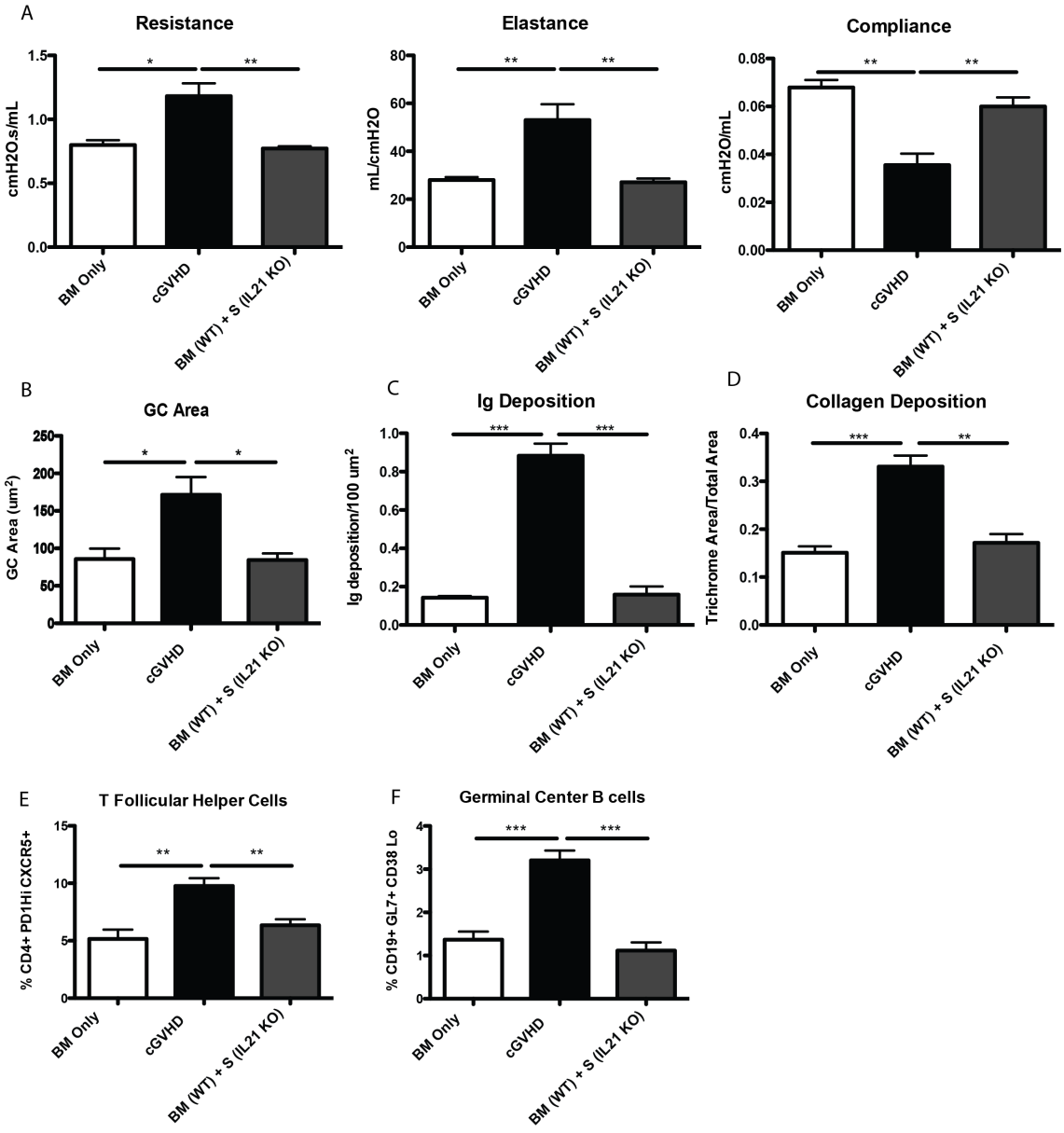
A
Resistance
cmH2O.s/mL
Elastance
mL/cmH2O
Compliance
cmH2O/mL
B
GC Area
GC Area (um2)
C
Ig Deposition
Ig deposition/100 um2
D
Collagen Deposition
Trichrome Area/Total Area
E
T Follicular Helper Cells
% CD4+ PD1Hi CXCR5+
F
Germinal Center B cells
% CD19+ GL7+ CD38 Lo
BM Only
cGVHD
BM (WT) + S (IL21 KO)

Figure 5

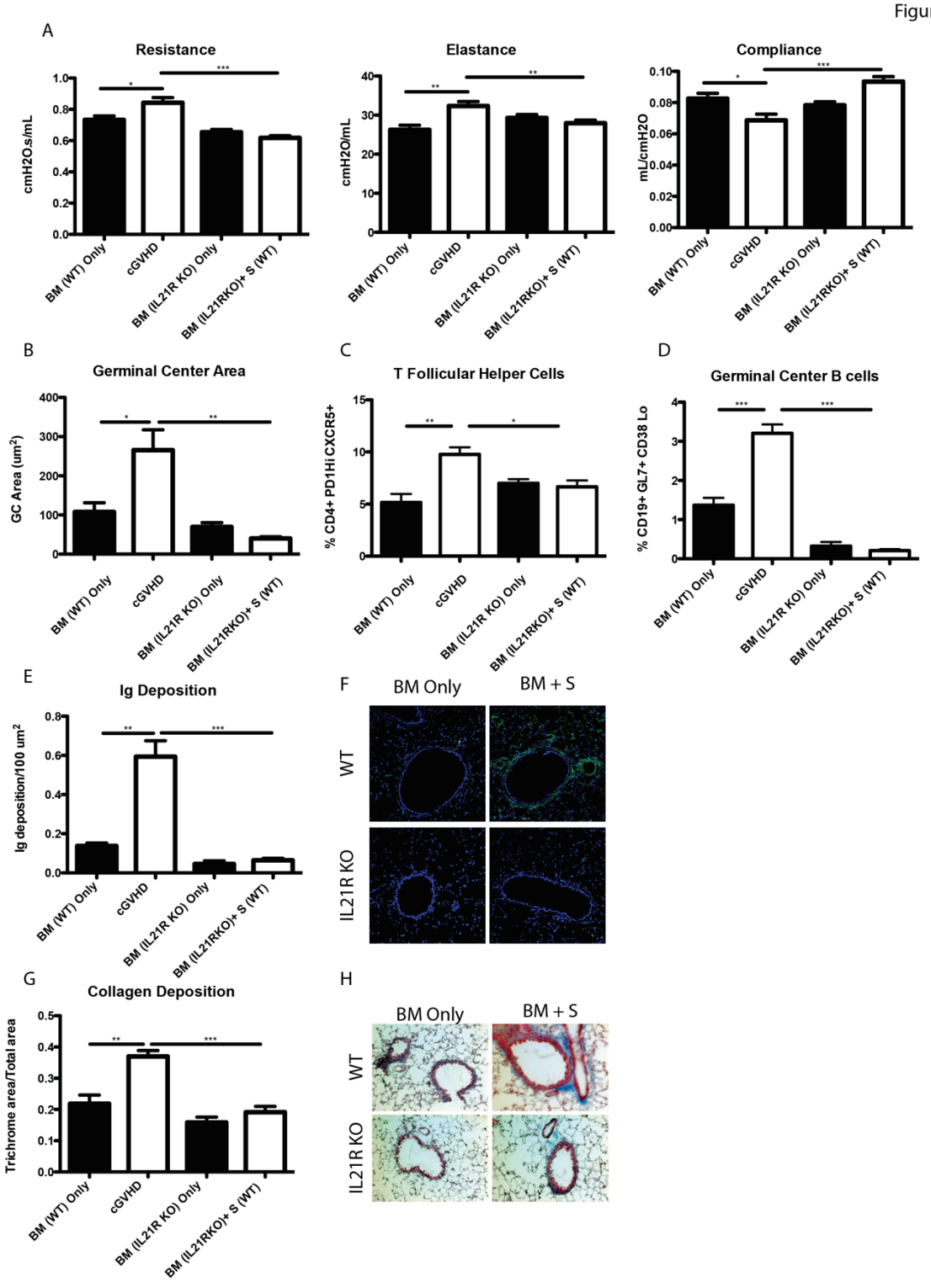
A
Resistance
cmH2Os/mL
Elastance
cmH2O/mL
Compliance
mL/cmH2O
BM (WT) Only
cGVHD
BM (IL21R KO) Only
BM (IL21RKO)+ S (WT)
B
Germinal Center Area
GC Area (um²)
C
T Follicular Helper Cells
% CD4+ PD1Hi CXCR5+
D
Germinal Center B cells
% CD19+ GL7+ CD38 Lo
E
Ig Deposition
Ig deposition/100 um²
F
BM Only
BM + S
WT
IL21R KO
G
Collagen Deposition
Trichrome area/Total area
H
BM Only
BM + S
WT
IL21R KO

Figure 6

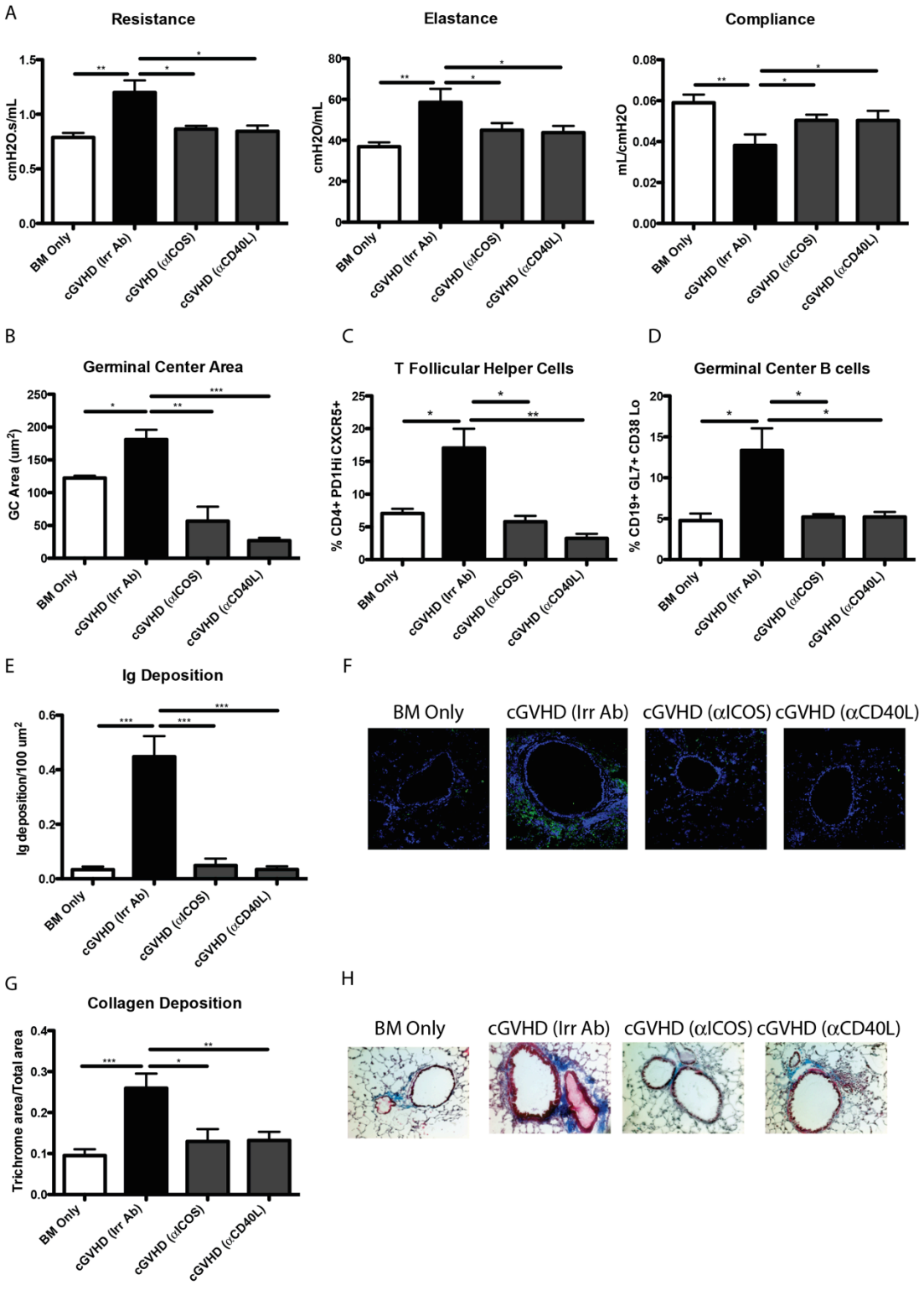
A
Resistance
cmH2O.s/mL
Elastance
cmH2O/mL
Compliance
mL/cmH2O
BM Only
cGVHD (Irr Ab)
cGVHD (αICOS)
cGVHD (αCD40L)
B
Germinal Center Area
GC Area (um2)
C
T Follicular Helper Cells
% CD4+ PD1Hi CXCR5+
D
Germinal Center B cells
% CD19+ GL7+ CD38 Lo
E
Ig Deposition
Ig deposition/100 um2
F
BM Only
cGVHD (Irr Ab)
cGVHD (αICOS)
cGVHD (αCD40L)
G
Collagen Deposition
Trichrome area/Total area
H
BM Only
cGVHD (Irr Ab)
cGVHD (αICOS)
cGVHD (αCD40L)

Figure 7

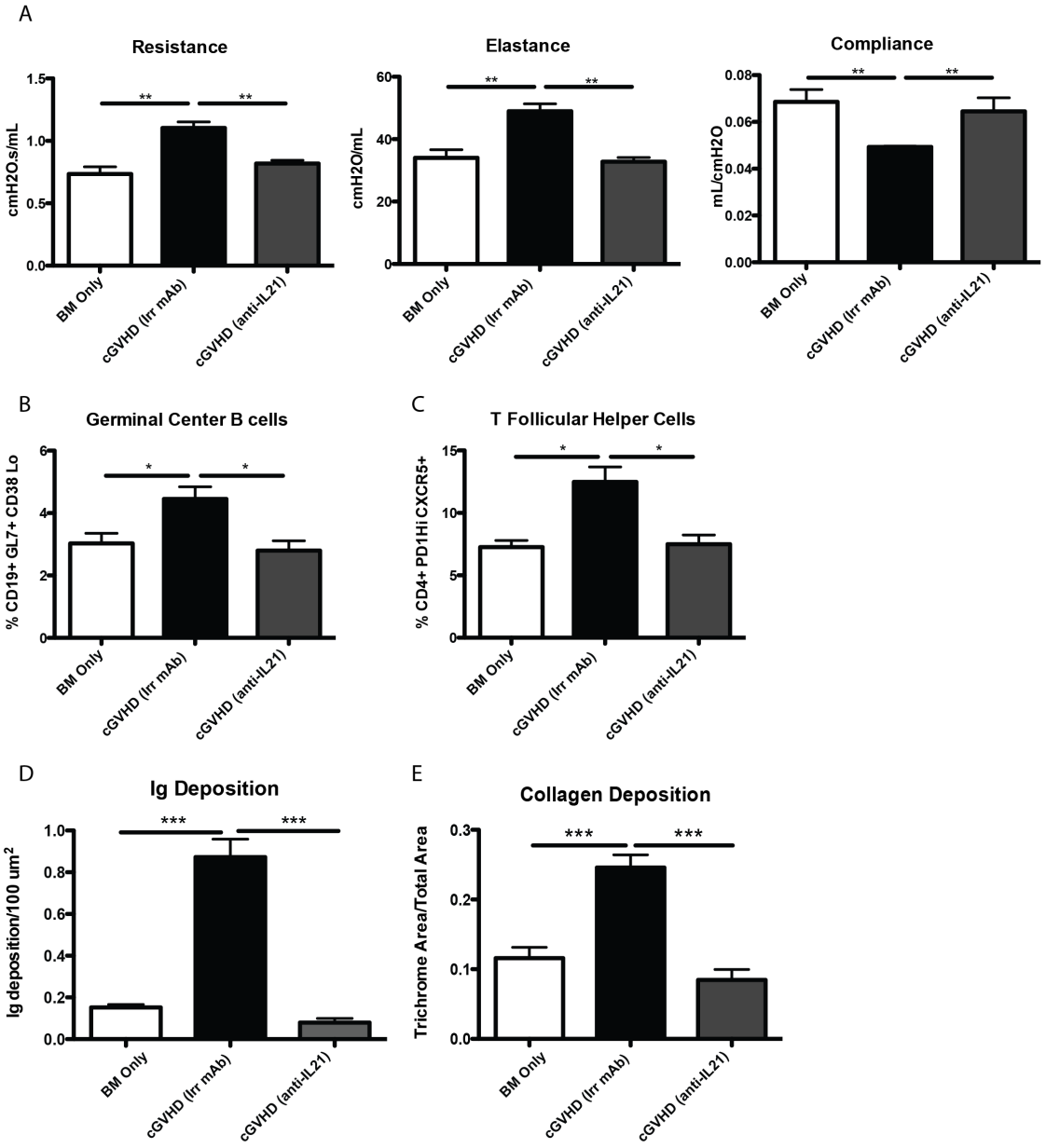
A
Resistance
cmH2Os/mL
1.5
1.0
0.5
0.0
**
**
BM Only
cGVHD (Irr mAb)
cGVHD (anti-IL21)
Elastance
cmH2O/mL
60
40
20
0
**
**
BM Only
cGVHD (Irr mAb)
cGVHD (anti-IL21)
Compliance
mL/cmH2O
0.08
0.06
0.04
0.02
0.00
**
**
BM Only
cGVHD (Irr mAb)
cGVHD (anti-IL21)
B
Germinal Center B cells
% CD19+ GL7+ CD38 Lo
6
4
2
0
*
*
BM Only
cGVHD (Irr mAb)
cGVHD (anti-IL21)
C
T Follicular Helper Cells
% CD4+ PD1Hi CXCR5+
15
10
5
0
*
*
BM Only
cGVHD (Irr mAb)
cGVHD (anti-IL21)
D
Ig Deposition
Ig deposition/100 um²
1.0
0.8
0.6
0.4
0.2
0.0
***
***
BM Only
cGVHD (Irr mAb)
cGVHD (anti-IL21)
E
Collagen Deposition
Trichrome Area/Total Area
0.3
0.2
0.1
0.0
***
***
BM Only
cGVHD (Irr mAb)
cGVHD (anti-IL21)

Supp Fig 1

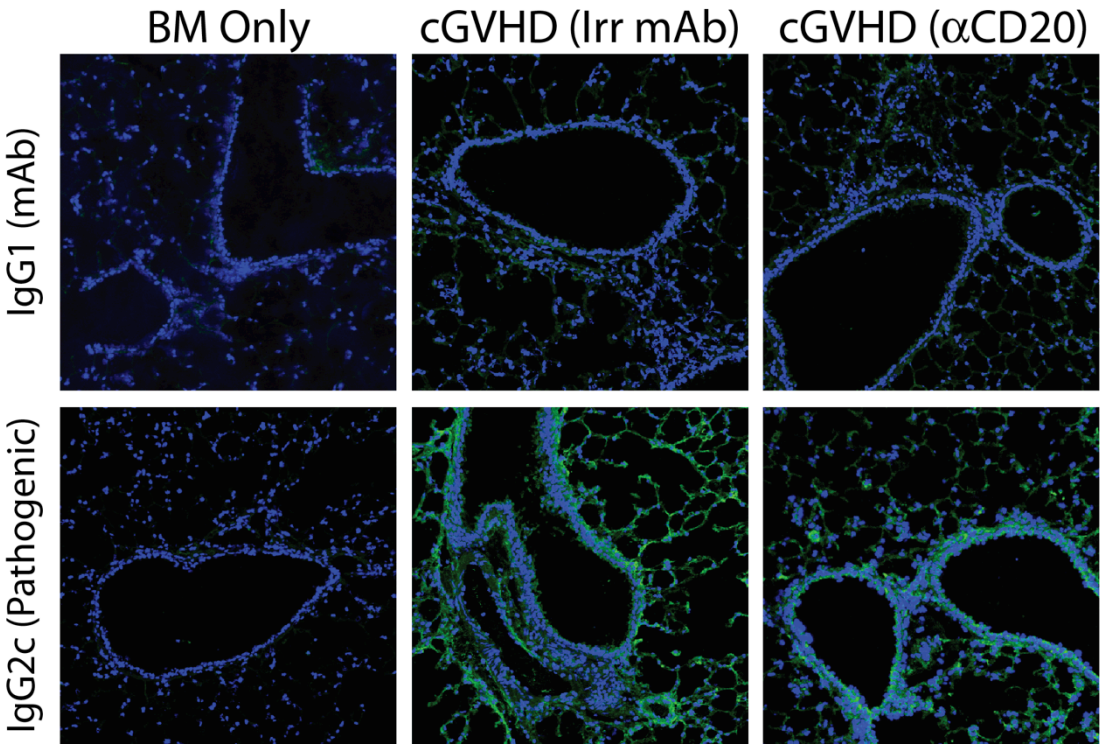

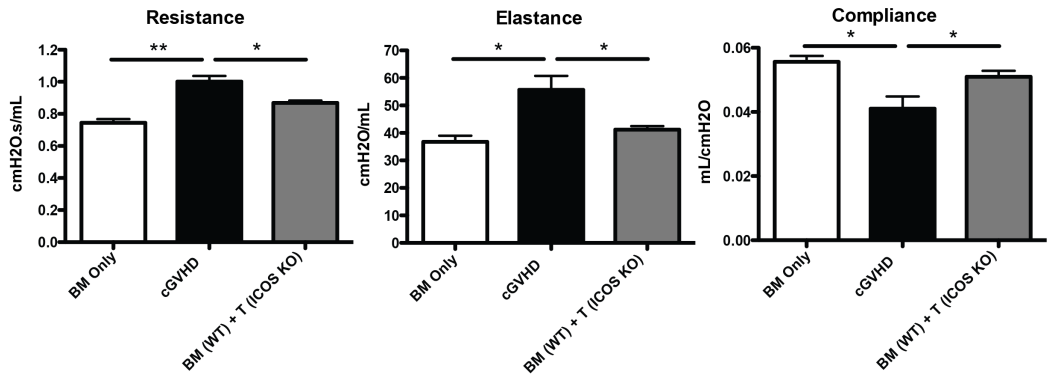
Resistance
cmH2O.s/mL
1.2
1.0
0.8
0.6
0.4
0.2
0.0
**
*
BM Only
cGVHD
BM (WT) + T (ICOS KO)
Elastance
cmH2O/mL
70
60
50
40
30
20
10
0
*
*
BM Only
cGVHD
BM (WT) + T (ICOS KO)
Compliance
mL/cmH2O
0.06
0.04
0.02
0.00
*
*
BM Only
cGVHD
BM (WT) + T (ICOS KO)

Chapter IV: Targeting of Syk in B-cells during murine and human chronic graft-versus-host disease

Submitted to the American Society of Hematology for publication in the journal Blood. Flynn R, Allen JA, Paz K, Du J, Panoskaltsis-Mortari A, Taylor PA, et. al.

Novel therapies for chronic graft-versus-host disease (cGVHD) are needed. Aberrant B cell activation has demonstrated in mice and humans with cGVHD. Having previously found that human cGVHD B cells are activated and primed for survival, we sought to further evaluate the role of the spleen tyrosine kinase (Syk) pathway in cGVHD. In murine models, we found that Syk expression was necessary in donor B but not T cells for disease progression in a model of antibody- and germinal center (GC) B cell dependent cGVHD. In cGVHD mice, a small molecule inhibitor of Syk, Fostamatinib, was effective in treating disease and normalizing GC formation. We further demonstrated that Syk inhibition was effective at inducing apoptosis of human cGVHD B cells. Together these data demonstrate the therapeutic potential of targeting B-cell Syk signaling in cGVHD.

Introduction

The development of cGVHD is a major complication following allogeneic hematopoietic stem cell transplantation. Discovery of new therapies has been limited by the absence on murine models that closely represent the clinical human disease and pathogenesis[65, 88]. Herein we use a mouse model of antibody-dependent, multi-organ system cGVHD, previously demonstrated to mimic several aspects of human cGVHD pathology[24, 89] to validate a novel therapeutic for cGVHD.

While the exact mechanisms of cGVHD remain unknown, recent studies have elucidated a role for antibody production by B-cells. The increase of B-cells in the germinal center (GC) has been shown to be necessary for the development of cGVHD[89]. Spleen tyrosine kinase (Syk) is activated by B-cell receptor (BCR engagement. After antigen-BCR engagement, Syk is phosphorylated at Y348, allowing for B-cell survival and proliferation. Increased proximal BCR signaling was recently described in cGVHD patient B cells.[90]

We sought to determine whether B-cell Syk activation was a critical component in cGVHD pathophysiology. First, we demonstrated that Syk was hyperactive in B-cells during cGVHD and that Syk expression was necessary in B- but not T-cells for murine cGVHD progression. Next, we demonstrated that *in vivo* molecular inhibition of Syk with Fostamatinib was sufficient for decreasing murine cGVHD manifestations and inducing apoptosis in human cGVHD B cells. These data together suggest that Syk targeting could be a novel therapeutic for cGVHD patients.

Results/Discussion

Syk activation and expression are necessary for the development of murine cGVHD

To determine if Syk is hyper-activated during murine cGVHD, purified B cells from day 60 cGVHD spleens were assayed for Syk phosphorylation. There was an increase in the percentage pSyk in both BCR stimulated B-cells (Figure 1A) and unstimulated B-cells in cGVHD (Supplemental Figure 1). These data extend a recent report that human B-cells have increased pSyk during cGVHD[81], potentially ascribed to increased soluble B-cell activating factor (BAFF)[19].

To test whether Syk is necessary for cGVHD progression, mice were transplanted with WT or conditional Syk KO BM and WT T-cells and analyzed for disease on day 60. Mice receiving Syk KO BM did not develop cGVHD pulmonary dysfunction compared to those receiving WT BM and T-cells (Figure 1B). In contrast, addition of Syk KO donor T-cells did not attenuate lung pathology compared to Syk-proficient WT T cell transplanted mice (Supplemental Figure 2). While T cell effects after Syk inhibition were previously described in acute[9] and sclerodermatous cGVHD[92], in this model donor T-cell Syk was not required for cGVHD development.

Since Syk is necessary for the proliferation of B-cells following antigen stimulation[93], we analyzed the spleens of transplanted mice to determine if there was a defect in the maintenance of Syk KO BM-derived B-cells. We found that B-cell frequency in mice receiving Syk KO BM was decreased 8-fold (Figure 1C), while T cell frequency was unaffected. These data are consistent with the

dependency of activated B-cells on Syk for proliferation and survival, and a requirement for activated donor-derived BM B-cells in cGVHD pathogenesis[24, 89].

Pharmacological inhibition of Syk decreases murine cGVHD and induces apoptosis in human cGVHD B-cells

Fostamatinib is a potent small molecule inhibitor of Syk. Studies in rheumatoid arthritis have demonstrated efficacy with Fostamatinib in randomized phase II clinical trials.[94, 95] Fostamatinib was notably safe in patients treated for non-Hodgkin's lymphoma, including some who had received prior autologous HCT.[96]. Additionally, Leonhardt et. al.[91] demonstrated that Syk inhibition decreased costimulatory molecules on antigen-presenting cells and increase survival of mice during acute GVHD while preserving anti-tumor and anti-viral immunity. To determine the effect of Fostamatinib on murine cGVHD, treatment was initiated on d28, a time of active disease.[24, 89] Mice receiving Fostamatinib had restoration of pulmonary function, similar to the healthy transplanted controls (Figure 2A). Improvement in pulmonary function correlated with a reduction in cGVHD pathology in the lung (Figure 2B). The number of GC reactions in the spleen was decreased in Fostamatinib versus vehicle treated cGVHD mice (Figure 2C). This is highlighted by a decrease in frequency of splenic GC B-cells in Fostamatinib treated cGVHD mice, matching healthy transplanted mice controls (Figure 2D).

To determine if human cGVHD B cells are more susceptible to Syk inhibition, B-cells purified from human peripheral blood were treated in vitro with

R406, the active form of R788. There was increased apoptosis in B cells in patients with cGVHD compared to healthy patients (Figure 2E and Supplemental Figure 3). These data, consistent with work by Allen et. al,[81] reveal that R406 preferentially kills cGVHD B cells via apoptosis. Global targeting of B cells with rituximab has been met with mixed success possibly due to altered B cell homeostasis perpetuated in some patients.[20, 97] We now demonstrate that constitutively activated B cells can be selectively targeted in cGVHD.

Materials and Methods

Mice

C57Bl/6 (B6; $H2^b$) mice were purchased from the National Cancer Institute. B10.BR ($H2^k$) mice were purchased from Jackson Laboratories. The Syk fl/fl x ERT2-cre mice were provided by RAC from Columbia University. Deletion of Syk occurred with daily administration of 1mg tamoxifen PO per mouse for 5 days (Sigma) and confirmed by Western Blot. Mice were housed in a specific pathogen-free facility and used with the approval of the UMN institutional animal care.

BMT

B10.BR recipients were conditioned with 120 mg/Kg cyclophosphamide and total body irradiation (8.3 Gy)[89]. Recipients received $10x10^6$ T cell depleted bone marrow (BM) cells from B6 wildtype (WT) or conditional Syk knockout (KO) BM cells with or without purified splenic T-cells ($0.1x10^6$) from WT vs KO donors. Where indicated, cGVHD recipients were given R788 (30 mg/Kg/animal/twice daily) or 0.4% methylcellulose vehicle from d28-56. Both pro-drug, R788, and its active metabolite, R406 (both known as Fostamatinib) were kindly provided by Rigel Pharmaceuticals. Lung function was assessed as previously described.[89]

Patient Samples

Samples were obtained from patients following written informed consent in accordance with the Declaration of Helsinki. The Institutional Review Boards at

the University of North Carolina Chapel Hill, Duke University Medical Center, and the Dana-Farber Cancer Institute approved all studies.

Flow Cytometry

B-cells were purified from murine cGVHD by magnetic separation with (Stem Cell Technologies) spleens on d60 and activated by 5 μg/mL anti-IgM Fab (Jackson Research), fixed and permeabilized and stained with anti-Syk Y348 PE (eBioscience). GC B cells were labeled with anti-CD19, anti-GL7 (eBioscience) and anti-CD95 (BD Biosciences) and analyzed on BD LSRFortessa. Ficoll purified human PBMC were stimulated and stained for Annexin V as previously described.[90, 98]

Frozen tissue preparation, pathology and immunofluorescence Organs harvested were embedded in Optimal Cutting Temperature compound, snap frozen, and stored at -80°. GC detection and pathologic scoring were accomplished as previously described[89].

Statistics

Group comparisons of pathology, pulmonary function tests, cell counts and flow cytometry data were analyzed by Student *t*-test.

Acknowledgements. We thank Rigel Pharmaceuticals for providing Fostamatinib (R788/R406). Supported in part by National Institutes of Health

National Cancer Institute grants P01 CA142106-06A1 and 5P01-CA047741-20, National Institutes of Allergy and Infectious Diseases grants P01 AI 056299 and T32 AI 007313 and K08HL107756.

Author contributions

RF designed and performed experiments and wrote the paper. JLA, KG and JD designed and performed experiments. AP-M discussed experimental design and edited the paper. PAT performed experiments and edited the paper. JSS, WJM, GRH, KPM, LL, IM, JK, CSC, RJS, and JR designed experiments and edited the paper; NJC and RAC provided reagents, discussed experiments and edited the paper, SS and BRB designed experiments and edited the paper.

Conflict of interest

No conflicts of interest are known.

Figure Legends

Figure 1: Syk activation during chronic GVHD is necessary during chronic GVHD in a murine model. A) Splenocytes from B10.BR mice transplanted with B6 BM and low numbers of T cells were analyzed for phosphorylated SYK at Y348 after ex vivo stimulation by 5 μg/mL of anti-IgM. B) Day 60 Pulmonary function tests of mice transplanted with conditional Syk deficient BM and WT T cells. C) Frequency of B cells in transplanted mice on day 60 after transplant. * $p < 0.5$; ** $p < 0.01$; *** $p < 0.001$.

Figure 2: Inhibition of Syk by R788 is capable of decreasing B cells in murine and human chronic GVHD. A) Pulmonary function tests on mice treated with 30 mg/Kg of R788 on day 56. B) GVHD pathology scores from the lungs of mice on Day 60. C) Number of germinal centers present in situ in spleens of mice. D) Frequency of germinal center B cells (gated on CD19+ GL7+ CD95hi) present in the spleens of transplanted mice on day 60. E) Peripheral blood mononuclear cells from patients without chronic GVHD (n = 3, open circles) and with chronic GVHD (n = 3, filled squares) treated with R406 (0, 0.01, and 0.1 μM) as indicated for 48 h. Apoptotic B cells were defined as CD19+ Annexin V+ 7AAD- cells. Fold increase in apoptosis by R406 divided by PBS is depicted. Data are mean +/- range pooled from 3 independent experiments. * $p < 0.5$; ** $p < 0.01$; *** $p < 0.001$.

Supplemental Figure 1. Phosphorylated Syk in purified B cells during chronic GVHD. B cells were purified from the spleens of healthy control (BM Only) or chronic GVHD (BM + T) mice and stimulated with anti-IgM at 5 μg/mL for 5 minutes.

Supplemental Figure 2. Syk in T cells has no effect on chronic GVHD progression. Pulmonary function tests from mice transplanted with WT BM and wither WT T cells of Syk deficient T cells. * $p < 0.5$; ** $p < 0.01$

Supplemental Figure 3. Increased apoptosis in human chronic GVHD B cells when treated with increasing concentrations of R406. Representative flow plots of purified B cells from human PBMC with or without chronic GVHD.

Figure 1

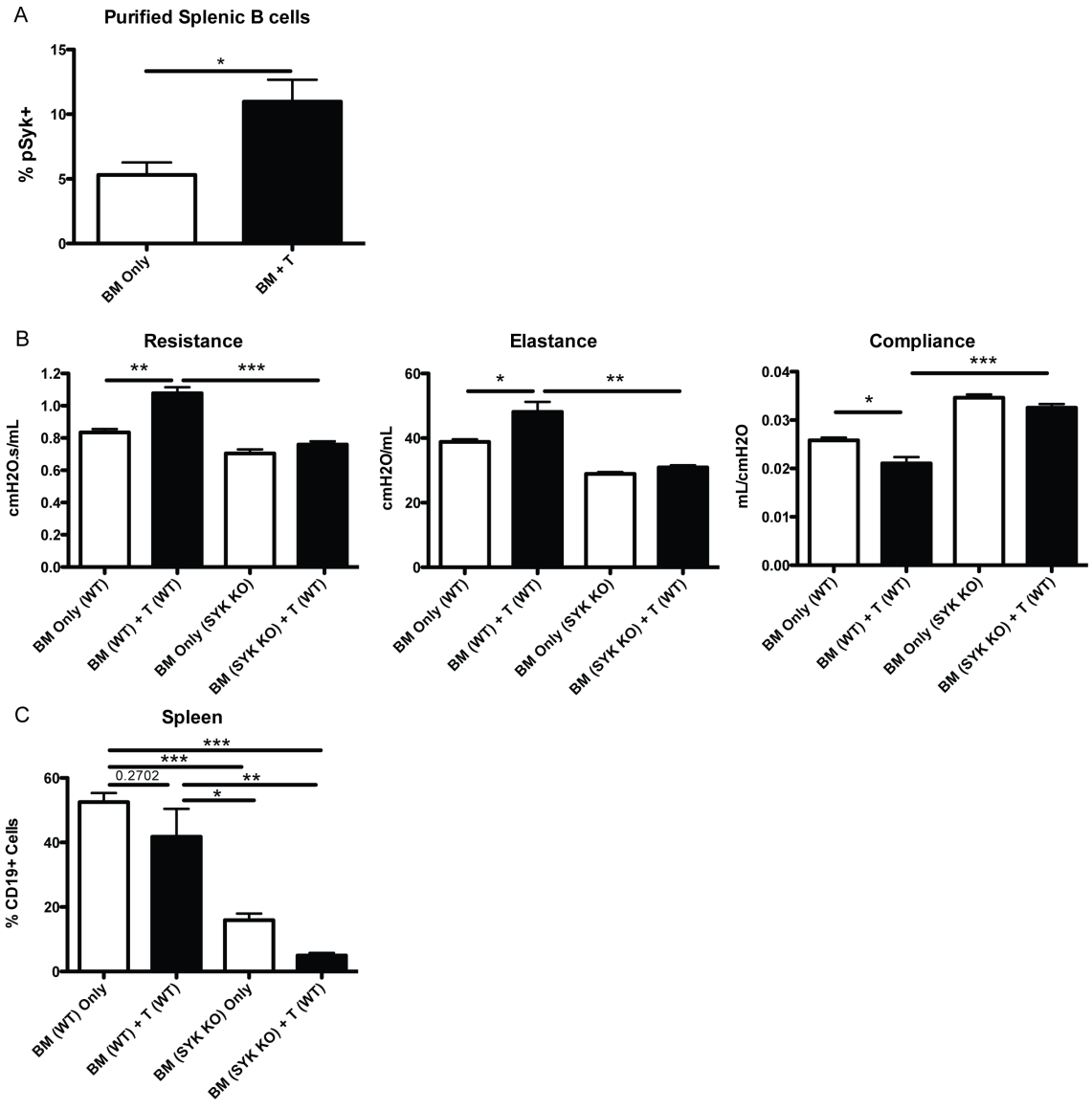
A
Purified Splenic B cells
% pSyk+
BM Only
BM + T
B
Resistance
cmH2O.s/mL
Elastance
cmH2O/mL
Compliance
mL/cmH2O
BM Only (WT)
BM (WT) + T (WT)
BM Only (SYK KO)
BM (SYK KO) + T (WT)
C
Spleen
% CD19+ Cells
0.2702
BM (WT) Only
BM (SYK KO) Only

Figure 2

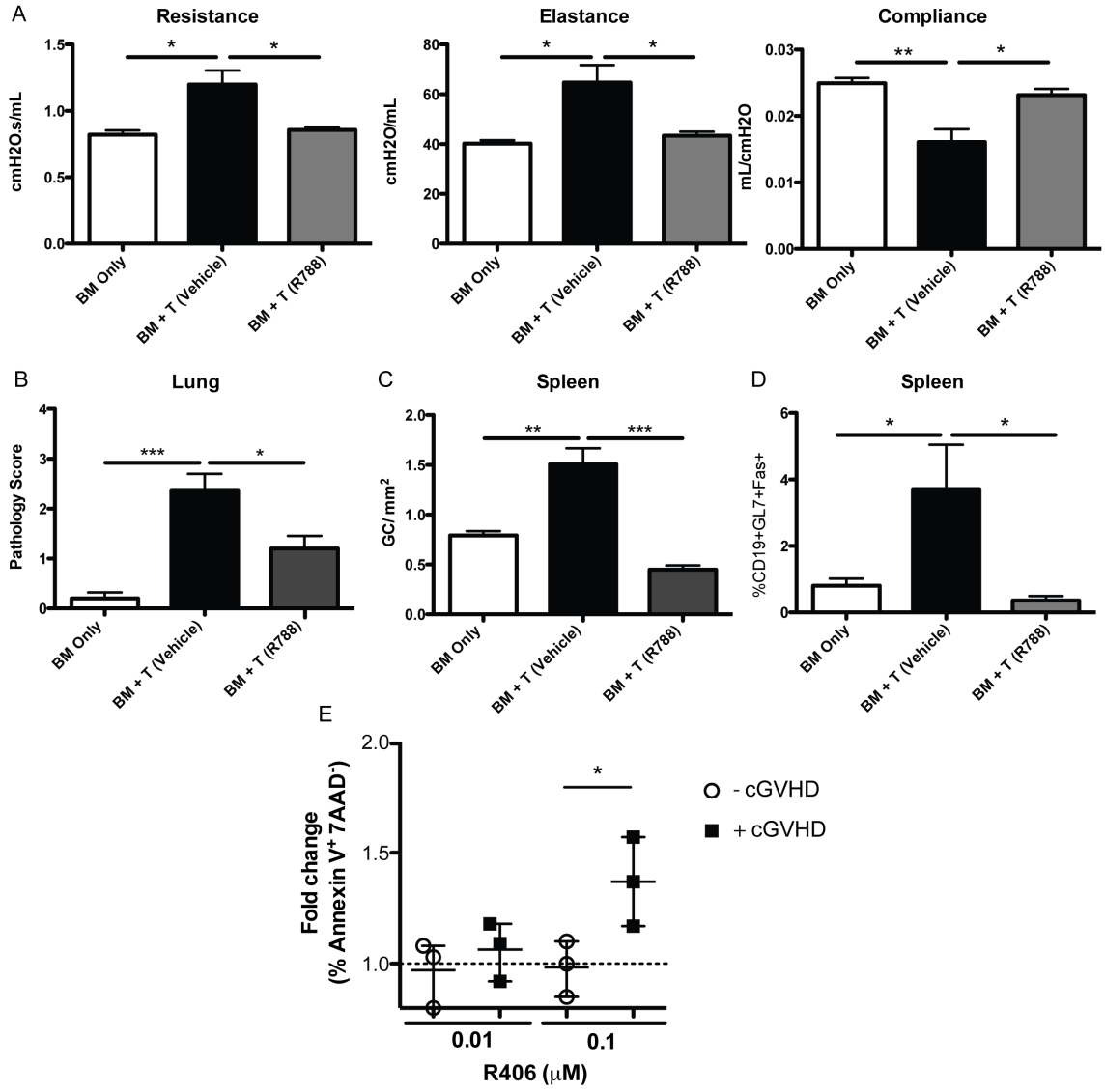
A
Resistance
cmH2O.s/mL
Elastance
cmH2O/mL
Compliance
mL/cmH2O
BM Only
BM + T (Vehicle)
BM + T (R788)
B
Lung
Pathology Score
C
Spleen
GC/ mm2
D
Spleen
%CD19+GL7+Fas+
E
Fold change
(% Annexin V+7AAD-)
- cGVHD
+ cGVHD
0.01
0.1
R406 (μM)

Supplemental Figure 1

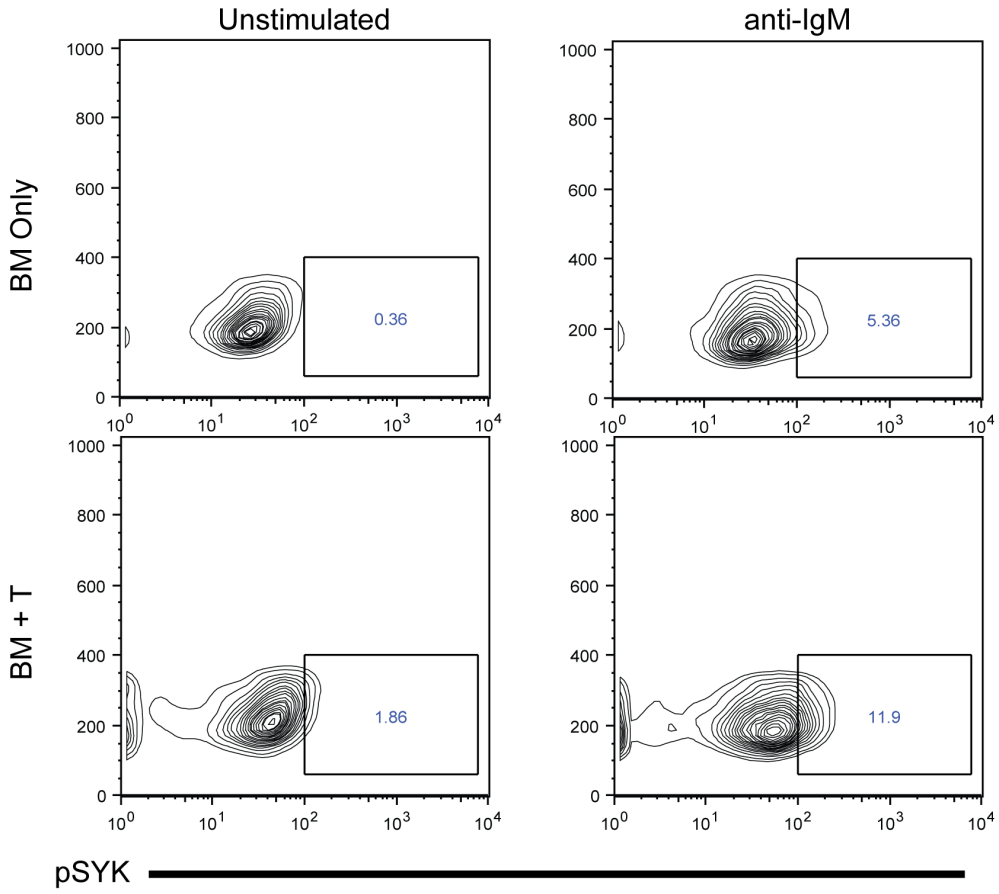

Supplemental Figure 2

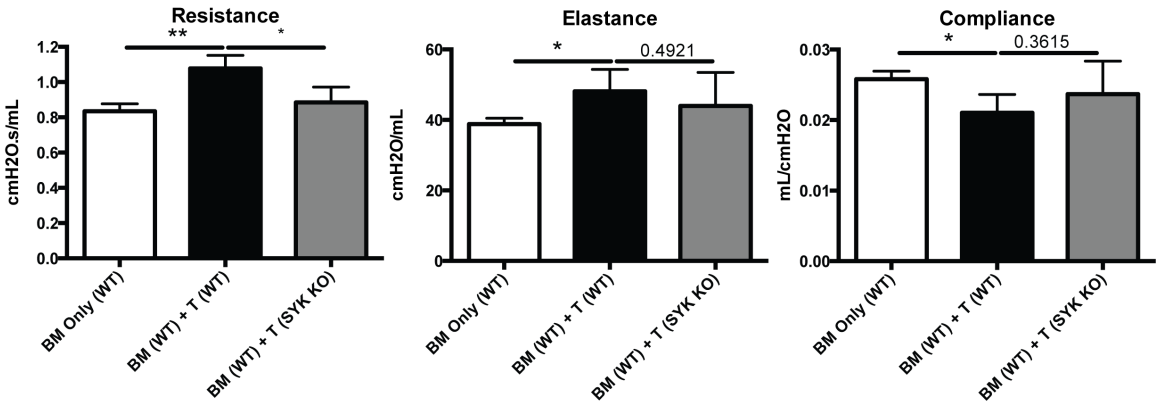

Supplemental Figure 3

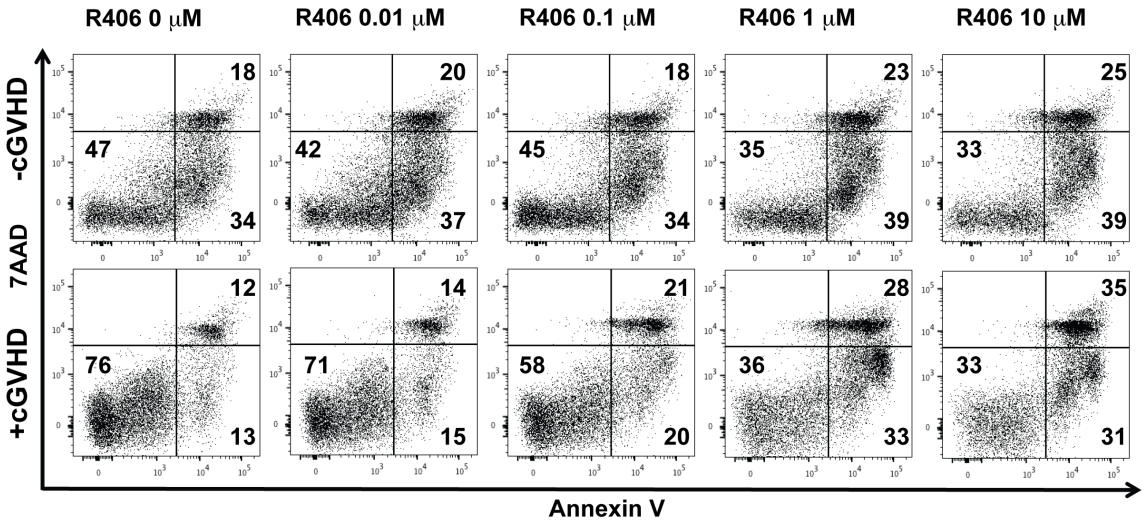

Chapter V: Ibrutinib Treatment Ameliorates Murine Chronic Graft-versus-Host Disease

Submitted to the American Society for Clinical Investigation for publication in the journal JCI. Ryan Flynn*, Jason A. Dubovsky*, Jing Du, Bonnie K. Harrington, Yiming Zhong, Benjamin Kaffenberger, et.al. 2014

Chronic graft-versus-host disease (cGVHD) is a life-threatening impediment to allogeneic hematopoietic stem cell transplantation that is mediated by CD4+ T-cells and B-cells. Current therapies are incompletely effective in preventing and treating cGVHD. Ibrutinib is an FDA-approved irreversible inhibitor of Bruton's tyrosine kinase (BTK) and IL-2 inducible T-cell kinase (ITK) that targets Th2 cells and B-cells and produces durable remissions in B-cell malignancies with minimal toxicity. To determine whether ibrutinib could reverse established cGVHD, we utilized two complementary murine models focused on interrogating T-cell driven sclerodermatous cGVHD (minor antigen disparate, LP/J→C57BL/6) or alloantibody driven multi-organ system cGVHD including bronchiolar obliterans (BO) (MHC disparate, C57BL/6→B10.BR). In the LPJ→C57BL/6 model, ibrutinib treatment delayed cGVHD progression, improved survival, and ameliorated cGVHD clinical and pathological manifestations. In the C57BL/6→B10.BR model, ibrutinib treatment restored pulmonary function, reduced germinal center reactions, and tissue immunoglobulin deposition. Genetic ablation studies confirmed that BTK and ITK were each critical to the development of cGVHD and further *ex vivo* human studies validate our findings in cells derived from patients with active cGVHD. Our data demonstrate that cGVHD is driven by B and T-cells and that ibrutinib is a potent and promising therapeutic agent that warrants consideration for cGVHD clinical trials.

Introduction

Chronic graft-versus-host disease (cGVHD) is a primary cause of non-relapse mortality after allogeneic hematopoietic stem cell transplantation (HSCT)[27, 99-101]. Drug therapy for cGVHD has been predominantly limited to calcineurin inhibitors and steroids, which are incompletely effective and associated with infections as well as long-term risks of toxicity[102]. Novel therapeutics that pinpoint pathogenic immune subsets might control cGVHD yet preserve immune effector function.

In contrast to acute GVHD, cGVHD is a relatively acellular process that has fibrosis as a dominant feature. The specific immune phenomena that underlie cGVHD are variable; however, recent studies show that B-cells, in addition to specific CD4 T-cell subsets, are key mediators of cGVHD[24, 103, 104]. It has been demonstrated that pathogenic antibody deposition occurs in human cGVHD[19, 30-32]. A network of alloreactive T-helper cells, including Th1, Th2, Th17, and T-follicular helper (Tfh) cells, infiltrate tissues and produce a milieu of effector cytokines resulting in antibody deposition, tissue fibrosis, and autoimmunity[105-107].

Many of the cellular activation and effector functions of these lymphoid subsets can be molecularly tethered to Bruton's tyrosine kinase (BTK) and IL-2 inducible kinase (ITK)[108, 109]. BTK and ITK are highly conserved TEC family kinases that propagate immune receptor-based signaling in B and T-lymphocytes, respectively[108]. These molecules are activated upstream by SRC

family kinases and, upon autophosphorylation, drive downstream activation of NF-κB, MAPK, and NFAT in lymphocytes, resulting in cellular activation, release of soluble effector molecules, and rapid proliferation[110]. Antibody production by B-cells hinges upon the function of BTK[109]. Whereas Th1, T-regulatory (Treg), and CD8 effector T-cells have both ITK and resting lymphocyte kinase (RLK, aka TXK) to drive activation, epigenetic evolution of Th2 and Th17 cells conserves a singular dominant role for ITK[109, 111-115]. This TEC- kinase profile difference provides an avenue to selectively target T-cell subsets that potentially are highly relevant to cGVHD. However, to date the individual impact of BTK or ITK on the development of cGVHD is unknown.

Ibrutinib is a first-in-class irreversible inhibitor of BTK and ITK that blocks downstream immune receptor activation[116-118]. Numerous *in vitro* and *in vivo* studies confirm the specific activity and clinical safety of ibrutinib for the treatment of specific TEC-kinase dependent malignancies[119-122]. Since ibrutinib can block the activation of B-cells via BTK inhibition as well as specific T-helper subsets that drive the development of cGVHD via ITK inhibition, we hypothesize that it may be ideally suited to the treatment of cGVHD.

To study the multifaceted effects of this inhibitor *in vivo* and interrogate the activity of both T and B-cells in the development of multi-organ systemic cGVHD*,* we used two complementary murine allogeneic HSCT models representing sclerodermatous and non-sclerodermatous cGVHD manifestations. Here, we show that ibrutinib treatment ameliorates the progression of cGVHD in the LP/J→C57BL/6 T-cell dependent murine model of sclerodermatous cGVHD,

reducing skin lesions, hair loss, and lymphohistiocytic infiltration[123]. Therapeutic administration of ibrutinib also proved effective at combating cGVHD in the C57BL/6→B10.BR model, which develops bronchiolitis obliterans syndrome (BO) and multi-organ cGVHD without skin involvement[36]. In this model, ibrutinib blocked germinal center (GC) formation and immunoglobulin (Ig) deposition, reduced tissue fibrosis, and reversed BO-associated pulmonary dysfunction. Genetic studies confirmed that ITK and BTK are independently critical for the development of cGVHD. These data strongly support the clinical investigation of ibrutinib as a novel therapeutic strategy for the treatment of cGVHD.

Results

Therapeutic administration of ibrutinib limits of the development of sclerodermatous lesions in a T-cell driven murine cGVHD model. To assess the efficacy of ibrutinib as a therapeutic intervention for cGVHD, we used the LP/J→C57BL/6 model of sclerodermatous cGVHD which develops dermal lesions characterized by hair loss, redness, flaking, scabbing, hunched posture, and thickened skin[123]. In this murine model, symptoms become apparent between days 20 and 25 and peak between days 37 and 47 after hematopoietic stem cell transplant (HSCT). Ibrutinib or vehicle treatment was initiated in randomized cohorts at day 25, after the initial signs of cGVHD (weight loss, hair loss, skin redness/flaking, hunched posture, or immobility) were visible in the majority (72%) of mice. Upon inspection at day 39 (14 days after starting therapy), ibrutinib-treated mice clearly lacked the sclerodermatous lesions, hair loss, hunched posture, and scabbing that were observed in both the vehicle and

cyclosporine treatment groups (Figure 1A). The development of cGVHD in this model was not effectively constrained by 10mg/kg/day cyclosporine (Supplementary Figure 1). Histology of representative skin lesions obtained at day 60 from vehicle- or cyclosporine-treated mice confirmed dermal fibrosis, epidermal hyperplasia, serocellular crusting, erosion, and lymphohistiocytic infiltration, which were not observed in skin samples from the ibrutinib-treated group (Figure 1B-C and Supplementary Figure 2-3).

Ibrutinib improves cGVHD progression-free survival and diminishes cGVHD.

To define cGVHD severity and progression in the LP/J→C57BL/6 model, we used a scoring system that quantitatively grades cGVHD metrics including: bodyweight, posture, mobility, hair loss, skin lesions, and vitality on a scale from 0 to 19 by a consistent and trained unbiased observer in a coded (blinded) manner[124]. Overall, 72% of mice (34 of 47) had active cGVHD on day 25 and the randomly assigned cohorts were very similar in initial (day 25) cGVHD score (ibrutinib = 1.5, vehicle =1, cyclosporine = 2.9). Using these metrics we found that mice treated with ibrutinib significantly reduced the overall intensity of cGVHD compared with vehicle treatment ($p=0.0184$) (Figure 2A and Supplementary Figure 4). Chronic GVHD progression in this model is defined as a >2 point increase in cGVHD score from the initiation of therapy. Data derived from two independent experiments show that ibrutinib significantly extended median time to cGVHD progression by 14 days; 33% (6 of 18) of ibrutinib treated mice remained progression-free as compared to 12% (2 of 18) of mice receiving

vehicle ($p<0.02$) (Figure 2B, and Supplementary Figure 5). During the study period, we observed 100% survival in the ibrutinib cohort compared with 82% and 88% survival for cyclosporine and vehicle groups, respectively (Supplementary Figure 6). Weekly evaluation of mouse body weights revealed little variation between groups (Supplementary Figure 7). To understand the sustained therapeutic benefits of ibrutinib and the potential for drug withdrawal we conducted an additional long-term therapeutic experiment (Figure 2C). Once again, in this separate experiment, ibrutinib significantly limited cGVHD progression as compared to vehicle control ($p=0.0019$). We also found that withdrawal of therapy at day 60 permitted breakthrough cGVHD in a single mouse (1 of 6); however this was not statistically significant. Analysis of internal cGVHD pathology within the pulmonary and renal tissues on day 75 suggested that continuous long-term ibrutinib was a more effective at controlling cGVHD (Supplementary Figures 8-9). Prophylactic ibrutinib treatment initiated pre-HSCT at day -2 and concluded at day 25 did not yield a significant improvement in cGVHD progression (Supplementary Figure 10).

Ibrutinib controls cGVHD-induced organ injury.

In addition to the externally measurable cGVHD metrics, we demonstrated that the LP/J→C57BL/6 model consistently develops pulmonary and renal cGVHD whereas other cGVHD pathologies are infrequently observed. Evaluation of H&E stained sections revealed that, compared with vehicle controls, ibrutinib therapy reduced cGVHD-related aggregation of lymphocytes, plasma cells, and histiocytes surrounding bronchioles and small caliber vessels throughout the

pulmonary parenchyma and within the renal interstitium. Immunohistochemistry revealed B220+ B-cell and CD3+ T-cell pulmonary infiltration in addition to CD3+ T-cell renal infiltration in both the vehicle and cyclosporine groups, which was not observed in ibrutinib treatment groups (Figure 3A and Supplementary Figure 11). Coded pathologic analysis confirmed that ibrutinib improved systemic cGVHD in this model (p=0.0099 for lung and p=0.0124 for kidney) (Figures 3B-C and Supplementary Figures 11).

Therapeutic administration of ibrutinib ameliorates pulmonary fibrosis and the development of bronchiolitis obliterans.

Chronic GVHD is characterized by a wide variety of autoimmune phenomena that are incompletely recapitulated by any single *in vivo* animal model. Recently published consensus criterion from the National Institutes of Health considers BO the only pathognomonic manifestation of cGVHD within the lung[17]. The C57BL/6→B10.BR model develops multi-organ system disease including BO starting at day 28 post-HSCT. Therapeutic administration of ibrutinib beginning at day 28 and continuing indefinitely curtailed the development of BO *in vivo* as measured by pulmonary resistance (p=0.0090), elastance (p=0.0019), and compliance (p=0.0071) (Figures 4A, B, and C). Masson trichrome staining of inflated pulmonary tissues from 4 mice derived from 3 experiments revealed less peribroncheolar collagen fibrosis among ibrutinib-treated animals (Figure 4D) and a significant reduction in pulmonary fibrosis (p<0.0001) (Figure 4E). We observed 100% survival in the ibrutinib cohort, versus 95% in the vehicle and 82% in the cyclosporine groups (Supplementary Figure 12). Weekly evaluation of mouse

body weight revealed little variation between groups. To examine the sustained benefit of ibrutinib therapy in this model we conducted a separate set of experiments where mice were withdrawn from ibrutinib on day 56 post transplant. Pulmonary function tests at day 60 and day 90 reveal that short-term ibrutinib therapy causes an eventual loss of benefit, supporting the need for continued therapy (Supplementary Figure 16). Day -2 to day 28 prophylactic administration of ibrutinib in this model also did not effectively combat cGVHD or BO (data not shown). Overall, these data indicate that ibrutinib therapy reduces the underlying fibrotic pathogenesis of BO in the C57BL/6→B10.BR cGVHD model.

Ibrutinib limits in vivo germinal center reactions and Ig deposition in pulmonary tissues.

Ibrutinib's ability to block BCR-induced activation of BTK is well defined; however, it remains unclear if GC reactions are effectively inhibited. To study this, we utilized the C57BL/6→B10.BR mouse model in which robust GC reactions sustain pathogenic B- lymphocytes and lead to Ig deposition within the liver and lungs and the development of BO. Peanut agglutinin staining revealed GC reactions within the spleen, and ibrutinib therapy reduced the overall size, cellularity, and number of GC reactions compared with vehicle treated mice with active cGVHD ($p<0.001$)(Figure 5A-B). On day 60 after HSCT, isolated splenocytes from chimeras were analyzed by flow cytometry for CD19+/GL7+/CD38lo germinal center B-cells. Ibrutinib significantly inhibited the cGVHD-induced formation of germinal centers within the spleen ($p=0.0222$) to numbers comparable to the no cGVHD, BM only control (Figure 5C).

The functional product of alloreactive GC B-cells is secreted Ig, which deposits within healthy tissues. In the C57BL/6→B10.BR cGVHD model, BO is inextricably related to the deposition of soluble Ig within pulmonary tissues and the fibrotic cascade that this initiates. By blocking B-cell reactivity, ibrutinib limited pulmonary deposition of Ig as quantified at day 60 post-HSCT using immunofluorescent microscopy (Figure 5D). Quantification of the immunofluorescent signal revealed elimination of pulmonary Ig deposition after therapeutic ibrutinib treatment ($p<0.001$) (Figure 5E). Together, these data confirm that a clinically relevant downstream effect of ibrutinib therapy in the setting of cGVHD is the blockade of Ig deposition within healthy tissues.

Genetic ablation of BTK or ITK activity in allogeneic donor cell engraftment confirms that both TEC kinases are required for the development of cGVHD.

The XID mouse in which the kinase activity of BTK is genetically abrogated and the Itk- /- mouse have been fully characterized on the C57BL/6 genetic background[125, 126]. Given ibrutinib's ability to inhibit both ITK and BTK, we sought to examine the relative independent contributions of ITK and BTK to the development of cGVHD. We therefore examined pulmonary function at day 60 after HSCT, as this represents a primary functional measurement of cGVHD-induced lung injury and fibrosis in the C57BL/6→B10.BR model.

Chronic GVHD sustaining T-cells in this model originate from mature lymphocytes in the donor cell graft. To recapitulate the effect of ITK inhibition

within these cGVHD causative T-lymphocytes, we administered Itk-/- splenic T-cells along with BM from wild- type mice to allogeneic recipients. Day 60 pulmonary function tests including resistance, elastance, and compliance were uniformly and significantly (p=0.0014; p=0.0028; p=0.0003) reduced in mice receiving Itk-/- vs. wild-type splenic T-cells and comparable to non-cGVHD, BM only controls. These data reveal that T-cell ITK activity is necessary for the development of cGVHD.

Data from both cGVHD models implicates hyper-reactive BTK. To genetically confirm the role of BTK signaling in cGVHD, we infused XID BM along with wild-type splenic T-cells to mimic BTK inhibition. Pulmonary function tests conducted at day 60 after HSCT revealed that BTK activity was essential to the development of BO (Figure 7). Pulmonary resistance, elastance, and compliance were significantly reduced in recipients of wild-type T cells and XID versus wild-type BM (p=0.0025; p=0.0025; p=00.496) and comparable to XID or wild- type BM only controls.

Ibrutinib blocks T and B-cell activation in samples obtained from patients with active cGVHD.

Our data confirm that BTK and ITK are critical to the development of cGVHD and that ibrutinib works to alleviate the symptoms associated with severe cGVHD in murine models. To confirm that this effect is not restricted to mouse models we tested the effects of ibrutinib on CD4-T and B-cells obtained from patients with active and persistent cGVHD. Data revealed that after pretreatment with 1μM

ibrutinib CD4 T-cells from these patients demonstrated lower surface expression of CD69 after *ex vivo* T-cell receptor (TCR) stimulation using anti-CD3 (p=0.033) (Figure 8A). Moreover, purified B- cells that were pretreated with 1μM ibrutinib showed lower levels of pBTK-Y223, pPLCγ2-Y1217, and pERK1/2 by immunoblot analysis (Figure 8B). These data confirm that ibrutinib can curtail immune receptor activation of human B and T-cells in the setting of active cGVHD.

Discussion

Chronic GVHD develops from coordinated effects of both B and T-cells, and multiple key functions of these cells are driven by TEC family kinases. Here, we show that that neither XID BM nor Itk-/- donor T-cells facilitate the development of systemic cGVHD in mice, identifying the importance of the TEC kinases BTK and ITK in cGVHD and identifying these two enzymes as therapeutic targets in this disease. Therefore, because of its ability to simultaneously target BTK and ITK, ibrutinib holds specific promise for the treatment of cGVHD. Our studies utilize two distinct but complementary, validated murine models of cGVHD; one that has dominant sclerodermatous features, and the other with a non-sclerodermatous, multi-organ system fibrotic disease with BO[36, 123]. Our results indicate that ibrutinib targets B and T-cell driven GC responses and is remarkably effective in treating cGVHD. In the sclerodermatous model, animals receiving therapeutic ibrutinib were often indistinguishable from their healthy counterparts, and in the non-sclerodermatous cGVHD model, no cGVHD manifestations were evident even at the end of the observation period. Moreover, GC reaction size,

cellularity, and number were lower in mice receiving ibrutinib, correlating to a partial but significant resolution of cGVHD symptoms. These data are consistent with preclinical data in which GC reactions are key to cGVHD pathogenesis; for instance, clinical responses to rituximab (anti-CD20 mAb) have been observed, implicating B cells as etiopathogenic in human cGVHD[45, 127]. Finally, we confirmed that our observation could be applied to human therapy by testing ibrutinib's capacity to block the molecular activation of T-cells and B-cells directly obtained from patients with active ongoing cGVHD.

our genetic ablation models reveal that BM-derived B cells are dependant upon BTK for GC formation. Similarly, Itk-/- splenocytes are unable to cause cGVHD, suggesting that ITK is critical for T-cell support of the fibrotic cascade. While XID and Itk-/- mice are useful in exploring the mechanisms responsible for cGVHD generation, there are caveats. For instance, TEC kinase can compensate for the lack of BTK in the XID mouse model, and complete genetic ablation of ITK blunts thymic maturation of functionally mature T-lymphocytes[128, 129]. As a result, we can conclude that ITK and BTK are necessary components for the development of cGVHD; however we cannot conclude that ibrutinib's therapeutic efficacy is solely driven by inhibition of these two TEC kinases.

In the cGVHD model that has BO as an important feature, fibrosis occurs by day 28 post-HSCT. Intriguingly, ibrutinib treatment beginning day 28 after HSCT in mice with established cGVHD resulted in resolution of fibrosis, suggesting that treatment in the early phase of cGVHD can permit tissue repair and further suggesting that ongoing antibody deposition in cGVHD target organs may be

required for a persistent fibrogenic process. Notably, for patients with debilitating cGVHD from fibrosis, therapies include supportive care, high dose steroids, rapamycin, mycophenolate, imatinib, extra-corporal photopheresis, IL-2 and lung transplant, all with incomplete efficacy and potentially serious complications[130, 131]. Although conclusions from rodent cGVHD must be validated in patients, our studies collectively indicate that a wide spectrum of cGVHD patients may benefit from ibrutinib therapy.

To examine the importance of sustained therapy we conducted studies using both cGVHD models in which mice were withdrawn from ibrutinib therapy around day 60 post HSCT. In general, we observed a loss of efficacy with removal of the drug, however not all metrics were statistically significant. These data are consistent with our molecular understanding which would imply that pathogenic T-cells and B-cells are restrained by the inhibitor but not actively depleted. Overall, these data would direct caution in the clinical setting when attempting to taper such an inhibitor.

To study prophylactic efficacy, we initiated ibrutinib treatment two days prior to HSCT and continued until we begin to observe cGVHD (approximately 28 days). Although post-transplant administration of ibrutinib effectively controlled cGVHD, we found that prophylactic treatment was ineffective under these conditions. The ideal time frame for ibrutinib administration may coincide with the establishment of robust T-cell driven GC reactions that may take up to 1 month; prophylactic treatment alone may be ineffective for this reason. Furthermore, unlike rituximab, ibrutinib does not directly kill B-cells; instead it prevents downstream BCR

activation, arresting cells in an unstimulated state. This effect can be lost after withdrawal of ibrutinib. Together, our data indicate that ibrutinib is likely to be better for cGVHD therapy as opposed to prophylaxis, should preclinical studies translate into the clinic.

Our studies focus on ibrutinib's effect on cGVHD; however the effects on infectious complications and leukemic relapse remain unanswered. Recent mouse and human studies indicate that ibrutinib improves the immune competence with regard to infectious complications, however this has yet to be tested in the HSCT setting[118, 121]. Ibrutinib also has direct anti-leukemic effects in both B-cell derived tumors and AML supporting the notion that it may directly aid in relapse prevention[132, 133].

Overall, our complementary *in vivo* models demonstrate a clear therapeutic benefit derived from therapeutic administration of ibrutinib to reduce the prolonged autoimmune effects of cGVHD. In addition, our ex vivo human data suggest that these conclusions likely extend to the setting of human cGVHD. These data support the future study of this promising therapeutic agent in cGVHD as well as the exploration of novel strategies which target specific TEC kinases in the setting of allo-HSCT.

Methods

Mice: C57BL/6 (H2b) mice were purchased from the National Cancer Institute or from The Jackson Laboratory (Bar Harbor, Maine). LP/J and B10.BR (H2k) mice were purchased from The Jackson Laboratory. The C57BL/6 XID mouse, in

which a specific mutation abrogates BTK kinase activity, was obtained from The Jackson Laboratory. The C57BL/6 Itk-/- mouse was a kind gift from Dr. Leslie Berg (University of Massachusetts)(58). Both strains are maintained on the defined C57BL/6 genetic background. All mice were housed in a pathogen-free facility at The Ohio State University or The University of Minnesota and used with the protocol approval of the respective institutional animal care committees.

Therapeutic HSCT models: The C57BL/6→B10.BR model has been described previously(7). In brief, B10.BR recipients conditioned with 120mg/kg/day I.P. cyclophosphamide (Cy) on days -3 and -2 and 8.3 Gy TBI (using a 137 Cesium irradiator) on day -1 were engrafted with $1X10^7$ Thy1.2 depleted C57BL/6 derived bone marrow (BM) cells with (or without) $1X10^6$ allogeneic splenocytes. Experiments with the LP/J→C57BL/6 model were conducted using similar methods to those previously described. Briefly, C57BL/6 recipients were conditioned with 8.5Gy X-ray TBI on day 0 and were provided $1X10^7$ LP/J-derived bone marrow (BM) cells and $2X10^6$ splenocytes by tail-vein injection. Mice surviving to day 25 begin to show clinical and pathologic changes consistent with systemic cGVHD frequently involving the skin, lung, and kidneys, and infrequently involving hepatic or salivary gland lymphohistiocytic infiltration, conjunctivitis, anterior uveitis, esophagitis and corneal ulcers. In our hands, this specific splenocyte and irradiation dose produces a cGVHD phenotype, devoid of the classic gastrointestinal lesions, splenic atrophy, or diarrhea associated with aGVHD. The development of cGVHD was measured in coded fashion using a modified version of the scoring system originally described by Cooke et al.

(Supplementary Table 1).Therapeutic administration of ibrutinib (kindly provided by Pharmacyclics, Inc.) via drinking water was conducted as previously described(27). Mice received a dose of 15 mg/Kg/day ibrutinib in 0.4% methylcellulose by intraperitoneal (IP) injection starting day 28 post-transplant for the C57BL/6→B10.BR model or 25 mg/kg/day via drinking water starting at day 25 post-transplant for the LP/J→C57BL/6 model. Drinking water administration daily dose was calculated previously. In the latter strain combination, a cohort of mice was given cyclosporine A administered IP in 0.2% CMC at 10 mg/kg/day starting at day 25 for 2 weeks followed by thrice weekly as previously described. Unless otherwise stated, ibrutinib was administered until the end of the study. For both cGVHD models the BTK pathway was found to be constitutively activated, similar to what has been identified in human cGVHD, and ex-vivo ibrutinib treatment yielded attenuation of this signaling pathway (Supplementary Figure 11).

Pulmonary function tests: Pulmonary function tests (PFTs) were performed on anesthetized mice using whole-body plethysmography with the Flexivent system (SCIREQ) as previously described.

Germinal Center (GC) detection: GC detection was conducted using 6 μm spleen cryosections stained using rhodamine peanut agglutinin as previously described.

Masson trichrome staining: Cryosections (6 μM) were fixed for 5 minutes in acetone and stained with hematoxylin and eosin and with the Masson trichrome

staining kit (Sigma, St. Louis MO) for detection of collagen deposition. Collagen deposition was quantified on trichrome stained sections as a ratio of area of blue staining to area of total staining using the Adobe Photoshop CS3 analysis tool.

Histopathological scoring: Coded pathologic analysis of H&E stained sections was performed by APM or BKH in an unbiased manner with scores ranging from 0 to 4(60). For pulmonary tissues, scores indicate the number of lymphoplasmacytic and histiocytic cellular cuffs infiltrating the surrounding airways or vasculature and the number of infiltrating aggregates. For renal H&E stained sections, both perivascular lymphoplasmacytic infiltration and intratubular protein were quantified. For additional details see supplementary methods.

Immunoblot analysis: Experiments were conducted using conventional methodology previously described. Blotting was conducted using pBTK-Y223, BTK, pPLCγ2- Y1217, PLCγ2, pERK1/2, ERK, and GAPDH (Cell Signaling Technologies, Danvers, MA) specific antibodies.

Statistical analysis: A two-tailed Student's T-test was used for normal data at equal variance. Significance was considered for $p<0.05$. For cGVHD scoring in the LP/J→C57BL/6 model, a linear mixed effects model was applied to assess the trends in cGVHD scores from days 33 – 52, using the measurement at day 25 as a covariate to account for differences in the initial measurement between treatments. Chronic GVHD progression in the LP/J→C57BL/6 model was prospectively defined as a >2 point increase in cGVHD score from the initiation of therapy.

Acknowledgements

The authors gratefully acknowledge Dr. Leslie J. Berg for providing critical reagents as well as Jessica MacMurray for experimental assistance. This work was supported by grants from the National Institutes of Health (P01 AI056299, P01 CA142106, R01 HL56067 and R01 AI34495) (B.R.B.) and T32 AI1007313 (R.F.). In addition, support was provided by NCI grants (P01 CA095426, K12 CA133250-05, and P50 CA140158) (J.C.B), and T32 CA009338-33-03 (JAD), as well as the American Cancer Society (125039-PF-13-246-01-LIB; J.A.D), the Leukemia & Lymphoma Society, the American Society of Hematology, Mr. and Mrs. Michael Thomas, the Harry Mangurian Foundation, the D. Warren Brown Family Foundation, and the Jock and Bunny Adams Research and Education Endowment (J.H.A.)

Authorship

JAD and RAF authored the manuscript and planned, organized, and performed the research. JD, BKH, YZ, CY, BK, and WT performed experiments; AL, HKW, AJ, NM, SD, SJ, JS, LE, WJM, DHM, LL, IM, JK, CC, RJS, JHA, JR, and AP-M supervised the research; JCB and BRB supervised the research, reviewed the manuscript, and obtained funding.

Conflict-of-interest disclosure: patents have been submitted on behalf of JCB, JAD, RAF, and BRB to cover the findings in this paper.

Figure Legends

Figure 1: Scleroderma and skin manisfestations of cGVHD are alleviated by ibrutinib therapy. At day 25 mice post-HSCT a total of 18 mice (from two independent experiments) were randomly assigned to ibrutinib (25mg/kg/day), 18 to vehicle, or 11 to cyclosporine (10mg/kg/day). Sclerodermatous lesions, hair loss, hunched posture, and gaunt appearance are characteristic visual indicators of cGVHD in this model. A) Representative visual analysis of 4 randomly selected mice at day 39 post-HSCT. B) H&E stained skin preparations of sclerodermatous skin lesions showing levels of dermal fibrosis, epidermal hyperplasia, serocellular crusting, erosion, and lymphohistiocytic infiltration, consistent with cGVHD. C) Pathologic cGVHD involvement of the skin was independently assessed on a scale from 0 to 8 for each mouse. Cohort averages are displayed, *=$p<0.05$, error bars = S.E.M.

Figure 2: Ibrutinib inhibits autoimmune manifestations of cGVHD. A) Weekly blinded analysis of cGVHD external metrics including weight, posture, vitality, mobility, coat, and skin in all mice from two independent experiments (18 vehicle, 18 ibrutinib, and 11 cyclosporine) (Supplementary Table 1). All cGVHD scores were corrected for individual scores at the beginning of treatment (day 25). Error bars = s.e.m. *=$p<0.01$ B) Kaplan Meier plot of cGVHD progression free survival. Data is derived from two independent experiments. Progression is defined a >2 point increase in day 25 cGVHD score (Supplementary Table 1) *=$p<0.01$. C) Kaplan Meier plot of cGVHD progression free survival in an independent experiment aimed to determine sustained benefits from continued ibrutinib

therapy. During the course of the experiment ibrutinib was withdrawn on day 60 from animals in the Ibrutinib Short Course cohort. **=p<0.001.

Figure 3: Ibrutinib therapy prevents autoimmune injury in a T-cell dependent model of cGVHD. A) Representative 20X images from H&E, B220, or CD3 stained lung and kidney tissues from mice sacrificed at day 125 post-HSCT from 6 mice/group. Images were taken by a trained veterinary pathologist who was blinded to animal cohorts. B) Blinded pathologic analysis of H&E stained lung tissues obtained from cGVHD cohorts (18 vehicle and 18 ibrutinib). Lymphohistiocytic infiltration was graded on a 0-4 scale for each animal. C) Blinded pathologic analysis of H&E stained kidney tissues obtained from cGVHD cohorts. Portal hepatitis and vasculitis was graded on a 0-4 scale for each animal. **=p<0.01, *=p<0.05.

Figure 4: Collagen deposition and pulmonary function are improved in a murine model of bronchiolitis obliterans. A-C) PFTs were performed at day 60 post- transplant on anesthetized animals. Animals (n=4/group) were artificially ventilated and A) resistance, B) elastance, and C) compliance were measured as parameters of distress in lung function in animals receiving $5x10^6$ splenocytes (S) in addition to bone marrow (BM). Error bars = s.e.m. D) and E) Collagen deposition within pulmonary tissues was determined with a Masson trichrome staining kit; blue indicates collagen deposition. D) Representative images of collagen deposition observed in each treatment cohort (n=8) Blue staining represents Masson Trichrome stained collagen. E) Quantification of collaged

deposition (n=8) as a ratio of blue area to total area of tissue was performed with the analysis tool in Photoshop CS3. Representative data from 3 independent experiments.

Figure 5: Germinal center reactions and pulmonary immunoglobulin deposition are reduced with administration of ibrutinib. A) Germinal centers were imaged by staining 6 um spleen sections with PNA conjugated to rhodamine (red) and DAPI (blue). B) Germinal center area (GC/mm^2) was calculated from PNA stained immunofluorescent images for each animal. The average area for each cohort is displayed. Error bars = s.e.m. C) Splenocytes were purified from transplanted mice on day 60 and frequency of germinal center B cells was quantified. D) 6μm lung sections from day 60 transplanted mice were stained with anti-mouse Ig conjugated to FITC (green) and DAPI (blue) and E) quantified with Adobe Photoshop CS3. Representative data from 3 independent experiments. For all graphs *= $p<0.05$, **=$p<0.001$. All measurements were conducted on day 60 post HSCT.

Figure 6: Development of BO is dependent on ITK expression in donor mature T cells. A) Day 60 pulmonary function tests Mice transplanted with WT bone marrow and low numbers of either WT T-cells or ITK deficient T cells. B) Pathologic scores in lung, liver and spleen of day 60 transplanted mice. n= 5 mice/group in 2 independent experiments.

Figure 7: Expression of BTK in donor-derived B cells is necessary for the development of BO. A) Day 60 pulmonary function tests from mice transplanted

with low levels of WT T-cells and either WT or XID (kinase inactive BTK) bone marrow. B) Pathology of lung, liver, and spleen of day 60 transplanted mice. n=5 mice/group from 2 independent experiments.

Figure 8: Ibrutinib limits activation of T-cells and B-cells from patients with active cGVHD. A) Primary CD4+ T-cells were isolated from patients with active cGVHD, pretreated with 1μM ibrutinib (or DMSO), and stimulated using anti-CD3 for 6 hours. Graph shows the mean florescent intensity (MFI) for CD69 amongst CD4+ T-cells for each patient. *=$p<0.05$. B) B-cells isolated from patients with cGVHD were pretreated with 1μM ibrutinib and stimulated with anti-IgM for 45 minutes. Immunoblot analysis of BTK, ERK, and PLCγ2 was conducted. The densitometric quantification of activated proteins relative to total proteins is provided. Data are representative of three experiments on three separate patients.

Supplementary Figure 1: At day 25 mice post-HSCT a total of 18 mice (from two independent experiments) were randomly assigned to ibrutinib (25mg/kg/day), 18 to vehicle, or 11 to cyclosporine (10mg/kg/day). Sclerodermatous lesions, hair loss, hunched posture, and gaunt appearance are characteristic visual indicators of cGVHD in this model. Representative visual analysis of 4 randomly selected mice at day 39 post-HSCT.

Supplementary Figure 2: H&E stained skin preparations of sclerodermatous skin lesions showing levels of dermal fibrosis, epidermal hyperplasia, serocellular crusting, erosion, and lymphohistiocytic infiltration, consistent with cGVHD.

Supplementary Figure 3: cGVHD involvement of the skin was assessed by a trained observer in a blinded fashion on a scale from 0 to 8. Cohort averages are displayed.

Supplementary Figure 4: Weekly blinded analysis of cGVHD external metrics including weight, posture, vitality, mobility, coat, and skin in all mice from two independent experiments (18 vehicle, 18 ibrutinib, and 11 cyclosporine) (Supplementary Table 1). All cGVHD scores were corrected for individual scores at the beginning of treatment (day 25). Error bars = s.e.m. *=$p<0.01$

Supplementary Figure 5: Kaplan Meier plot of cGVHD progression free survival. Progression is defined a >2 point increase in day 25 cGVHD score (Supplementary Table 1) *=$p<0.01$

Supplementary Figure 6: Kaplan Meier plot of overall survival for vehicle, ibrutinib, or cyclosporine treatment groups.

Supplementary Figure 7: Weekly bodyweight measurements for vehicle, ibrutinib, and cyclosporine treatment groups. Bodyweight was calculated to the nearest 0.1 gram at a similar time each day. Error bars = s.e.m., samples derived from two independent experiments.

Supplementary Figure 8: Blinded pathologic analysis of H&E stained lung tissues obtained from cGVHD cohorts derived from the sustained benefit experiment on day 75 post HSCT. Lymphohistiocytic infiltration was graded on a 0-4 scale for each animal. *=$p<0.05$.

Supplementary Figure 9: Blinded pathologic analysis of H&E stained kidney tissues obtained from cGVHD cohorts derived from the sustained benefit experiment on day 75 post HSCT. Portal hepatitis and vasculitis was graded on a 0-4 scale for each animal. *=$p<0.05$, **=$p<0.01$.

Supplementary Figure 10: Prophylactic treatment of cGVHD. 2-days prior to HSCT mice are randomly assigned to ibrutinib (25mg/kg/day), vehicle, or cyclosporine (10mg/kg/day) groups. Weekly blinded analysis of cGVHD external metrics including weight, posture, vitality, mobility, coat, and skin (Supplementary Table 1). All cGVHD scores were corrected for individual scores at the beginning of treatment (day -2). Error bars = s.e.m.

Supplementary Figure 11: Representative 20X images from H&E, B220, or CD3 stained lung and kidney tissues from mice sacrificed at day 125 post-HSCT from 6 mice/group. Images were taken by a trained veterinary pathologist who was blinded to animal cohorts. Blinded pathologic analysis of H&E stained lung tissues obtained from cGVHD cohorts (18 vehicle, 18 ibrutinib, and 11 cyclosporine). Lymphohistiocytic infiltration was graded on a 0-4 scale for each animal. *=$p<0.05$, **=$p<0.01$. Blinded pathologic analysis of H&E stained kidney tissues obtained from cGVHD cohorts. Portal hepatitis and vasculitis was graded on a 0-4 scale for each animal. *=$p<0.05$.

Supplementary Figure 12: PFTs were performed at day 60 or day 90 post-transplant on anesthetized animals to understand sustained benefits. Animals were artificially ventilated and resistance, elastance, and compliance were

measured as parameters of distress in lung function in animals receiving $5x10^6$ splenocytes (S) in addition to bone marrow (BM). Treatment cohorts were administered vehicle or ibrutinib starting on day 28 and ending on day 56 post transplant; Error bars = s.e.m

Figure 1

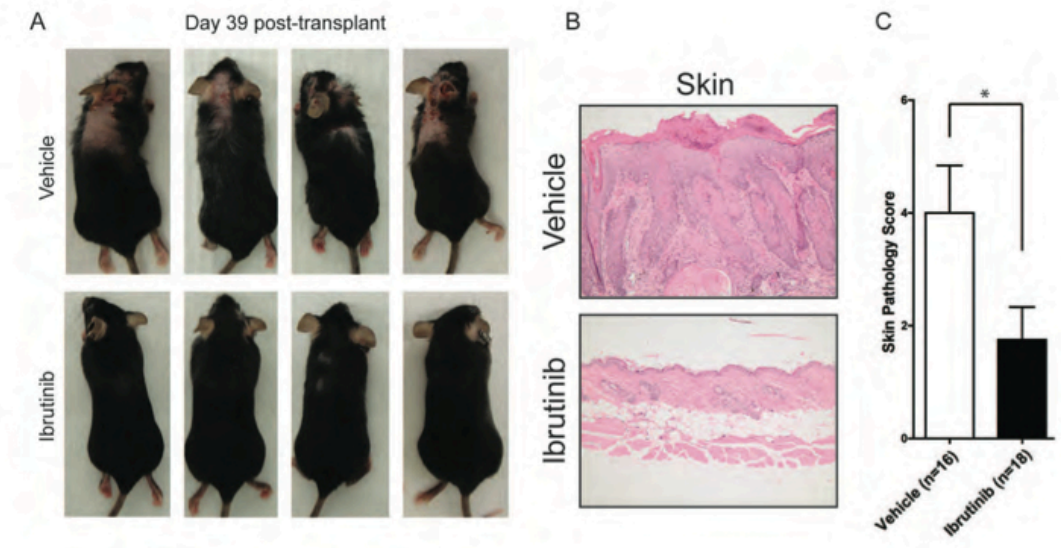
A
Day 39 post-transplant
Vehicle
Ibrutinib
B
Skin
Vehicle
Ibrutinib
C
Skin Pathology Score
*
0
2
4
6
Vehicle (n=16)
Ibrutinib (n=18)

Figure 2

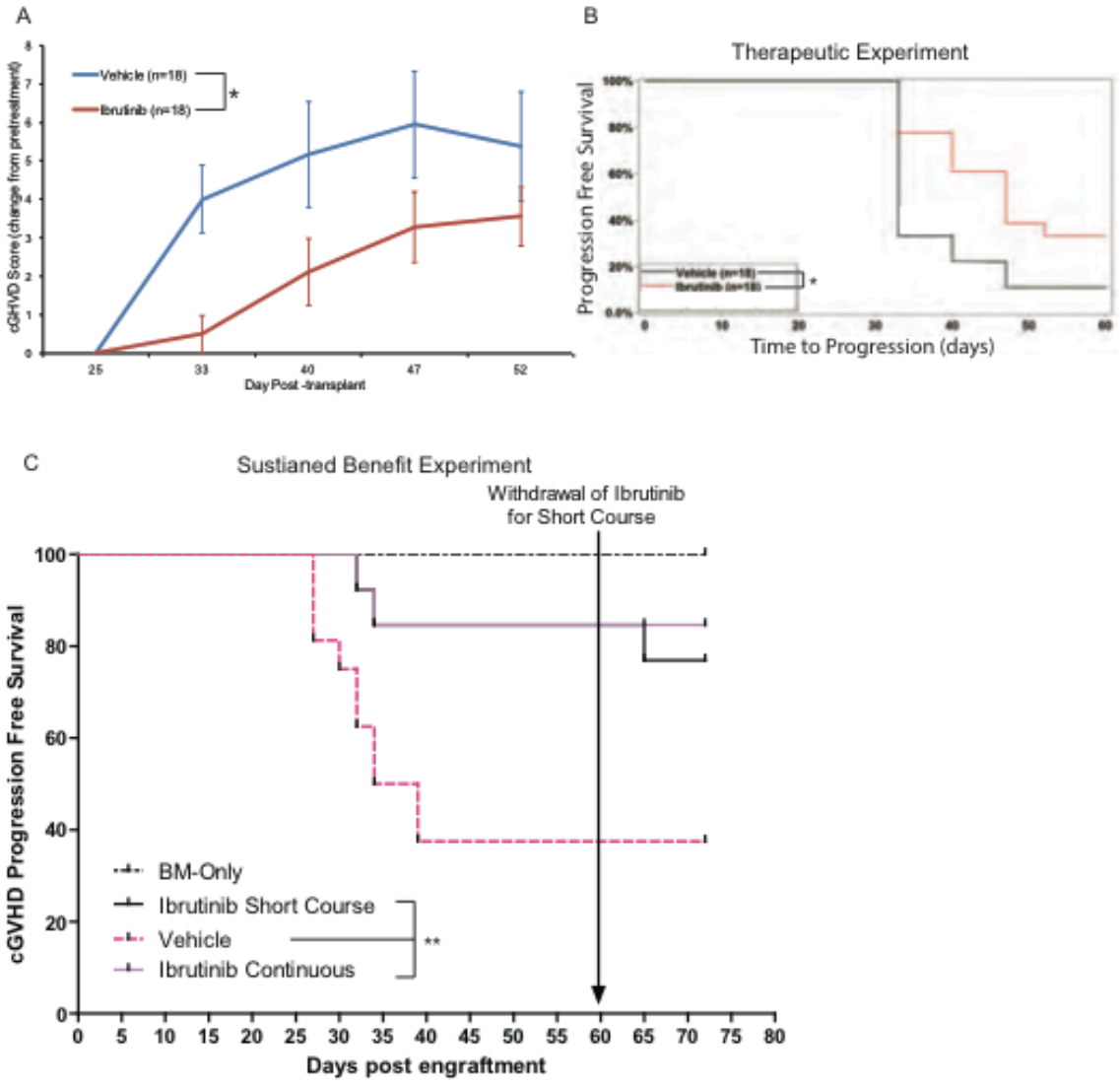
A
Vehicle (n=18)
Ibrutinib (n=18)
*
cGVHD Score (change from pretreatment)
Day Post -transplant
B
Therapeutic Experiment
Progression Free Survival
Time to Progression (days)
C
Sustianed Benefit Experiment
Withdrawal of Ibrutinib
for Short Course
cGVHD Progression Free Survival
BM-Only
Ibrutinib Short Course
Vehicle
Ibrutinib Continuous
**
Days post engraftment

Figure 3

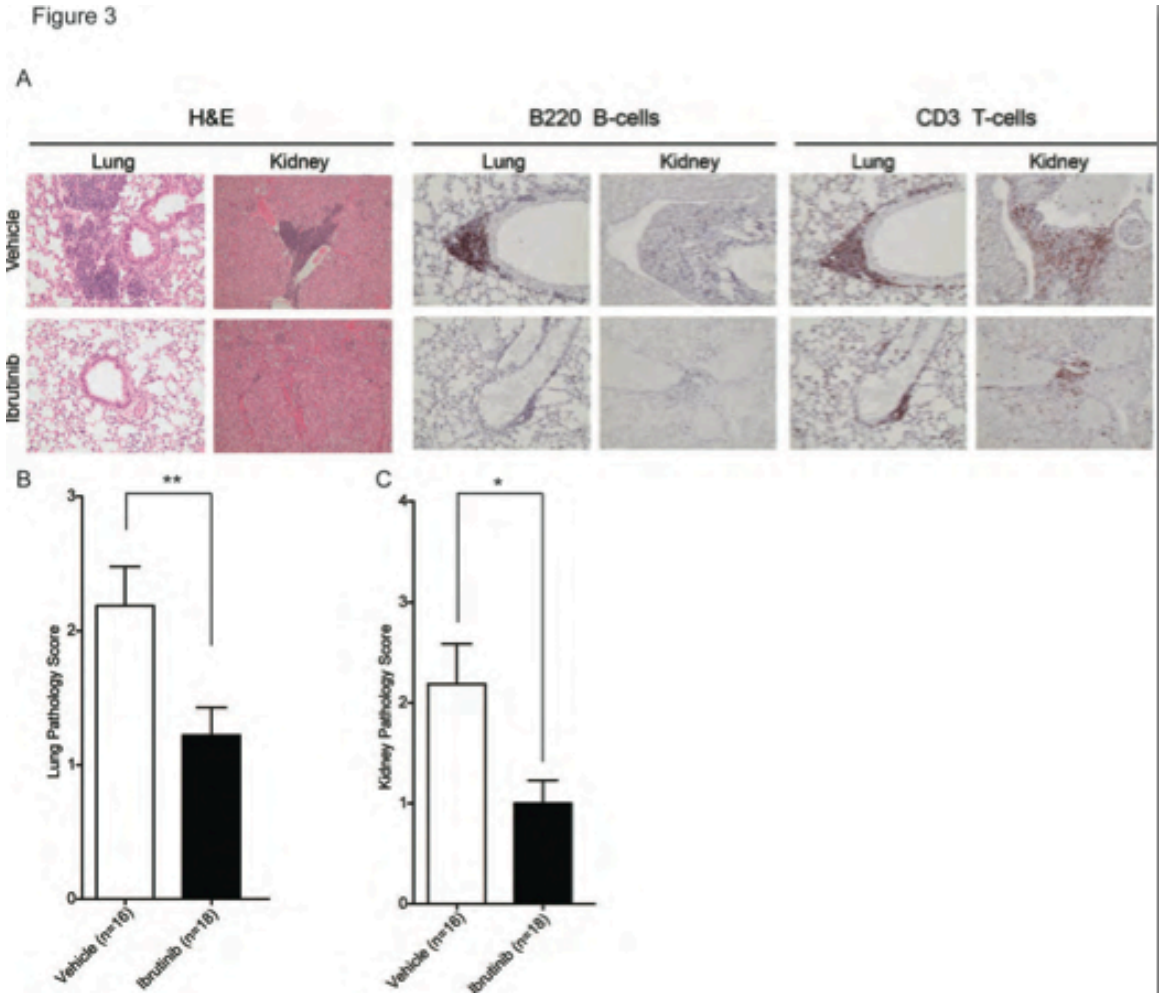
A
H&E
B220 B-cells
CD3 T-cells
Lung
Kidney
Lung
Kidney
Lung
Kidney
Vehicle
Ibrutinib
B
**
Lung Pathology Score
Vehicle (n=16)
Ibrutinib (n=18)
C
*
Kidney Pathology Score
Vehicle (n=16)
Ibrutinib (n=18)

Figure 4

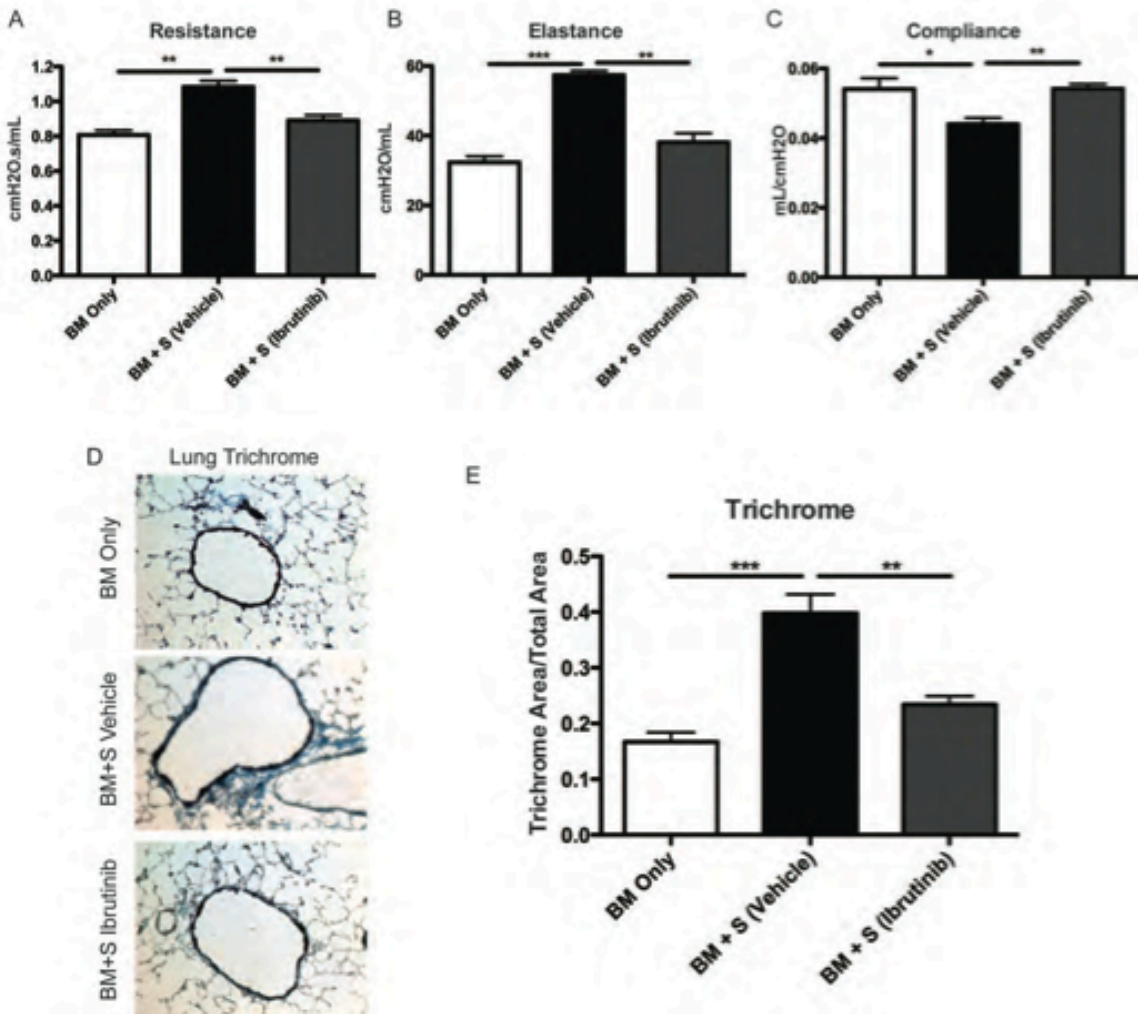
A
Resistance
cmH2O.s/mL
1.2
1.0
0.8
0.6
0.4
0.2
0.0
**
**
BM Only
BM + S (Vehicle)
BM + S (Ibrutinib)
B
Elastance
cmH2O/mL
60
40
20
0
***
**
BM Only
BM + S (Vehicle)
BM + S (Ibrutinib)
C
Compliance
mL/cmH2O
0.06
0.04
0.02
0.00
*
**
BM Only
BM + S (Vehicle)
BM + S (Ibrutinib)
D
Lung Trichrome
BM Only
BM+S Vehicle
BM+S Ibrutinib
E
Trichrome
Trichrome Area/Total Area
0.5
0.4
0.3
0.2
0.1
0.0
***
**
BM Only
BM + S (Vehicle)
BM + S (Ibrutinib)

Figure 5

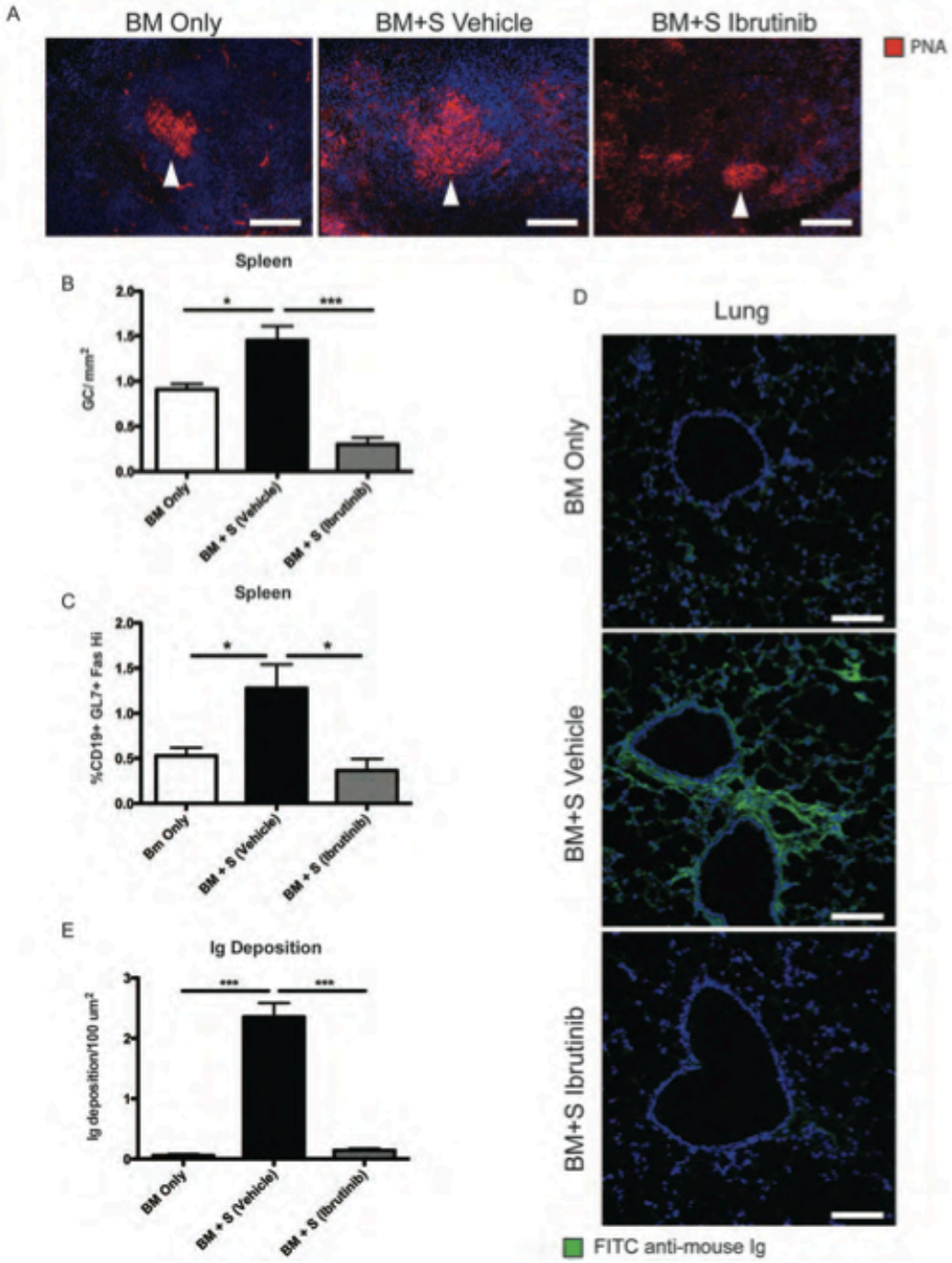
A
BM Only
BM+S Vehicle
BM+S Ibrutinib
PNA
Spleen
B
GC/ mm²
BM Only
BM + S (Vehicle)
BM + S (Ibrutinib)
Spleen
C
%CD19+ GL7+ Fas Hi
Bm Only
BM + S (Vehicle)
BM + S (Ibrutinib)
E
Ig Deposition
Ig deposition/100 um²
BM Only
BM + S (Vehicle)
BM + S (Ibrutinib)
D
Lung
BM Only
BM+S Vehicle
BM+S Ibrutinib
FITC anti-mouse Ig

Figure 6

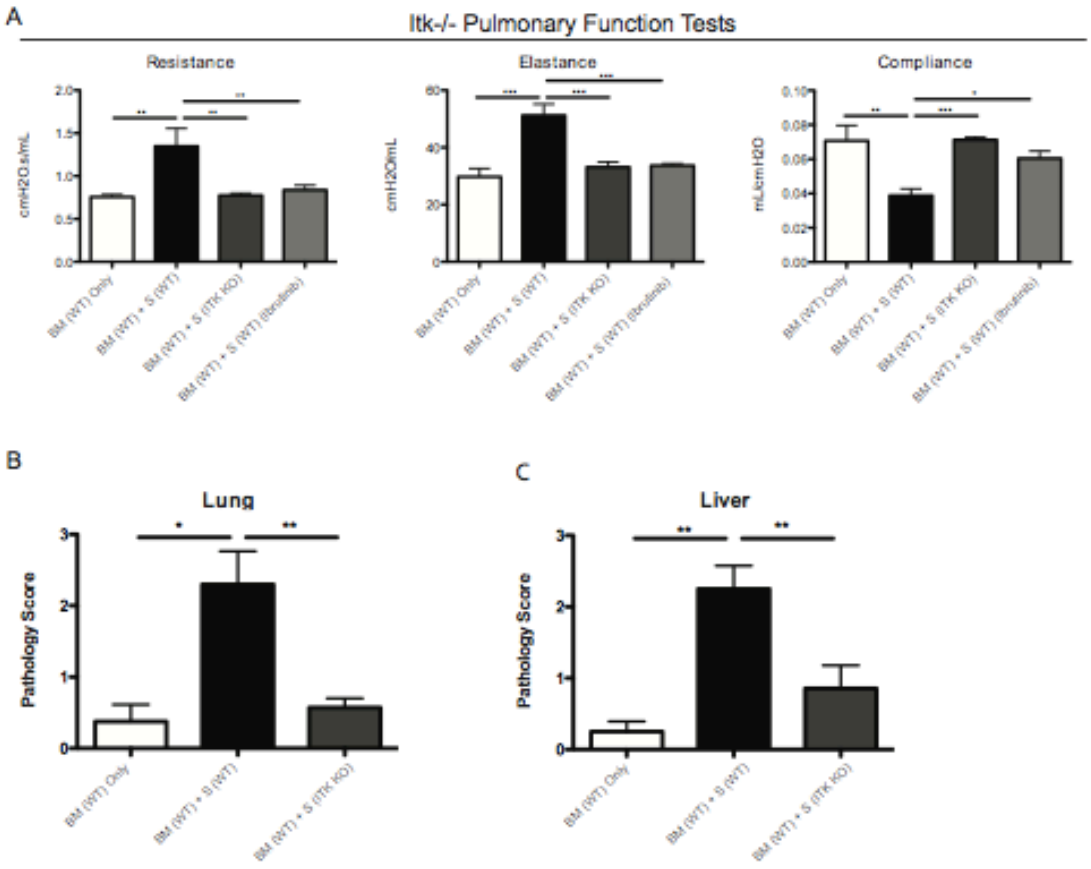
A
Itk-/- Pulmonary Function Tests
Resistance
Elastance
Compliance
cmH2Os/mL
cmH2O/mL
mLcmH2O
BM (WT) Only
BM (WT) + S (WT)
BM (WT) + S (ITK KO)
BM (WT) + S (WT) (Ibrutinib)
B
Lung
Pathology Score
C
Liver
Pathology Score

Figure 7

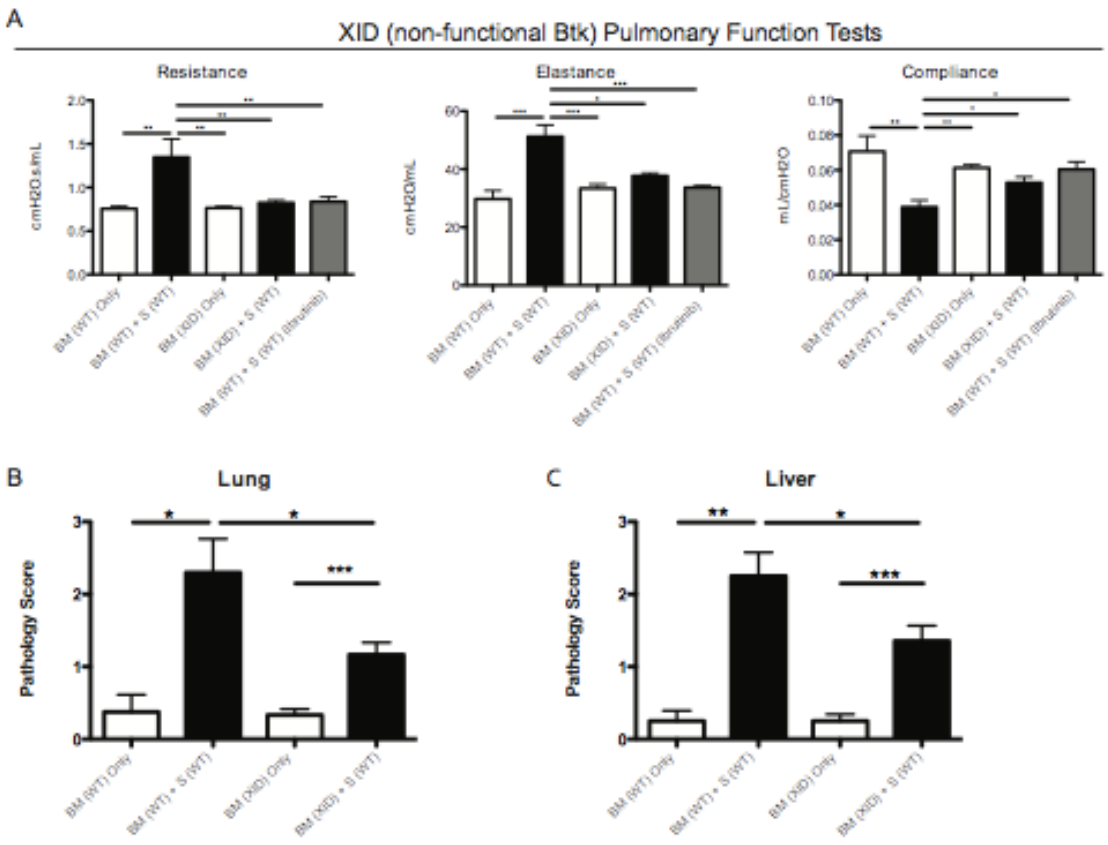
A
XID (non-functional Btk) Pulmonary Function Tests
Resistance
Elastance
Compliance
cmH2O·s/mL
cmH2O/mL
mL/cmH2O
BM (WT) Only
BM (WT) + S (WT)
BM (XID) Only
BM (XID) + S (WT)
BM (WT) + S (WT) (Ibrutinib)
B
Lung
C
Liver
Pathology Score

Figure 8

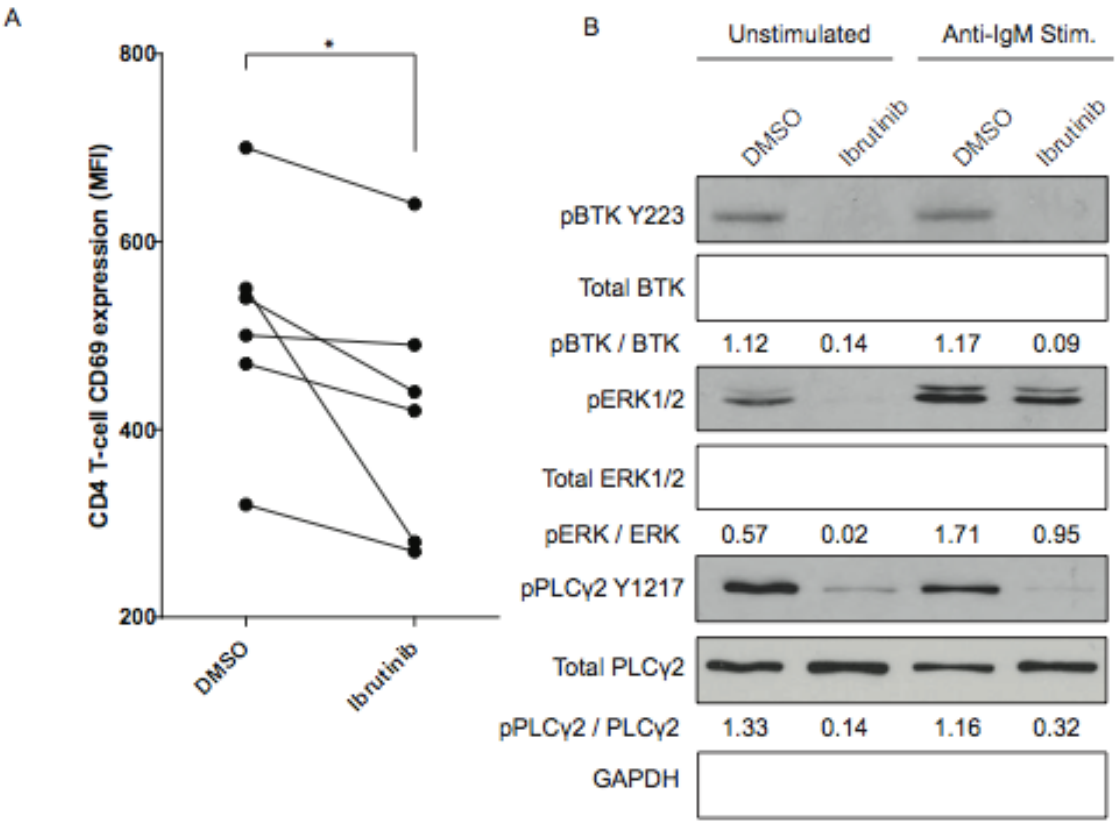
A
800
600
400
200
CD4 T-cell CD69 expression (MFI)
*
DMSO
Ibrutinib
B
Unstimulated
Anti-IgM Stim.
DMSO
Ibrutinib
DMSO
Ibrutinib
pBTK Y223
Total BTK
pBTK / BTK
1.12
0.14
1.17
0.09
pERK1/2
Total ERK1/2
pERK / ERK
0.57
0.02
1.71
0.95
pPLCγ2 Y1217
Total PLCγ2
pPLCγ2 / PLCγ2
1.33
0.14
1.16
0.32
GAPDH

Supplementary Figure 1

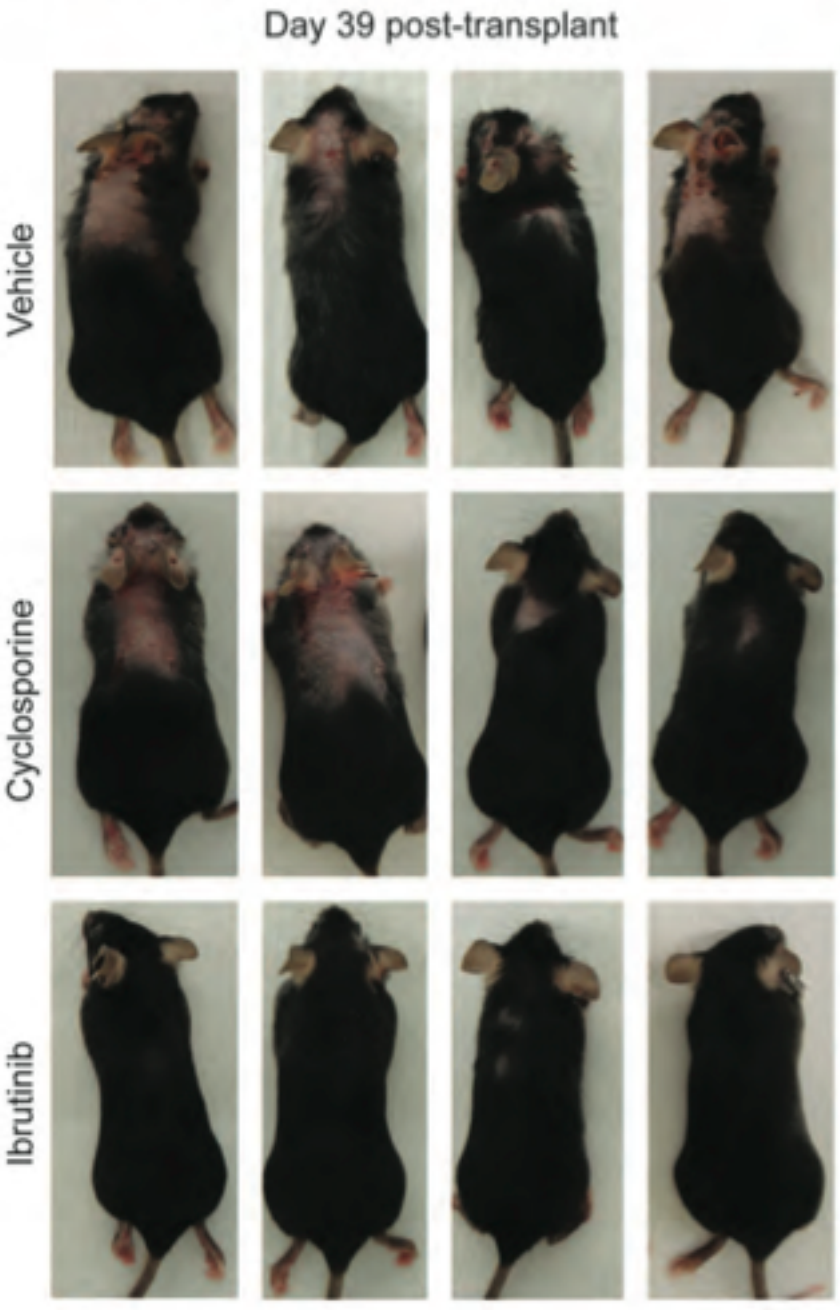

Supplementary Figure 2

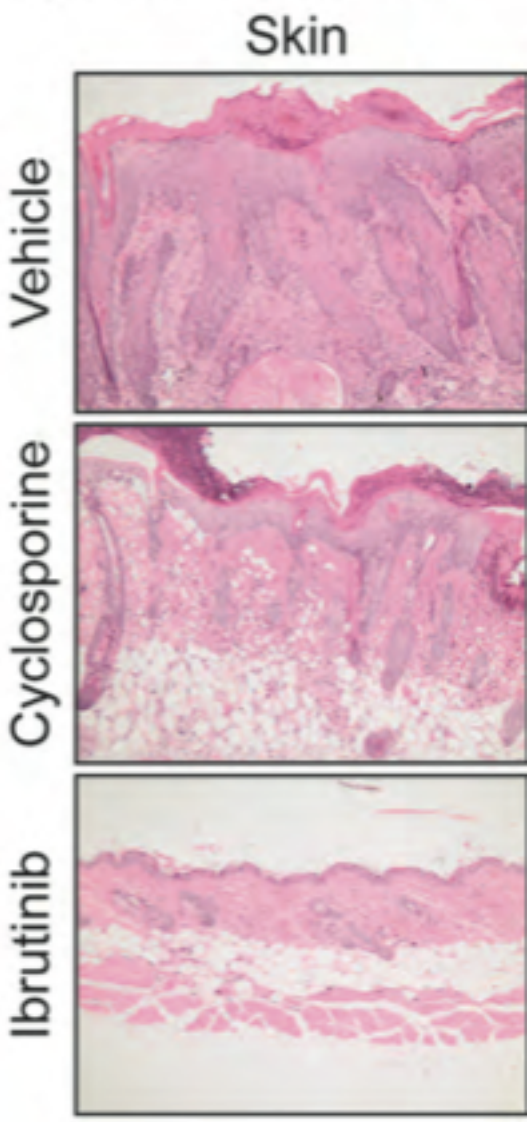

Supplementary Figure 3

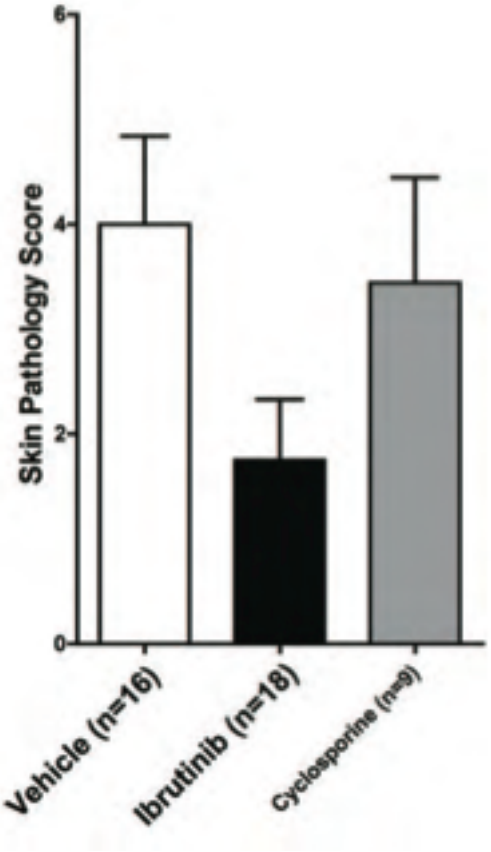

Supplementary Figure 4

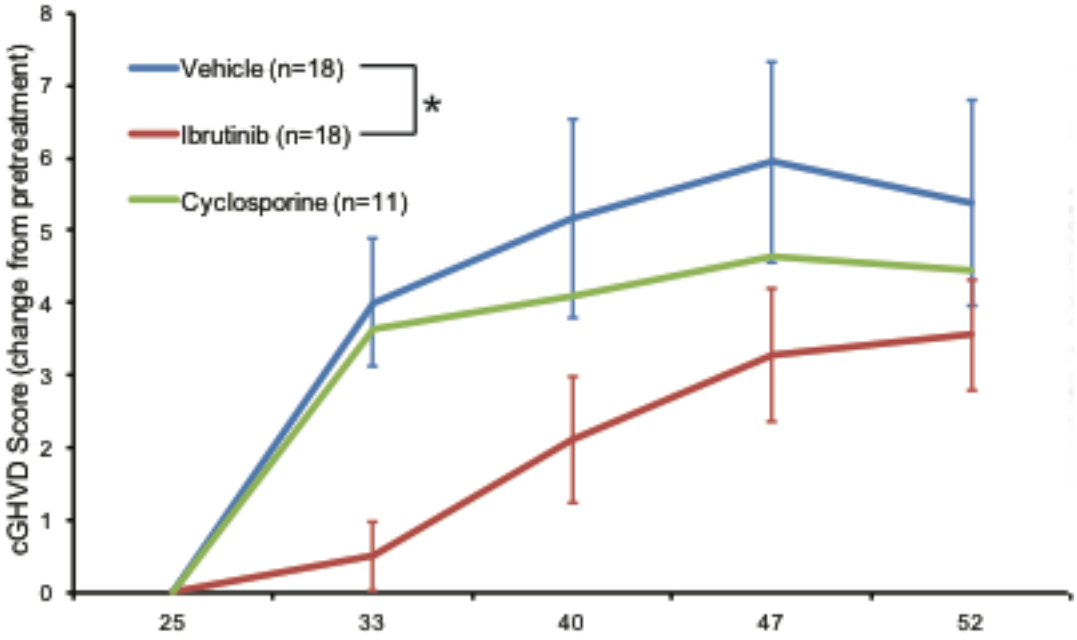

Supplementary Figure 5

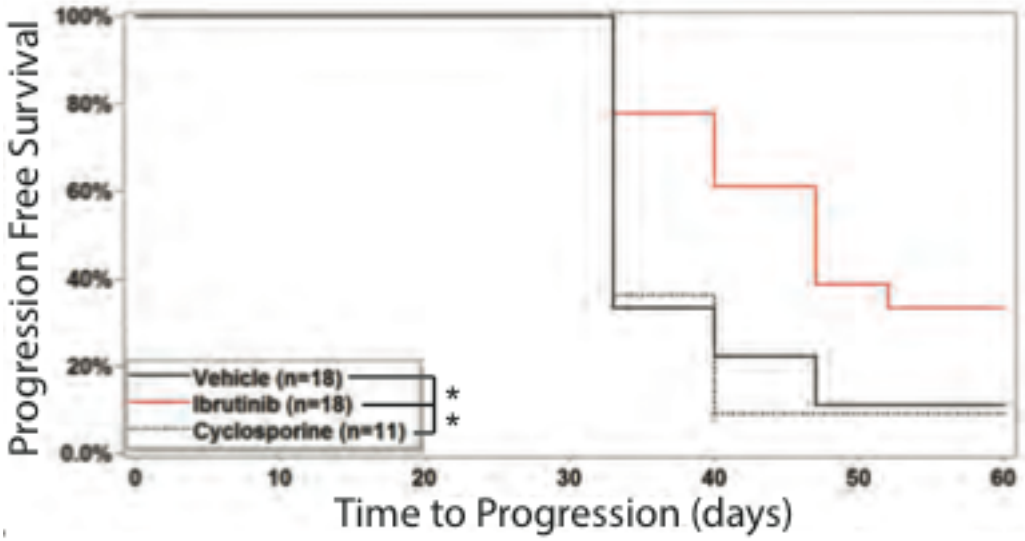

Supplementary Figure 6

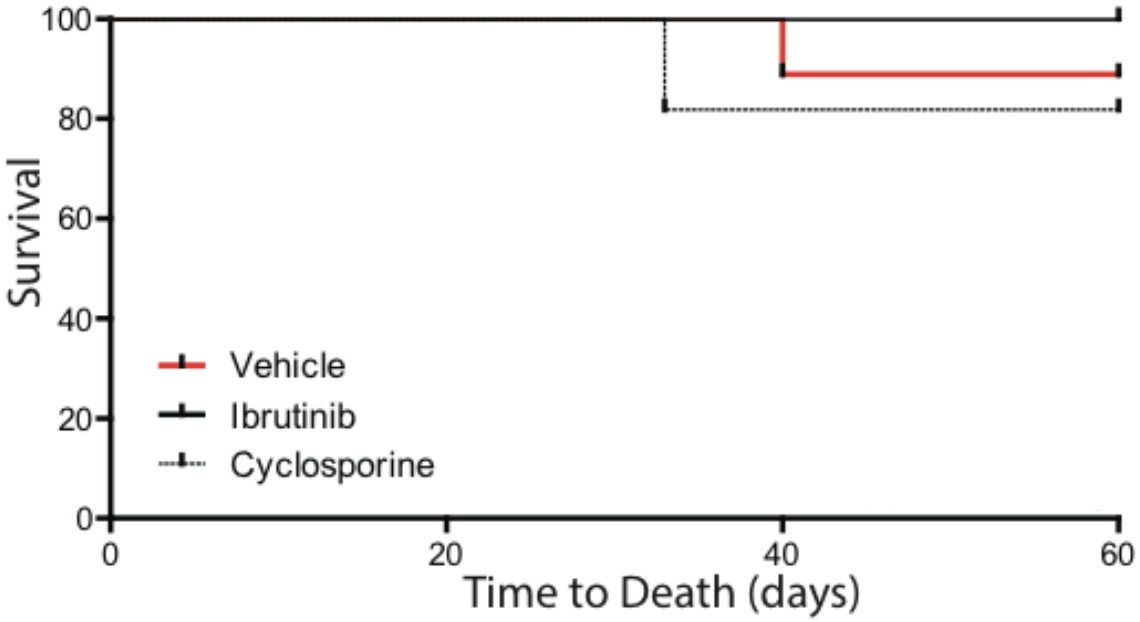

Supplementary Figure 7

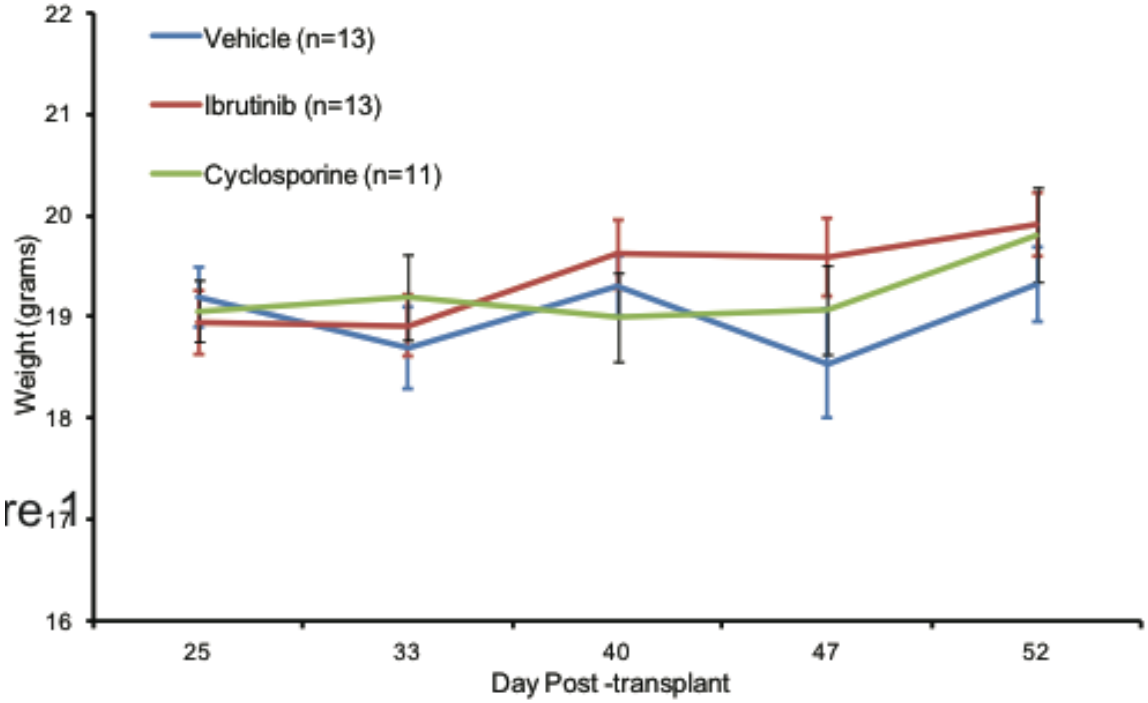

Supplementary Figure 8

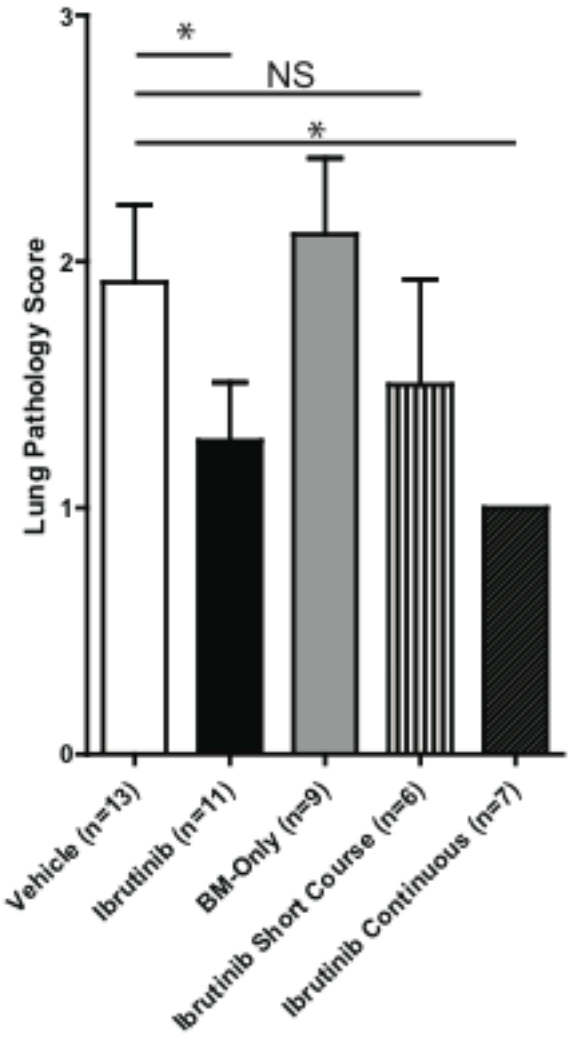

Supplementary Figure 9

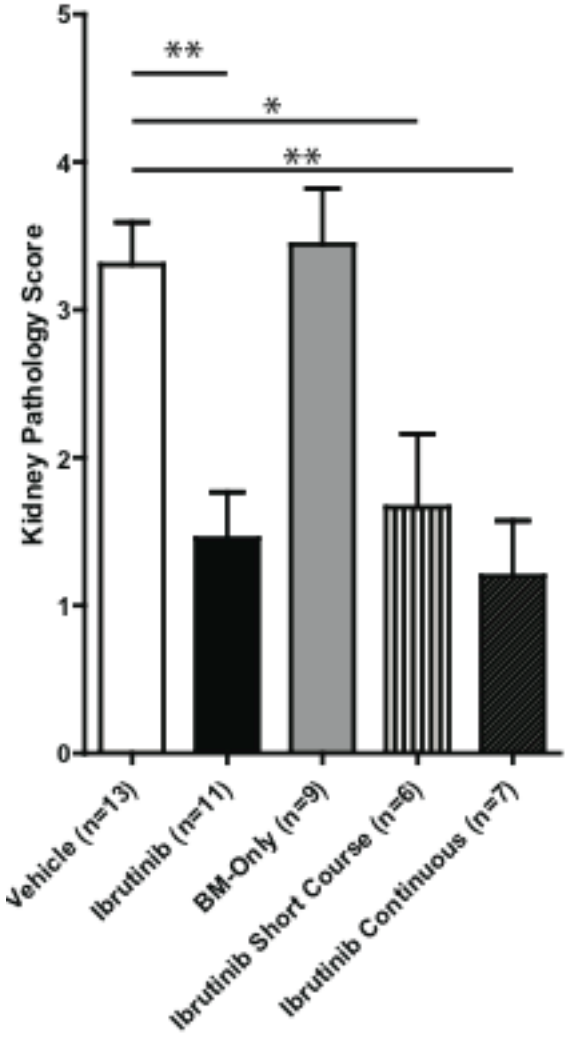

Supplementary Figure 10

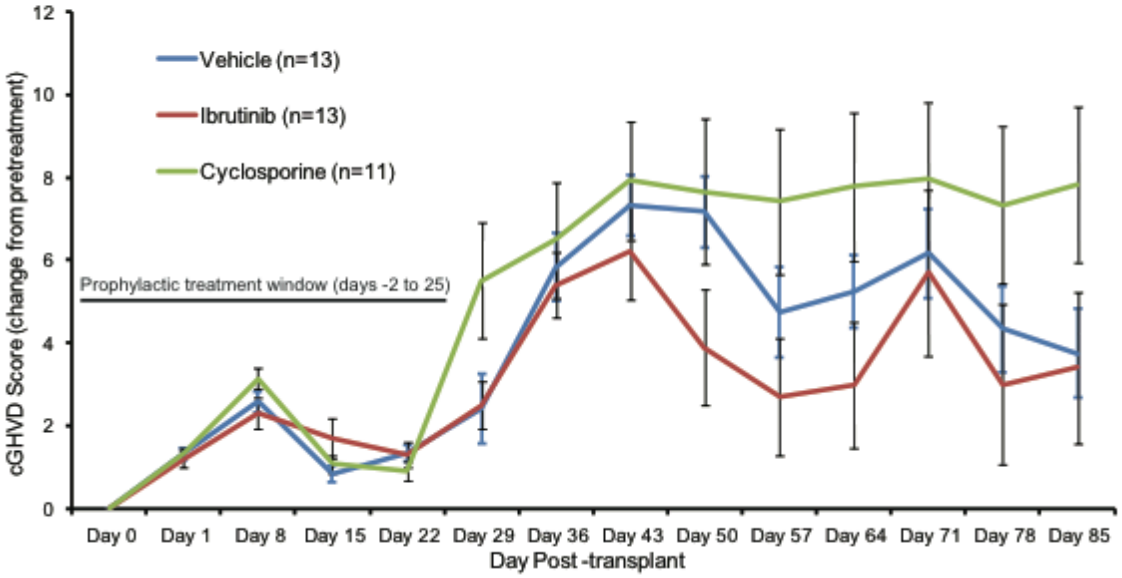

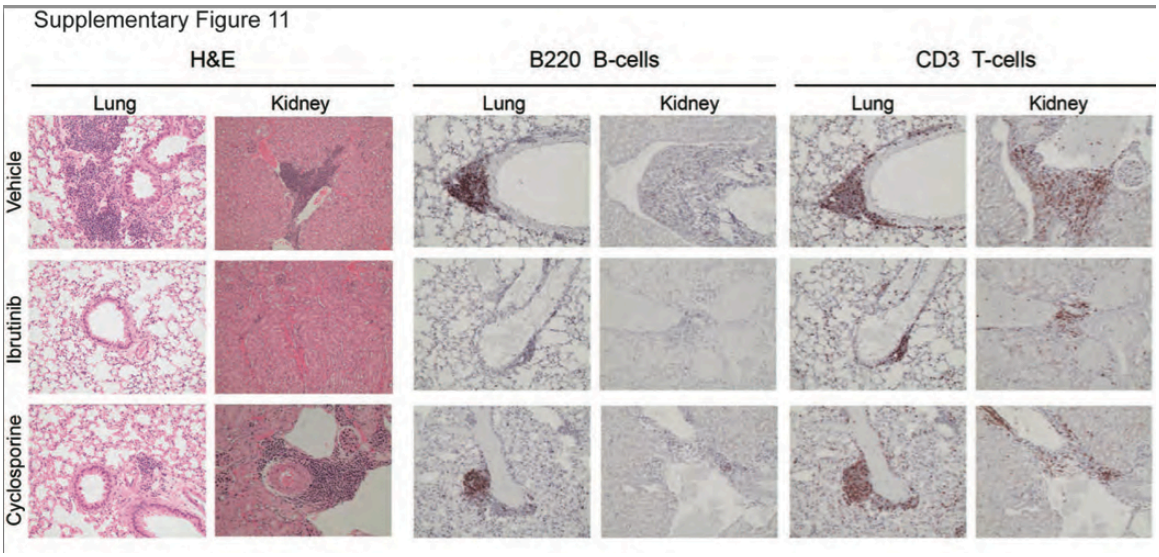
Supplementary Figure 11
H&E
B220 B-cells
CD3 T-cells
Lung
Kidney
Lung
Kidney
Lung
Kidney
Vehicle
Ibrutinib
Cyclosporine

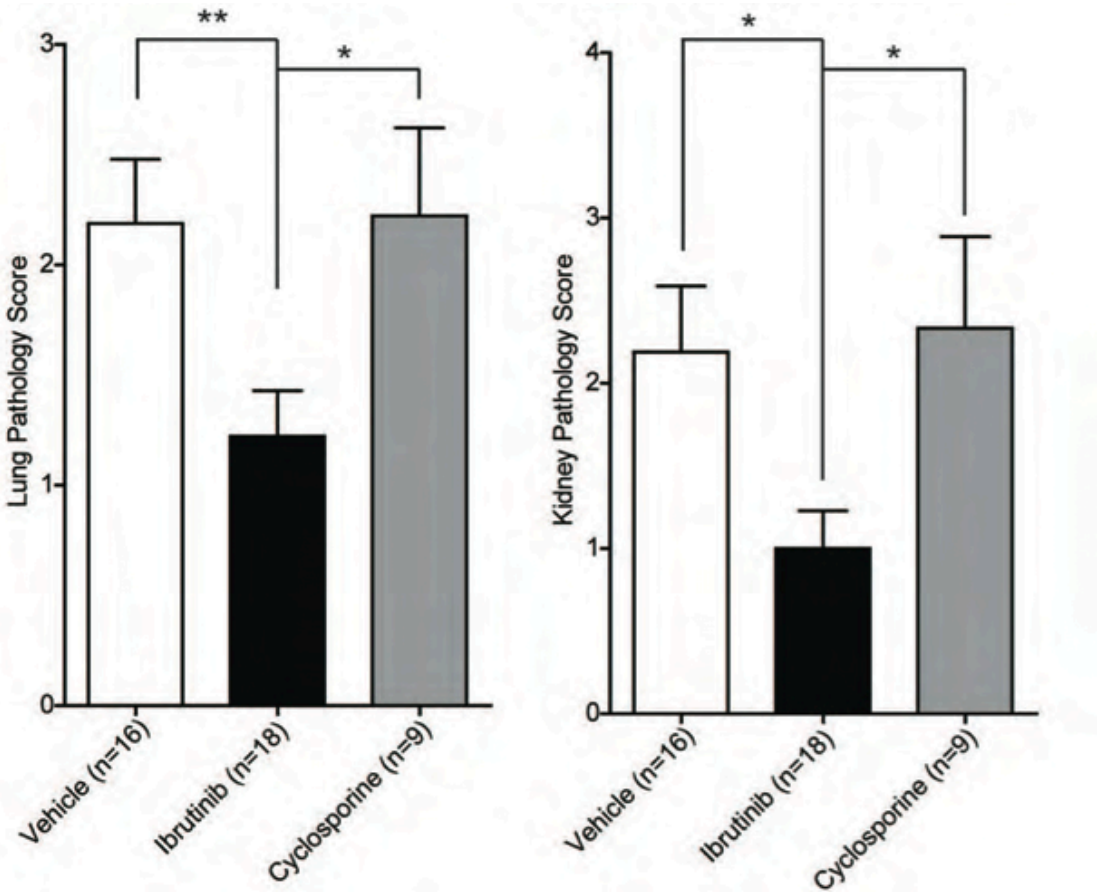
**
*
Lung Pathology Score
0
1
2
3
Vehicle (n=16)
Ibrutinib (n=18)
Cyclosporine (n=9)
*
*
Kidney Pathology Score
0
1
2
3
4
Vehicle (n=16)
Ibrutinib (n=18)
Cyclosporine (n=9)

Supplemental Figure 12

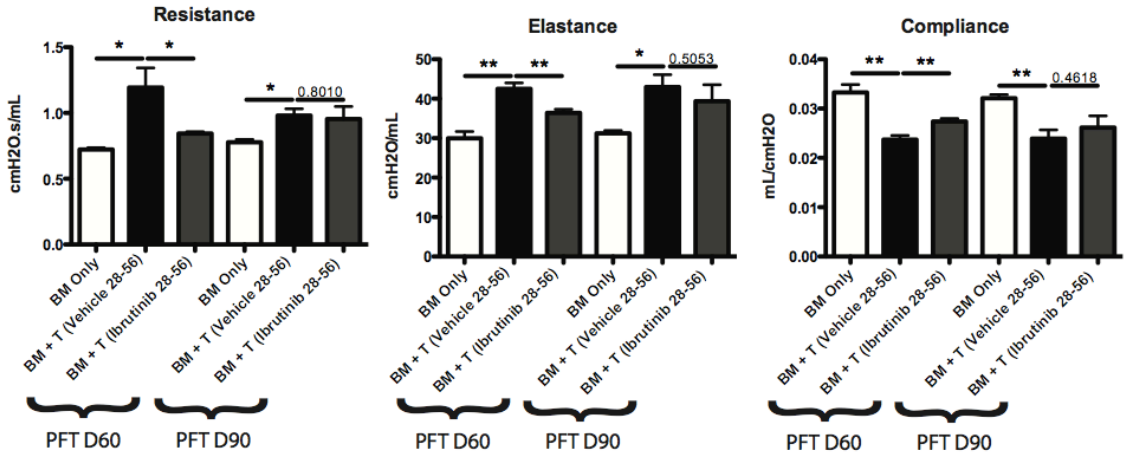

Chapter VI: Concluding Statements

The clinical benefits of HSCT are only hindered by the development of GVHD. With greater understanding of the underlying mechanisms involved in the development of chronic GVHD new therapies can be brought into the clinic. The data presented here are the first to demonstrate the underlying mechanisms and pathogenesis in a clinically relevant murine model. We demonstrated the necessity of B cells to develop from bone marrow derived cells to drive chronic GVHD pathogenesis. We also showed that there was an increase in GC activity and that by eliminating follicular dendritic cells by blocking LTβR signaling we could therapeutically decrease chronic GVHD pathology. However, depleting B cells after the onset of disease was not sufficient for preventing disease progression. The therapeutic depletion of B cells has had controversial results, but prophylactic depletion of B cells could be beneficial for disease treatment. Building off of these findings, we investigated the role T cells play in the GC reaction. We demonstrated that the increase in GC size and frequency correlated with an increase in Tfh cells. These cells demonstrated to be required for the progression of disease. IL21 is a key cytokine produced by donor T cells for development of chronic GVHD. These cells required the chemokine receptor CXCR5 for migration of T cells to the B cell follicle for iniation of disease. The discovery that GCs are important for the development of chronic GVHD has many implications on the development of new therapies. Furthermore, blocking BCR signaling is important for the disruption of disease. Using inhibitors for Syk and Btk have demonstrated to be successful in preventing disease progression. By treating mice with inhibitors to key B cell survival and proliferation molecules

the development of chronic GVHD is prevented by targeting hyperactive B cells. This demonstrates the importance of preventing B cell activation and not just depletion of the cells. These data are confirmed when we target the Tec-family kinases, BTK and ITK during chronic GVHD. We verified hyperactivity in BTK phosphorylation in B cells during chronic GVHD and revealed that inhibition with Ibrutinib was sufficient for prevention of disease. This was due to BTK expression in B cells and possibly ITK expression in T cells.

These data presented from the chronic GVHD murine model with associated BOS are key in linking experimental data to clinical applications. All of the proposed therapeutic approaches have effects on the progression of disease and potentially reverses some of the features of chronic GVHD. It will be necessary to determine the effects the proposed therapeutics have on infections and future malignancies due to immunosuppression. Experiments challenging mice with virus and bacteria will be necessary for determining the effects on other aspects of the immune system. However, in many of the therapies proposed we are potentially restoring homeostatic levels of stimulation (anti-ICOS, anti-CD40L, anti-IL21) or targeting hyperactive B cells (Fostamatinib and Ibrutinib); this could allow for a therapeutic effect with minimal immunosuppressive side effects. Finally, since chronic GVHD is a late-term disease it is unlikely that relapse of malignancies would occur, but the occurrence of new malignancies could be increased due to decreased immune surveillance.

Here we have presented data mainly from one murine model, the BOS model of chronic GVHD, with supplemental data from a scleroderma model of chronic GVHD. The use of multiple models will be necessary to evaluate potential mechanisms of disease as well as evaluate novel therapies for multiple syndromes. We have demonstrated several overlapping pathologies of these models even though the disease manifestations might be divergent. For example, both models demonstrated an increase in BTK and ITK activity and treatment with Ibrutinib was able to ameliorate disease progression. Finally other models of chronic GVHD have demonstrated the importance of IL21 production and IL17 production consistent with the BOS model[134].

Even though novel findings have been discovered, new questions have emerged. Plasma cells are antibody-producing cells that differentiate from GC B cells. The generation of plasma cells could be an explanation for the ineffectiveness of therapeutic B cell depletion due to their lack of expression of key B cell surface molecules. The role of plasma cells during chronic GVHD needs to be fully evaluated to determine if depletion therapies could have beneficial effects. The roles of regulatory cells in chronic GVHD have yet to be determined. It has been well documented that regulatory T (Treg) cells play a pivotal role in the prevention of acute GVHD[135]. T follicular regulatory cells are involved in controlling the GC response. T follicular regulatory cells might prevent the GC reaction and prevent the progression of chronic GVHD. The regulation of the GC response could prevent the production of high-affinity antibodies and the progression of B cells to differentiated plasma cells. Novel therapies could be

applied by understanding the induction of T follicular regulatory. The PD-1 pathway is necessary for maintenance of T follicular regulatory cells[136]. Unpublished data demonstrates that blocking PD-1 with a mAb during active chronic GVHD increases T follicular regulatory cell numbers in the GC and prevents the development of BOS. However, recent findings in a scleroderma model of chronic GVHD found that PD-1 blockade increases severity of chronic GVHD[137]. It will be important to compare the progression of disease between multiple models to determine the full mechanism of PD-1 during chronic GVHD.

Finally, data presented here have paved the way for novel therapeutic studies using direct or epigenetic inhibition of the GC response. The master transcriptional regulator Bcl6 is necessary for GC B cells as well as Tfh cells. By direct inhibition of the Bcl6 regulator by petidomimetics[138] we can prevent the development of chronic GVHD by blocking the germinal center reaction (unpublished data). Furthermore, epigenetic regulation of the GC is another potential target for amelioration of chronic GVHD. The EZH2 protein complex is upregulated in GC B cells and alloreactive T cells[139, 140]. Targeting EZH2 expression has a therapeutic effect in Diffuse Large B cell Lymphoma. New pharmaceutical inhibitors of the EZH2 complex are being generated and have demonstrated to have positive effects on the progression of chronic GVHD (Unpublished Data). These new findings are consistent with the presented data that GCs and Tfh are necessary for the progression of chronic GVHD.

Support from other CD4 helper T cells is necessary for chronic GVHD as well, however, less is known. For example the role of Th17 cells and

the production of IL17 has been demonstrated to be important. Th17 cells are have demonstrated to be involved in the initiation of the germinal center response and have demonstrated to increase the B cell activation following immunization[141]. In addition, Th17 cells are important for the initiation of ectopic lymphoid follicles in autoimmune diseases[142]. While Th17 cells have been demonstrated to increase chronic GVHD[105, 143, 144], their exact role in development of disease remains undefined. Pathways for TH17 differentiation have been implicated in disease progression in models of scleraderma chronic GVHD. The induction of STAT3, a necessary transcription factor for Th17 differentiation, is necessary for the manifestation of scleroderma lesions[107]. Unpublished observations have demonstrated the importance of STAT3 induction in both bone marrow derived B cells and donor mature T cells. Finally, G-CSF administration promotes the induction of Th17 cells and has been linked to increased pathology in the scleroderma model of cGVHD[143, 145]. Together these data indicate a role for Th17 cells during both scleroderma and BOS chronic GVHD. Therapeutic interventions that block IL17 production could be beneficial. A novel regulator of Th17 cells is the Endothelial Protein C Receptor (EPCR), which binds Activated Protein C. After binding the ligand, EPCR is endocytosed and provides anti-inflammatory and barrier cytoprotective effects. We have seen a decrease in pathogenic pulmonary function when mice with chronic GVHD were treated with Activated Protein C (unpublished observations), indicating that the EPCR pathway might be a novel regulator of Th17 cells during chronic GVHD. In addition, inhibition of IL17 by pharmaceutical inhibitors has

demonstrated to have beneficial effects. The selective ROCK2 inhibitor KD025 was demonstrated to decrease both IL21 and IL17 production from healthy donor peripheral blood cells[146]. We were able to reduce lung pathology in mice when we administered KD025 during chronic GVHD (Unpublished Data). The regulation or inhibition of pathogenic Th17 cells during chronic GVHD has great therapeutic potential. Since multiple models of both lung and skin pathology demonstrate a role of Th17 involvement, these data have strong implications for clinical translation.

Presented have defined potential mechanisms in support of our hypothetical model of chronic GVHD (Chapter 1, Figure 1). We have defined the GC reaction as a mandatory process for the production of high-affinity pathogenic antibodies facilitated by Tfh. We have demonstrated the cell-signaling cascade necessary for B cell proliferation and maintenance. New understanding of disease progression and evaluation of novel therapeutics will be necessary for the successful treatment of chronic GVHD. The key findings presented lay the foundation of novel research to lead to potential therapies.

Bibliography

1. Ferrara JL, Levine JE. Graft-versus-host disease in the 21st century: new perspectives on an old problem. *Seminars in hematology* 2006; **43**(1)**:** 1-2.

2. Pasquini MC, Wang Z, Horowitz MM, Gale RP. 2010 report from the Center for International Blood and Marrow Transplant Research (CIBMTR): current uses and outcomes of hematopoietic cell transplants for blood and bone marrow disorders. *Clinical transplants* 2010**:** 87-105.

3. Barnes DW, Loutit JF, Micklem HS. "Secondary disease" of radiation chimeras: a syndrome due to lymphoid aplasia. *Annals of the New York Academy of Sciences* 1962; **99:** 374-85.

4. Billingham RE. The biology of graft-versus-host reactions. *Harvey Lect* 1966; **62:** 21-78.

5. Loutit JF, Micklem HS. "Secondary disease" among lethally irradiated mice restored with haematopoietic tissues from normal or iso-immunized foreign mice. *British journal of experimental pathology* 1962; **43:** 77-87.

6. Korngold R, Sprent J. Lethal graft-versus-host disease after bone marrow transplantation across minor histocompatibility barriers in mice. Prevention by removing mature T cells from marrow. *J Exp Med* 1978; **148**(6)**:** 1687-98.

7. Ferrara JL, Yanik G. Acute graft versus host disease: pathophysiology, risk factors, and prevention strategies. *Clin Adv Hematol Oncol* 2005; **3**(5)**:** 415-9, 428.

8. Schwarer AP, Jiang YZ, Brookes PA, Barrett AJ, Batchelor JR, Goldman JM *et al.* Frequency of anti-recipient alloreactive helper T-cell precursors in donor blood and graft-versus-host disease after HLA-identical sibling bone-marrow transplantation. *Lancet* 1993; **341**(8839)**:** 203-5.

9. Jenkins MK, Moon JJ. The role of naive T cell precursor frequency and recruitment in dictating immune response magnitude. *J Immunol* 2012; **188**(9)**:** 4135-40.

10. Hill GR, Crawford JM, Cooke KR, Brinson YS, Pan L, Ferrara JL. Total body irradiation and acute graft-versus-host disease: the role of gastrointestinal damage and inflammatory cytokines. *Blood* 1997; **90**(8)**:** 3204-13.

11. Shlomchik WD, Couzens MS, Tang CB, McNiff J, Robert ME, Liu J *et al.* Prevention of graft versus host disease by inactivation of host antigen-presenting cells. *Science* 1999; **285**(5426)**:** 412-5.

12. Antin JH. Acute graft-versus-host disease: inflammation run amok? *J Clin Invest* 2001; **107**(12)**:** 1497-8.

13. Chung B, Barbara-Burnham L, Barsky L, Weinberg K. Radiosensitivity of thymic interleukin-7 production and thymopoiesis after bone marrow transplantation. *Blood* 2001; **98**(5)**:** 1601-6.

14. Sayegh MH, Watschinger B, Carpenter CB. Mechanisms of T cell recognition of alloantigen. The role of peptides. *Transplantation* 1994; **57**(9)**:** 1295-302.

15. Wysocki CA, Panoskaltsis-Mortari A, Blazar BR, Serody JS. Leukocyte migration and graft-versus-host disease. *Blood* 2005; **105**(11)**:** 4191-9.

16. Socie G, Ritz J, Martin PJ. Current challenges in chronic graft-versus-host disease. *Biol Blood Marrow Transplant* 2010; **16**(1 Suppl)**:** S146-51.

17. Filipovich AH, Weisdorf D, Pavletic S, Socie G, Wingard JR, Lee SJ *et al.* National Institutes of Health consensus development project on criteria for clinical trials in chronic graft-versus-host disease: I. Diagnosis and staging working group report. *Biol Blood Marrow Transplant* 2005; **11**(12)**:** 945-56.

18. Miklos DB, Kim HT, Miller KH, Guo L, Zorn E, Lee SJ *et al.* Antibody responses to H-Y minor histocompatibility antigens correlate with chronic graft-versus-host disease and disease remission. *Blood* 2005; **105**(7)**:** 2973-8.

19. Sarantopoulos S, Stevenson KE, Kim HT, Cutler CS, Bhuiya NS, Schowalter M *et al.* Altered B-cell homeostasis and excess BAFF in human chronic graft-versus-host disease. *Blood* 2009; **113**(16)**:** 3865-74.

20. Sarantopoulos S, Stevenson KE, Kim HT, Washel WS, Bhuiya NS, Cutler CS *et al.* Recovery of B-cell homeostasis after rituximab in chronic graft-versus-host disease. *Blood* 2011; **117**(7)**:** 2275-83.

21. Banovic T, MacDonald KP, Morris ES, Rowe V, Kuns R, Don A *et al.* TGF-beta in allogeneic stem cell transplantation: friend or foe? *Blood* 2005; **106**(6)**:** 2206-14.

22. Svegliati S, Olivieri A, Campelli N, Luchetti M, Poloni A, Trappolini S *et al.* Stimulatory autoantibodies to PDGF receptor in patients with extensive chronic graft-versus-host disease. *Blood* 2007; **110**(1)**:** 237-41.

23. Gabrielli A, Svegliati S, Moroncini G, Luchetti M, Tonnini C, Avvedimento EV. Stimulatory autoantibodies to the PDGF receptor: a link to fibrosis in scleroderma and a pathway for novel therapeutic targets. *Autoimmun Rev* 2007; **7**(2)**:** 121-6.

24. Srinivasan M, Flynn R, Price A, Ranger A, Browning JL, Taylor PA *et al.* Donor B-cell alloantibody deposition and germinal center formation are required for the development of murine chronic GVHD and bronchiolitis obliterans. *Blood* 2012; **119**(6)**:** 1570-80.

25. Murphy K, Travers P, Walport M, Janeway C. *Janeway's immunobiology*, 8th edn Garland Science: New York, 2012.

26. Ozaki K, Spolski R, Feng CG, Qi CF, Cheng J, Sher A *et al.* A critical role for IL-21 in regulating immunoglobulin production. *Science* 2002; **298**(5598)**:** 1630-4.

27. Baird K, Pavletic SZ. Chronic graft versus host disease. *Curr Opin Hematol* 2006; **13**(6)**:** 426-35.

28. Baird K, Cooke K, Schultz KR. Chronic graft-versus-host disease (GVHD) in children. *Pediatric clinics of North America* 2010; **57**(1)**:** 297-322.

29. Kapur R, Ebeling S, Hagenbeek A. B-cell involvement in chronic graft-versus-host disease. *Haematologica* 2008; **93**(11)**:** 1702-11.

30. Fujii H, Cuvelier G, She K, Aslanian S, Shimizu H, Kariminia A *et al.* Biomarkers in newly diagnosed pediatric-extensive chronic graft-versus-host disease: a report from the Children's Oncology Group. *Blood* 2008; **111**(6)**:** 3276-85.

31. Sarantopoulos S, Stevenson KE, Kim HT, Bhuiya NS, Cutler CS, Soiffer RJ *et al.* High levels of B-cell activating factor in patients with active chronic graft-versus-host disease. *Clin Cancer Res* 2007; **13**(20)**:** 6107-14.

32. She K, Gilman AL, Aslanian S, Shimizu H, Krailo M, Chen Z *et al.* Altered Toll-like receptor 9 responses in circulating B cells at the onset of extensive chronic graft-versus-host disease. *Biol Blood Marrow Transplant* 2007; **13**(4)**:** 386-97.

33. Zhang C, Todorov I, Zhang Z, Liu Y, Kandeel F, Forman S *et al.* Donor CD4+ T and B cells in transplants induce chronic graft-versus-host disease with autoimmune manifestations. *Blood* 2006; **107**(7)**:** 2993-3001.

34. Chu YW, Gress RE. Murine models of chronic graft-versus-host disease: insights and unresolved issues. *Biol Blood Marrow Transplant* 2008; **14**(4)**:** 365-78.

35. Zhang Y, McCormick LL, Desai SR, Wu C, Gilliam AC. Murine sclerodermatous graft-versus-host disease, a model for human scleroderma: cutaneous cytokines, chemokines, and immune cell activation. *J Immunol* 2002; **168**(6)**:** 3088-98.

36. Panoskaltsis-Mortari A, Tram KV, Price AP, Wendt CH, Blazar BR. A new murine model for bronchiolitis obliterans post-bone marrow transplant. *American journal of respiratory and critical care medicine* 2007; **176**(7)**:** 713-23.

37. Dudek AZ, Mahaseth H, DeFor TE, Weisdorf DJ. Bronchiolitis obliterans in chronic graft-versus-host disease: analysis of risk factors and treatment outcomes. *Biol Blood Marrow Transplant* 2003; **9**(10)**:** 657-66.

38. Al-Githmi I, Batawil N, Shigemura N, Hsin M, Lee TW, He GW *et al.* Bronchiolitis obliterans following lung transplantation. *Eur J Cardiothorac Surg* 2006; **30**(6)**:** 846-51.

39. Chien JW, Duncan S, Williams KM, Pavletic SZ. Bronchiolitis obliterans syndrome after allogeneic hematopoietic stem cell transplantation-an increasingly recognized manifestation of chronic graft-versus-host disease. *Biol Blood Marrow Transplant* 2010; **16**(1 Suppl)**:** S106-14.

40. Dudek AZ, Mahaseth H. Hematopoietic stem cell transplant-related airflow obstruction. *Curr Opin Oncol* 2006; **18**(2)**:** 115-9.

41. Browning JL. B cells move to centre stage: novel opportunities for autoimmune disease treatment. *Nat Rev Drug Discov* 2006; **5**(7)**:** 564-76.

42. Ratanatharathorn V, Ayash L, Reynolds C, Silver S, Reddy P, Becker M *et al.* Treatment of chronic graft-versus-host disease with anti-CD20 chimeric monoclonal antibody. *Biol Blood Marrow Transplant* 2003; **9**(8)**:** 505-11.

43. Cutler C, Miklos D, Kim HT, Treister N, Woo SB, Bienfang D *et al.* Rituximab for steroid-refractory chronic graft-versus-host disease. *Blood* 2006; **108**(2)**:** 756-62.

44. Canninga-van Dijk MR, van der Straaten HM, Fijnheer R, Sanders CJ, van den Tweel JG, Verdonck LF. Anti-CD20 monoclonal antibody treatment in 6 patients with therapy-refractory chronic graft-versus-host disease. *Blood* 2004; **104**(8)**:** 2603-6.

45. Kharfan-Dabaja MA, Mhaskar AR, Djulbegovic B, Cutler C, Mohty M, Kumar A. Efficacy of rituximab in the setting of steroid-refractory chronic graft-versus-host disease: a systematic review and meta-analysis. *Biol Blood Marrow Transplant* 2009; **15**(9)**:** 1005-13.

46. Browning JL. Inhibition of the lymphotoxin pathway as a therapy for autoimmune disease. *Immunol Rev* 2008; **223:** 202-20.

47. Baumgarth N, Jager GC, Herman OC, Herzenberg LA. CD4+ T cells derived from B cell-deficient mice inhibit the establishment of peripheral B cell pools. *Proc Natl Acad Sci U S A* 2000; **97**(9)**:** 4766-71.

48. Chan OT, Hannum LG, Haberman AM, Madaio MP, Shlomchik MJ. A novel mouse with B cells but lacking serum antibody reveals an antibody-independent role for B cells in murine lupus. *J Exp Med* 1999; **189**(10)**:** 1639-48.

49. Ziegler TR, Panoskaltsus-Mortari A, Gu LH, Jonas CR, Farrell CL, Lacey DL *et al.* Regulation of glutathione redox status in lung and liver by conditioning regimens and keratinocyte growth factor in murine allogeneic bone marrow transplantation. *Transplantation* 2001; **72**(8)**:** 1354-62.

50. Crawford SW, Clark JG. Bronchiolitis associated with bone marrow transplantation. *Clinics in chest medicine* 1993; **14**(4)**:** 741-9.

51. Imanguli MM, Atkinson JC, Mitchell SA, Avila DN, Bishop RJ, Cowen EW *et al.* Salivary gland involvement in chronic graft-versus-host disease: prevalence, clinical significance, and recommendations for evaluation. *Biol Blood Marrow Transplant* 2010; **16**(10)**:** 1362-9.

52. Nagler RM, Nagler A. The molecular basis of salivary gland involvement in graft--vs.--host disease. *J Dent Res* 2004; **83**(2)**:** 98-103.

53. Levy S, Nagler A, Okon S, Marmary Y. Parotid salivary gland dysfunction in chronic graft-versus-host disease (cGVHD): a longitudinal study in a mouse model. *Bone Marrow Transplant* 2000; **25**(10)**:** 1073-8.

54. Novobrantseva TI, Majeau GR, Amatucci A, Kogan S, Brenner I, Casola S *et al.* Attenuated liver fibrosis in the absence of B cells. *J Clin Invest* 2005; **115**(11)**:** 3072-82.

55. Anderson SM, Hannum LG, Shlomchik MJ. Memory B cell survival and function in the absence of secreted antibody and immune complexes on follicular dendritic cells. *J Immunol* 2006; **176**(8)**:** 4515-9.

56. Gong Q, Ou Q, Ye S, Lee WP, Cornelius J, Diehl L *et al.* Importance of cellular microenvironment and circulatory dynamics in B cell immunotherapy. *J Immunol* 2005; **174**(2)**:** 817-26.

57. Hamaguchi Y, Uchida J, Cain DW, Venturi GM, Poe JC, Haas KM *et al.* The peritoneal cavity provides a protective niche for B1 and conventional B lymphocytes during anti-CD20 immunotherapy in mice. *J Immunol* 2005; **174**(7)**:** 4389-99.

58. Gatto D, Brink R. The germinal center reaction. *J Allergy Clin Immunol* 2010; **126**(5)**:** 898-907; quiz 908-9.

59. Gommerman JL, Browning JL. Lymphotoxin/light, lymphoid microenvironments and autoimmune disease. *Nat Rev Immunol* 2003; **3**(8)**:** 642-55.

60. Doherty TA, Soroosh P, Khorram N, Fukuyama S, Rosenthal P, Cho JY *et al.* The tumor necrosis factor family member LIGHT is a target for asthmatic airway remodeling. *Nat Med* 2011; **17**(5)**:** 596-603.

61. Kuzmina Z, Greinix HT, Weigl R, Kormoczi U, Rottal A, Frantal S *et al.* Significant differences in B-cell subpopulations characterize patients with chronic graft-versus-host disease-associated dysgammaglobulinemia. *Blood* 2011; **117**(7)**:** 2265-74.

62. Narimatsu H, Miyakoshi S, Yamaguchi T, Kami M, Matsumura T, Yuji K *et al.* Chronic graft-versus-host disease following umbilical cord blood transplantation: retrospective survey involving 1072 patients in Japan. *Blood* 2008; **112**(6)**:** 2579-82.

63. Brunstein CG, Barker JN, Weisdorf DJ, DeFor TE, Miller JS, Blazar BR *et al.* Umbilical cord blood transplantation after nonmyeloablative conditioning: impact on transplantation outcomes in 110 adults with hematologic disease. *Blood* 2007; **110**(8)**:** 3064-70.

64. Pavletic SZ, Lee SJ, Socie G, Vogelsang G. Chronic graft-versus-host disease: implications of the National Institutes of Health consensus development project on criteria for clinical trials. *Bone Marrow Transplant* 2006; **38**(10)**:** 645-51.

65. Shlomchik WD, Lee SJ, Couriel D, Pavletic SZ. Transplantation's greatest challenges: advances in chronic graft-versus-host disease. *Biol Blood Marrow Transplant* 2007; **13**(1 Suppl 1)**:** 2-10.

66. Choi YS, Yang JA, Crotty S. Dynamic regulation of Bcl6 in follicular helper CD4 T (Tfh) cells. *Curr Opin Immunol* 2013; **25**(3)**:** 366-72.

67. Choi YS, Kageyama R, Eto D, Escobar TC, Johnston RJ, Monticelli L *et al.* ICOS receptor instructs T follicular helper cell versus effector cell differentiation via induction of the transcriptional repressor Bcl6. *Immunity* 2011; **34**(6)**:** 932-46.

68. Zotos D, Coquet JM, Zhang Y, Light A, D'Costa K, Kallies A *et al.* IL-21 regulates germinal center B cell differentiation and proliferation through a B cell-intrinsic mechanism. *J Exp Med* 2010; **207**(2)**:** 365-78.

69. Vu F, Dianzani U, Ware CF, Mak T, Gommerman JL. ICOS, CD40, and lymphotoxin beta receptors signal sequentially and interdependently to initiate a germinal center reaction. *J Immunol* 2008; **180**(4)**:** 2284-93.

70. Ballesteros-Tato A, Leon B, Graf BA, Moquin A, Adams PS, Lund FE *et al.* Interleukin-2 inhibits germinal center formation by limiting T follicular helper cell differentiation. *Immunity* 2012; **36**(5)**:** 847-56.

71. Conlon TM, Saeb-Parsy K, Cole JL, Motallebzadeh R, Qureshi MS, Rehakova S *et al.* Germinal center alloantibody responses are mediated exclusively by indirect-pathway CD4 T follicular helper cells. *J Immunol* 2012; **188**(6)**:** 2643-52.

72. Kerfoot SM, Yaari G, Patel JR, Johnson KL, Gonzalez DG, Kleinstein SH *et al.* Germinal center B cell and T follicular helper cell development initiates in the interfollicular zone. *Immunity* 2011; **34**(6)**:** 947-60.

73. Luthje K, Kallies A, Shimohakamada Y, Belz GT, Light A, Tarlinton DM *et al.* The development and fate of follicular helper T cells defined by an IL-21 reporter mouse. *Nat Immunol* 2012; **13**(5)**:** 491-8.

74. Martin F, Chan AC. B cell immunobiology in disease: evolving concepts from the clinic. *Annu Rev Immunol* 2006; **24:** 467-96.

75. Linterman MA, Beaton L, Yu D, Ramiscal RR, Srivastava M, Hogan JJ *et al.* IL-21 acts directly on B cells to regulate Bcl-6 expression and germinal center responses. *J Exp Med* 2010; **207**(2)**:** 353-63.

76. Taylor PA, Panoskaltsis-Mortari A, Freeman GJ, Sharpe AH, Noelle RJ, Rudensky AY *et al.* Targeting of inducible costimulator (ICOS) expressed on alloreactive T cells down-regulates graft-versus-host disease (GVHD) and facilitates engraftment of allogeneic bone marrow (BM). *Blood* 2005; **105**(8)**:** 3372-80.

77. Pesce J, Kaviratne M, Ramalingam TR, Thompson RW, Urban JF, Jr., Cheever AW *et al.* The IL-21 receptor augments Th2 effector function and alternative macrophage activation. *J Clin Invest* 2006; **116**(7)**:** 2044-55.

78. Odegard JM, Marks BR, DiPlacido LD, Poholek AC, Kono DH, Dong C *et al.* ICOS-dependent extrafollicular helper T cells elicit IgG production via IL-21 in systemic autoimmunity. *J Exp Med* 2008; **205**(12)**:** 2873-86.

79. Herber D, Brown TP, Liang S, Young DA, Collins M, Dunussi-Joannopoulos K. IL-21 has a pathogenic role in a lupus-prone mouse model and its blockade with IL-21R.Fc reduces disease progression. *J Immunol* 2007; **178**(6)**:** 3822-30.

80. Feldmann M, Maini RN, Bondeson J, Taylor P, Foxwell BM, Brennan FM. Cytokine blockade in rheumatoid arthritis. *Adv Exp Med Biol* 2001; **490:** 119-27.

81. Allen JL, Tata PV, Fore MS, Wooten J, Rudra S, Deal AM *et al.* Increased BCR responsiveness in B cells from patients with chronic GVHD. *Blood* 2014.

82. Di Carlo E, D'Antuono T, Contento S, Di Nicola M, Ballone E, Sorrentino C. Quilty effect has the features of lymphoid neogenesis and shares CXCL13-CXCR5 pathway with recurrent acute cardiac rejections. *Am J Transplant* 2007; **7**(1)**:** 201-10.

83. Silverman GJ, Weisman S. Rituximab therapy and autoimmune disorders: prospects for anti-B cell therapy. *Arthritis Rheum* 2003; **48**(6)**:** 1484-92.

84. Bucher C, Koch L, Vogtenhuber C, Goren E, Munger M, Panoskaltsis-Mortari A *et al.* IL-21 blockade reduces graft-versus-host disease mortality by supporting inducible T regulatory cell generation. *Blood* 2009; **114**(26)**:** 5375-84.

85. Deenick EK, Chan A, Ma CS, Gatto D, Schwartzberg PL, Brink R *et al.* Follicular helper T cell differentiation requires continuous antigen presentation that is independent of unique B cell signaling. *Immunity* 2010; **33**(2)**:** 241-53.

86. Foy TM, Laman JD, Ledbetter JA, Aruffo A, Claassen E, Noelle RJ. gp39-CD40 interactions are essential for germinal center formation and the development of B cell memory. *J Exp Med* 1994; **180**(1)**:** 157-63.

87. Bossaller L, Burger J, Draeger R, Grimbacher B, Knoth R, Plebani A *et al.* ICOS deficiency is associated with a severe reduction of CXCR5+CD4 germinal center Th cells. *J Immunol* 2006; **177**(7)**:** 4927-32.

88. Schultz KR, Miklos DB, Fowler D, Cooke K, Shizuru J, Zorn E *et al.* Toward biomarkers for chronic graft-versus-host disease: National Institutes of Health consensus development project on criteria for clinical trials in chronic graft-versus-host disease: III. Biomarker Working Group Report. *Biol Blood Marrow Transplant* 2006; **12**(2)**:** 126-37.

89. Flynn R, Du J, Veenstra RG, Reichenbach DK, Panoskaltsis-Mortari A, Taylor PA *et al.* Increased T follicular helper cells and germinal center B cells are required for cGVHD and bronchiolitis obliterans. *Blood* 2014; **123**(25)**:** 3988-98.

90. Allen JL, Tata PV, Fore MS, Wooten J, Rudra S, Deal AM *et al.* Increased BCR responsiveness in B cells from patients with chronic GVHD. *Blood* 2014; **123**(13)**:** 2108-15.

91. Leonhardt F, Zirlik K, Buchner M, Prinz G, Hechinger AK, Gerlach UV *et al.* Spleen tyrosine kinase (Syk) is a potent target for GvHD prevention at different cellular levels. *Leukemia* 2012; **26**(7)**:** 1617-29.

92. Le Huu D, Kimura H, Date M, Hamaguchi Y, Hasegawa M, Hau KT *et al.* Blockade of Syk ameliorates the development of murine sclerodermatous chronic graft-versus-host disease. *Journal of dermatological science* 2014; **74**(3)**:** 214-21.

93. Craxton A, Jiang A, Kurosaki T, Clark EA. Syk and Bruton's tyrosine kinase are required for B cell antigen receptor-mediated activation of the kinase Akt. *J Biol Chem* 1999; **274**(43)**:** 30644-50.

94. Genovese MC, Kavanaugh A, Weinblatt ME, Peterfy C, DiCarlo J, White ML *et al.* An oral Syk kinase inhibitor in the treatment of rheumatoid arthritis: a three-month randomized, placebo-controlled, phase II study in patients with active rheumatoid arthritis that did not respond to biologic agents. *Arthritis and rheumatism* 2011; **63**(2)**:** 337-45.

95. Weinblatt ME, Kavanaugh A, Burgos-Vargas R, Dikranian AH, Medrano-Ramirez G, Morales-Torres JL *et al.* Treatment of rheumatoid arthritis with a Syk kinase inhibitor: a twelve-week, randomized, placebo-controlled trial. *Arthritis Rheum* 2008; **58**(11)**:** 3309-18.

96. Friedberg JW, Sharman J, Sweetenham J, Johnston PB, Vose JM, Lacasce A *et al.* Inhibition of Syk with fostamatinib disodium has significant clinical activity in non-Hodgkin lymphoma and chronic lymphocytic leukemia. *Blood* 2010; **115**(13)**:** 2578-85.

97. Cutler C, Kim HT, Bindra B, Sarantopoulos S, Ho VT, Chen YB *et al.* Rituximab prophylaxis prevents corticosteroid-requiring chronic GVHD after allogeneic

peripheral blood stem cell transplantation: results of a phase 2 trial. *Blood* 2013; **122**(8)**:** 1510-7.

98. Allen JL, Fore MS, Wooten J, Roehrs PA, Bhuiya NS, Hoffert T *et al.* B cells from patients with chronic GVHD are activated and primed for survival via BAFF-mediated pathways. *Blood* 2012; **120**(12)**:** 2529-36.

99. Lee SJ, Vogelsang G, Flowers ME. Chronic graft-versus-host disease. *Biol Blood Marrow Transplant* 2003; **9**(4)**:** 215-33.

100. Pidala J, Kurland B, Chai X, Majhail N, Weisdorf DJ, Pavletic S *et al.* Patient-reported quality of life is associated with severity of chronic graft-versus-host disease as measured by NIH criteria: report on baseline data from the Chronic GVHD Consortium. *Blood* 2011; **117**(17)**:** 4651-7.

101. Arai S, Jagasia M, Storer B, Chai X, Pidala J, Cutler C *et al.* Global and organ-specific chronic graft-versus-host disease severity according to the 2005 NIH Consensus Criteria. *Blood* 2011; **118**(15)**:** 4242-9.

102. Holler E. Risk assessment in haematopoietic stem cell transplantation: GvHD prevention and treatment. *Best Pract Res Clin Haematol* 2007; **20**(2)**:** 281-94.

103. Coghill JM, Sarantopoulos S, Moran TP, Murphy WJ, Blazar BR, Serody JS. Effector CD4+ T cells, the cytokines they generate, and GVHD: something old and something new. *Blood* 2011; **117**(12)**:** 3268-76.

104. Lim JY, Cho BS, Min CK, Park G, Kim YJ, Chung NG *et al.* Fluctuations in pathogenic CD4+ T-cell subsets in a murine sclerodermatous model of chronic graft-versus-host disease. *Immunol Invest* 2014; **43**(1)**:** 41-53.

105. Carlson MJ, West ML, Coghill JM, Panoskaltsis-Mortari A, Blazar BR, Serody JS. In vitro-differentiated TH17 cells mediate lethal acute graft-versus-host disease with severe cutaneous and pulmonary pathologic manifestations. *Blood* 2009; **113**(6)**:** 1365-74.

106. Zhang Y, Hexner E, Frank D, Emerson SG. CD4+ T cells generated de novo from donor hemopoietic stem cells mediate the evolution from acute to chronic graft-versus-host disease. *J Immunol* 2007; **179**(5)**:** 3305-14.

107. Radojcic V, Pletneva MA, Yen HR, Ivcevic S, Panoskaltsis-Mortari A, Gilliam AC *et al.* STAT3 signaling in CD4+ T cells is critical for the pathogenesis of chronic sclerodermatous graft-versus-host disease in a murine model. *J Immunol* 2010; **184**(2)**:** 764-74.

108. Berg LJ, Finkelstein LD, Lucas JA, Schwartzberg PL. Tec family kinases in T lymphocyte development and function. *Annu Rev Immunol* 2005; **23:** 549-600.

109. Satterthwaite AB, Witte ON. The role of Bruton's tyrosine kinase in B-cell development and function: a genetic perspective. *Immunol Rev* 2000; **175:** 120-7.

110. Gomez-Rodriguez J, Kraus ZJ, Schwartzberg PL. Tec family kinases Itk and Rlk / Txk in T lymphocytes: cross-regulation of cytokine production and T-cell fates. *Febs J* 2011; **278**(12)**:** 1980-9.

111. Mueller C, August A. Attenuation of immunological symptoms of allergic asthma in mice lacking the tyrosine kinase ITK. *J Immunol* 2003; **170**(10)**:** 5056-63.

112. Au-Yeung BB, Katzman SD, Fowell DJ. Cutting edge: Itk-dependent signals required for CD4+ T cells to exert, but not gain, Th2 effector function. *J Immunol* 2006; **176**(7)**:** 3895-9.

113. Sahu N, Venegas AM, Jankovic D, Mitzner W, Gomez-Rodriguez J, Cannons JL *et al.* Selective expression rather than specific function of Txk and Itk regulate Th1 and Th2 responses. *J Immunol* 2008; **181**(9)**:** 6125-31.

114. Fowell DJ, Shinkai K, Liao XC, Beebe AM, Coffman RL, Littman DR *et al.* Impaired NFATc translocation and failure of Th2 development in Itk-deficient CD4+ T cells. *Immunity* 1999; **11**(4)**:** 399-409.

115. Miller AT, Wilcox HM, Lai Z, Berg LJ. Signaling through Itk promotes T helper 2 differentiation via negative regulation of T-bet. *Immunity* 2004; **21**(1)**:** 67-80.

116. Chang BY, Huang MM, Francesco M, Chen J, Sokolove J, Magadala P *et al.* The Bruton tyrosine kinase inhibitor PCI-32765 ameliorates autoimmune arthritis by inhibition of multiple effector cells. *Arthritis Res Ther* 2011; **13**(4)**:** R115.

117. Herman SE, Gordon AL, Hertlein E, Ramanunni A, Zhang X, Jaglowski S *et al.* Bruton tyrosine kinase represents a promising therapeutic target for treatment of chronic lymphocytic leukemia and is effectively targeted by PCI-32765. *Blood* 2011; **117**(23)**:** 6287-96.

118. Dubovsky JA, Beckwith KA, Natarajan G, Woyach JA, Jaglowski S, Zhong Y *et al.* Ibrutinib is an irreversible molecular inhibitor of ITK driving a Th1-selective pressure in T lymphocytes. *Blood* 2013; **122**(15)**:** 2539-49.

119. Woyach JA, Johnson AJ, Byrd JC. The B-cell receptor signaling pathway as a therapeutic target in CLL. *Blood* 2012; **120**(6)**:** 1175-84.

120. Honigberg LA, Smith AM, Sirisawad M, Verner E, Loury D, Chang B *et al.* The Bruton tyrosine kinase inhibitor PCI-32765 blocks B-cell activation and is efficacious in models of autoimmune disease and B-cell malignancy. *Proc Natl Acad Sci U S A* 2010; **107**(29)**:** 13075-80.

121. Byrd JC, Furman RR, Coutre SE, Flinn IW, Burger JA, Blum KA *et al.* Targeting BTK with ibrutinib in relapsed chronic lymphocytic leukemia. *N Engl J Med* 2013; **369**(1)**:** 32-42.

122. Wang ML, Rule S, Martin P, Goy A, Auer R, Kahl BS *et al.* Targeting BTK with ibrutinib in relapsed or refractory mantle-cell lymphoma. *N Engl J Med* 2013; **369**(6)**:** 507-16.

123. Hamilton BL, Parkman R. Acute and chronic graft-versus-host disease induced by minor histocompatibility antigens in mice. *Transplantation* 1983; **36**(2)**:** 150-5.

124. Cooke KR, Kobzik L, Martin TR, Brewer J, Delmonte J, Jr., Crawford JM *et al.* An experimental model of idiopathic pneumonia syndrome after bone marrow transplantation: I. The roles of minor H antigens and endotoxin. *Blood* 1996; **88**(8)**:** 3230-9.

125. Numata F, Hitoshi Y, Uehara S, Takatsu K. The xid mutation plays an important role in delayed development of murine acquired immunodeficiency syndrome. *Int Immunol* 1997; **9**(1)**:** 139-46.

126. Liu KQ, Bunnell SC, Gurniak CB, Berg LJ. T cell receptor-initiated calcium release is uncoupled from capacitative calcium entry in Itk-deficient T cells. *J Exp Med* 1998; **187**(10)**:** 1721-7.

127. Teshima T, Nagafuji K, Henzan H, Miyamura K, Takase K, Hidaka M *et al.* Rituximab for the treatment of corticosteroid-refractory chronic graft-versus-host disease. *Int J Hematol* 2009; **90**(2)**:** 253-60.

128. Tomlinson MG, Kane LP, Su J, Kadlecek TA, Mollenauer MN, Weiss A. Expression and function of Tec, Itk, and Btk in lymphocytes: evidence for a unique role for Tec. *Mol Cell Biol* 2004; **24**(6)**:** 2455-66.

129. Ellmeier W, Jung S, Sunshine MJ, Hatam F, Xu Y, Baltimore D *et al.* Severe B cell deficiency in mice lacking the tec kinase family members Tec and Btk. *J Exp Med* 2000; **192**(11)**:** 1611-24.

130. Inamoto Y, Flowers ME. Treatment of chronic graft-versus-host disease in 2011. *Curr Opin Hematol* 2011; **18**(6)**:** 414-20.

131. Matsuoka K, Koreth J, Kim HT, Bascug G, McDonough S, Kawano Y *et al.* Low-dose interleukin-2 therapy restores regulatory T cell homeostasis in patients with chronic graft-versus-host disease. *Sci Transl Med* 2013; **5**(179)**:** 179ra43.

132. Woyach JA, Bojnik E, Ruppert AS, Stefanovski MR, Goettl VM, Smucker KA *et al.* Bruton's tyrosine kinase (BTK) function is important to the development and expansion of chronic lymphocytic leukemia (CLL). *Blood* 2014; **123**(8)**:** 1207-13.

133. Rushworth SA, Murray MY, Zaitseva L, Bowles KM, MacEwan DJ. Identification of Bruton's tyrosine kinase as a therapeutic target in acute myeloid leukemia. *Blood* 2014; **123**(8)**:** 1229-38.

134. Serody JS, Hill GR. The IL-17 differentiation pathway and its role in transplant outcome. *Biol Blood Marrow Transplant* 2012; **18**(1 Suppl)**:** S56-61.

135. Taylor PA, Lees CJ, Blazar BR. The infusion of ex vivo activated and expanded CD4(+)CD25(+) immune regulatory cells inhibits graft-versus-host disease lethality. *Blood* 2002; **99**(10)**:** 3493-9.

136. Sage PT, Francisco LM, Carman CV, Sharpe AH. The receptor PD-1 controls follicular regulatory T cells in the lymph nodes and blood. *Nat Immunol* 2013; **14**(2)**:** 152-61.

137. Fujiwara H, Maeda Y, Kobayashi K, Nishimori H, Matsuoka KI, Fujii N *et al.* Programmed Death-1 Pathway in Host Tissues Ameliorates Th17/Th1-Mediated Experimental Chronic Graft-versus-Host Disease. *J Immunol* 2014.

138. Polo JM, Dell'Oso T, Ranuncolo SM, Cerchietti L, Beck D, Da Silva GF *et al.* Specific peptide interference reveals BCL6 transcriptional and oncogenic mechanisms in B-cell lymphoma cells. *Nat Med* 2004; **10**(12)**:** 1329-35.

139. Velichutina I, Shaknovich R, Geng H, Johnson NA, Gascoyne RD, Melnick AM *et al.* EZH2-mediated epigenetic silencing in germinal center B cells contributes to proliferation and lymphomagenesis. *Blood* 2010; **116**(24)**:** 5247-55.

140. He S, Xie F, Liu Y, Tong Q, Mochizuki K, Lapinski PE *et al.* The histone methyltransferase Ezh2 is a crucial epigenetic regulator of allogeneic T-cell responses mediating graft-versus-host disease. *Blood* 2013; **122**(25)**:** 4119-28.

141. Patakas A, Benson RA, Withers DR, Conigliaro P, McInnes IB, Brewer JM *et al.* Th17 effector cells support B cell responses outside of germinal centres. *PLoS One* 2012; **7**(11)**:** e49715.

142. Peters A, Pitcher LA, Sullivan JM, Mitsdoerffer M, Acton SE, Franz B *et al.* Th17 cells induce ectopic lymphoid follicles in central nervous system tissue inflammation. *Immunity* 2011; **35**(6)**:** 986-96.

143. Hill GR, Olver SD, Kuns RD, Varelias A, Raffelt NC, Don AL *et al.* Stem cell mobilization with G-CSF induces type 17 differentiation and promotes scleroderma. *Blood* 2010; **116**(5)**:** 819-28.

144. Dander E, Balduzzi A, Zappa G, Lucchini G, Perseghin P, Andre V *et al.* Interleukin-17-producing T-helper cells as new potential player mediating graft-versus-host disease in patients undergoing allogeneic stem-cell transplantation. *Transplantation* 2009; **88**(11)**:** 1261-72.

145. Kolls JK, Linden A. Interleukin-17 family members and inflammation. *Immunity* 2004; **21**(4)**:** 467-76.

146. Zanin-Zhorov A, Mo R, Scher J, Nyuydzefe M, Weiss J, Schueller O *et al.* Selective ROCK2 inhibitor down-regulates pro-inflammatory T cell responses via shifting Th17/Treg balance (IRM6P.711). *The Journal of Immunology* 2014; **192**(1 Supplement)**:** 63.3.